Frequency Synchronization Techniques in Wireless Communication

Thesis submitted to the University of Cardiff in candidature for the degree of Doctor of Philosophy.

Qiang Yu

CARDIFF
UNIVERSITY

PRIFYSGOL
CAERDYⅅ

Centre of Digital Signal Processing

Cardiff University

2007

UMI Number: U584985

UMI U584985

Abstract

In this thesis various iterative channel estimation and data detection techniques for time-varying frequency selective channels with multiple frequency offsets are proposed.

Firstly, a maximum likelihood approach for the estimation of complex multipath gains (MGs) and real Doppler shifts (DSs) for a single input single output (SISO) frequency selective channel is proposed. In a time division multiple access (TDMA) system, for example the third-generation global system, or mobile GSM communications, the pilot symbols are generally inadequate to provide enough resolution to estimate frequency offsets. Therefore, our approach is to use the pilot sequence for the estimation and equalization of the channel without consideration to frequency offsets, and then to use the soft estimates of the transmitted signal as a long pilot sequence to determine iteratively the multiple frequency offsets and refine the channel estimates. Inter-symbol interference (ISI) is removed with a linear structure turbo equalizer where the filter coefficients are chosen based on the minimum mean square error (MMSE) criterion. The detection performance is verified using the bit error rate (BER) curves and the frequency offset estimation performance through comparison with appropriate Cramer-Rao lower bounds.

This work is then extended for a multi-user transmission system where the channel is modelled as a multi input multi output (MIMO) TDMA system. For the iterative channel estimation, the MIMO frequency selective channel is decoupled into multiple SISO flat fading sub-channels through appropriately cancelling both inter-symbol-interference (ISI) and inter-user-interference (IUI) from the received signal. The refined channel

estimates and the corresponding frequency offset estimates are then obtained for each resolved MIMO multipath tap. Simulation results confirm a superior BER and estimation performance.

Finally, these iterative equalization and estimation techniques are extended to orthogonal frequency division multiplexing (OFDM) based SISO and MIMO systems. For OFDM, the equalization is performed in two stages. In the first stage, the channel and the frequency offsets are estimated in the time domain, while in the second stage, the transmitted symbols are estimated in the frequency domain and the mean values and the variances of the symbols are determined in the frequency domain. These two procedures interact in an iterative manner, exchanging information between the time and frequency domains. Simulation studies show that the proposed iterative scheme has the ability to track frequency offsets and provide a superior BER performance as compared to a scheme that does not track frequency offsets.

Abbreviations and Acronyms

AML   Approximate Maximum Likelihood

AWGN   Additive White Gaussian Noise

BER   Bit Error Rate

BPSK   Binary Phase Shift Keying

CDMA   Code Division Multiple Access

CIR   Channel Impulse Response

CP   Cyclic Prefix

CRLB   Cramér-Rao Lower Bound

CSI   Channel State Information

DFE   Decision Feedback Equalizer

DFT   Discrete Fourier Transform

DS   Doppler Shift

FBF   Feedback Filter

FDM   Frequency Division Multiplexing

FFF   Feedforward Filter

FFT   Fast Fourier Transform

FIR   Finite Impulse Response

FIM   Fisher Information Matrix

FO   Frequency Offset

GSM   Global System for Mobile Communications

ICI   Inter-Carrier Interference

ISI   Inter-Symbol Interference

iff   If and only if

IFFT   Inverse Fast Fourier Transform

LE   Linear Equalizer

LS   Least Squares

LLR   Log-likelihood Ratios

LOS   Line of Sight

LTE   Linear Transversal Equalizer

LTI   Linear Time Invariant

LTV   Linear Time Variant

MAP   Maximum A Posteriori

MCM   Multi Carrier Modulation

MIMO   Multiple Input and Multiple Output

MG   Multipath Gain

ML   Maximum Likelihood

MLE   Maximum Likelihood Estimator

MLSE   Maximum Likelihood Sequence Estimation

MMSE   Minimum Mean Square Error

MS   Mobile Station

MSE   Mean Square Error

MVUE   Minimum Variance Unbiased Estimator

OFDM   Orthogonal Frequency Division Multiplexing

PDF   Probability Density Function

SISO   Single Input and Single Output

SNR   Signal-to-Noise Ratio

SOVA   Soft Output Viterbi Algorithm

TDMA   Time Division Multiple Access

VA   Viterbi Algorithm

ZF   Zero Forcing

List of Symbols

$\lvert . \rvert$	Absolute value
$\odot$	Schur-Hadamard product
$(.)^H$	Hermitian transpose operator
$(.)^T$	Transpose operator
$(.)^\dagger$	Pseudo-inverse
$\triangleq$	Definition
θ	unknown parameter
Λ	Diagonal matrix
$\mathbf{b}$	feedback tap weight vector
$\mathbf{c}_d$	dth element of coordinate vector
f_d	Doppler shift
$\mathbf{f}$	forward filter tap weight
$\mathbf{H}_d$	dth column vector of convolution matrix
$\mathbf{H}$	Channel convolution matrix
$Im(.)$	Imaginary part of a complex number
$In(.)$	Natural logarithm
$J(.)$	Mean square error cost function

$diag(\mathbf{v})$	Diagonal matrix with vector $\boldsymbol{v}$ on its main diagonal
$\mathbf{C}ov(.)$	Covariance operator
$E\{\cdot\}$	Expectation operator
$\mathbf{I}$	Identity matrix
L	Length of the channel
M	Equalizer length
n	Number of sample
ω	Zero mean white Gaussian noise
$p(.)$	Probability density function
R	Covariance matrix
$Re\{.\}$	Real part
$\mathbf{S}$	Training signal matrix
$\mathbf{U}$	Received signal vector
$Var(.)$	Variance
$\mathbf{w}$	Equalizer tap weight vector
Y	Frequency domain signal

Statement of Originality

The contributions in this thesis are on the proposal and analysis of iterative channel and frequency offset estimation and detection algorithms for multipath channels with multiple frequency offsets. New techniques have been proposed for both SISO and MIMO systems and for TDMA and OFDM access schemes. The novel contributions are supported by one IEEE journal, four IEEE conference papers. The summary of these contributions are given below.

1. In chapter 3, and [I, II] an iterative approximate maximum likelihood (AML) estimator for a SISO multipath channel with distinct frequency offsets (FOs) has been proposed. The pilot symbols are generally inadequate to obtain an accurate estimate of the FOs due to limitation on the frequency resolution of the estimator. Hence the soft estimate of the transmitted signal are treated as a long pilot sequence to determine multiple FOs and to refine channel estimates iteratively. The performance of the proposed scheme has been studied for both flat-fading and frequency selective fading channels in a GSM system. The performance of the proposed scheme has been investigated with and without error control coding, and compared with appropriate Cramer-Rao Lower bounds (CRLB).

2. In chapter 4, the parameter estimation and equalization proposed for a SISO channel has been extended to MIMO multipath channels with distinct FOs. The soft estimates of the transmitted signal has been used as a pilot signal to resolve multiple users and multipaths and estimate and correct FOs in each resolved paths. The simulation results include BER

curves and comparison of the variance of the FO estimates with the corresponding CRLBs. The results have been published in [III, V].

3. In chapter 5 and [IV], iterative FO estimation and correction techniques for an OFDM system have been proposed to track multiple FOs due to distinct Doppler shifts associated with multipaths. The long training signal available in an OFDM symbol has been used to obtain initial estimates of the channel and FOs. Then the soft estimates of the data symbols are obtained in an iterative manner to track carrier frequency offsets and multipath channels coefficients in the subsequent packets. The proposed iterative technique has the ability to resolve multipaths, thereby converting the joint multiple FO estimation problem into estimation of distinct FOs. The technique has also been extended to a MIMO OFDM system [VI].

Publications

Journal Papers

I) Q. Yu, S. Lambotharan, "Iterative (Turbo) Estimation and Detection Techniques for Frequency Selective Channels with Multiple Frequency Offsets," *IEEE Signal Process. Lett.,* vol. 14, pp. 236-239, Apr. 2007.

Conference Papers

II) Q. Yu, S. Lambotharan, "Iterative Channel Estimation and Equalization Techniques for Multipath Channels with Multiple Frequency Offsets", *The Tenth IEEE International Conference on Communications Systems (ICCS)*, Singapore, Nov. 2006.

III) Q. Yu, S. Lambotharan, "Iterative (Turbo) Estimation and Detection Techniques for Frequency Selective Channels with Multiple Frequency Offsets in MIMO System", *IEEE 65th Vehicular Technology Conference (VTC)*, Dublin, Ireland, April 2007.

IV) Q. Yu, S. Lambotharan, "An Iterative Estimation and Detection Technique for OFDM Systems with Multiple Frequency Offsets (Doppler Shifts)," *The 18th IEEE personal, indoor and mobile radio communications (PIMRC)*, Athens, Greece, Sept. 2007.

V) K. Cumanan, R. Krishna, Q. Yu and S. Lambotharan, "Maximum likelihood frequency offset estimation for frequency selective MIMO channels: An average periodogram interpretation and iterative techniques," *The 15th European Signal Processing Conference (EUSIPCO)*, Poznan, Poland, Sept. 2007.

VI) Q. Yu, S. Lambotharan, "Iterative Estimation and Detection Technique for a MIMO OFDM channel with Multiple Frequency Offsets", *Submitted to IEEE 67th Vehicular Technology Conference (VTC)*, Singapore, May 2008.

Acknowledgment

I would like to thank especially my respected supervisor Dr. S. Lambotharan for his invaluable suggestions, and constant support in the development of this research. His invaluable expertise, advice, and encouragement made this work possible.

I am also extremely grateful to Prof. Jonathon A. Chambers for his help, invaluable discussions, and comments on this research. I am also grateful to him for proof reading this thesis.

I also wish to thank Dr. Sajid Ahmed for his advice on iterative methods, help in using LaTex and various practical problems.

I am greatly indebted to my parents for their constant support and encouragement of pursuing my education. I could not have succeeded without their support.

My study here at Cardiff University was valuable and enjoyable due to the excellent faculty, staff, and students. I wish to thank all my colleagues, in particular, I would like to thank Dr. Wenwu Wang, Dr. Zhuo Zhang, Dr. Lay Teen Ong, Dr. Rab Nawaz, Dr. Thomas Bowles, Dr. Yonggang Zhang, Dr. Clive Cheong Took, Vimal Sharma, Tariq Qaisirani, Loukianos Spyrou, Li Zhang, Min Jing, Cheng Shen, Lei Lei Li and Andrew Aubrey, for their insightful discussions and support.

Finally, I am grateful to my girlfriend, Yue Zheng, and her family for their caring support.

CONTENTS

List of Figures

Chapter 1

INTRODUCTION

The demand for high data rate applications such as multimedia and interactive services over wireless links is steadily increasing [1]. The research activities in wireless communication systems such as 3G [2], 4G, WLAN [3], DAB [4] and DVB [5] are focussed on supporting high bandwidth and high data rate services. In order to meet these requirements, development of advanced signal processing algorithms for mitigating channel impairments becomes an important task.

In this thesis, various transmitter and receiver signal processing techniques are proposed in order to improve the system performance, specifically through the use of multiple antennas at the transmitter and the receiver. High data rate communications are limited by several factors, among which intersymbol interference (ISI), which results from the signal spreading characteristic of the channel, plays an important role. Moreover, the effect of frequency offset (FO) introduced by local oscillator mismatch or Doppler shifts (DS) will become more severe as the data rate is increased.

1.1 Signal fading

In a wireless system, a communication channel is often no longer a single line of sight path, particularly in an urban environment. The received sig-

1

nal consists of a large number of reflected, refracted and scattered waves. The signal from the transmitter to the receiver arrives via more than one path. Due to multipath propagation, different attenuated versions of the transmitted signal arrive sequentially at the receiver. The differential time delay introduces a relative phase shift between different components. These signals could add constructively or distractively at the receiver so that the received signal could vary significantly. In a dynamic environment, due to the motion between the transmitter and the receiver, there is a continuous change in path lengths. The amplitude and the phase of the signal could continuously vary with time whereby there are constructive additions in some locations and distractive additions in certain other locations. This phenomenon is known as signal fading.

LARGE-SCALE FADING AND SMALL-SCALE FADING

Large-scale fading represents the average signal power attenuation or path loss due to motion over large areas [6]. This phenomenon is affected by prominent terrain such as hills, forests and buildings between the transmitter and receiver. Small-scale fading is used to describe the rapid fluctuation of the amplitude of a radio signal over a short period of time or travel distance, so that large-scale path loss effects may be ignored. Small-scale fading is caused by interference between two or more versions of the transmitted signal which arrive at the receiver at slightly different times. For mobile radio applications, the channel is time-variant because motion between the transmitter and receiver results in propagation path changes. Multipath in the radio channel creates small-scale fading effects. The three most important effects are [6]:

- Rapid changes in signal strength over a small travel distance or time interval.

- Random frequency modulation due to varying Doppler shifts on different multipath signals.

- Time dispersion (echoes) caused by multipath propagation delays.

This thesis is aimed at providing various signal processing techniques to mitigate the effect of small scale fading, in particular for high data rate transmission over wireless links. The work covers both single input and single output (SISO) and multiple input and multiple output (MIMO) systems as well as time division multiple access (TDMA) and orthogonal frequency division multiple (OFDM) access schemes.

1.1.1 Doppler shift

Due to relative motion between the mobile and the basestation, each multipath wave experiences an apparent shift in frequency. The shift in the received signal frequency due to this motion is named "Doppler shift" (DS). In order to improve the link layer performance of the receiver, the effects of the time selectivity of the channel due to DS must be cancelled. In most of the available literature [7–10], all multipaths have been assumed to have identical DSs. In this case, the DS can be compensated for prior to equalization. The phase change in the received signal is defined is [6]

$$\Delta\phi = \frac{2\pi v \Delta t}{\lambda} cos\theta \tag{1.1.1}$$

where v is the velocity of the transmitter relative to the receiver in meters/second: positive when moving towards one another, negative when moving away. Δt is the time required for the signal to travel from the transmitter to the receiver. λ is the wavelength, and θ is the angle of arrival in radians. Therefore, the DS is given is [6]

$$f_d = \frac{1}{2\pi} \cdot \frac{\Delta\phi}{\Delta t} = \frac{v}{\lambda} cos\theta \tag{1.1.2}$$

The equation in (1.1.2) shows that if the relative speed between the transmitter and receiver is constant, then the DS is a function of the angle of arrival. Therefore, each multipath which arrives with different angle of arrival could have different frequency offsets, and this effect should be accounted for in the receiver design. This is one of the main motivation of this thesis.

1.1.2 Channel Classification

A channel is said to be non-distorting if, within the bandwidth, BW, occupied by the transmitted signal, the amplitude response, $A(\omega)$, of the channel is constant, time-invariant and the phase response, $\theta(\omega)$, is a linear function of ω. However, if the amplitude of the spectrum is time varying, the fading in the signal is called frequency non-selective or flat fading. In the time domain, it can be said that the delay spread denoted as T_d, is less than the symbol period, T_s [11,12]. Flat fading does not produce ISI. Therefore, for flat fading, the channel satisfies

$$T_d < T_s \qquad\qquad (1.1.3)$$

On the other hand, multipath propagation can spread the transmitted signal over an interval of time which is longer than the symbol period, which can cause ISI, that limits the data rate of a communication system and increases the associated bit error rate. In the frequency domain, it means that the frequency response is not flat for the entire bandwidth of the signal. Hence, each frequency component of the signal is amplified and phase shifted differently. The fading in the received signal in this case is called frequency selective fading. Therefore, for frequency selective fading,

$$T_d > T_s \qquad\qquad (1.1.4)$$

Frequency selective fading occurs in the so-called 'small scale' multipath fading which dictates the instantaneous behaviour of the underlying channel conditions; whereas "Large scale" refers to long term effects of the channel over a longer period of time. The design of a relatively low complexity receiver that can provide significant improvement in BER performance over a conventional receiver in a frequency selective environment is the focus of this thesis.

1.2 Outline of the Thesis

Chapter 2: A detailed literature survey is provided together with necessary theoretical background. Various FO and channel estimation techniques are reviewed followed by the introduction of minimum variance unbiased estimation techniques. A detailed discussion on the existing equalization techniques is also provided.

Chapter 3: Parameter estimation and iterative equalization techniques for a SISO system are proposed. The FOs associated with each path of the channel have been assumed to be distinct. Unlike an identical DS problem as in [7,13,14], the distinct DSs can not be compensated prior to equalization. Hence a sophisticated equalizer is required. In order to design such an equalizer, the complex multipath gains (MGs) and FOs are required. A maximum likelihood (ML) estimation approach is used to obtain the complex MGs and FOs. In a TDMA based communication system, such as GSM, the pilot symbols are generally inadequate to obtain an accurate estimate of the FOs due to limitation on the frequency resolution of the estimator. Therefore, in the proposed technique, an initial channel estimate is obtained using a very short pilot (training) signal and the soft estimate of the transmitted signal is then treated as a pilot signal to determine

multiple FOs and to refine channel estimates iteratively. The proposed iterative technique has the ability to resolve multipaths, thereby modifying the multiple FO problem into one in which distinct frequency offsets are estimated. The performance of the estimator is assessed through comparison of the variance of estimates with the Cramér-Rao lower bound (CRLB).

Chapter 4: The work presented in chapter 3 is extended to a MIMO frequency selective channel. MIMO systems are very attractive in order to boost the capacity of a wireless communication system that operates in a rich multipath environment. In this chapter, communication over a MIMO system, allowing for a frequency selective channel between each transmit and receive antenna is considered with each path having distinct DSs. The training signals transmitted from the antennas are assumed to be spatially and temporally uncorrelated. An iterative channel parameter estimator is provided whereby the MIMO frequency selective channel is decoupled into multiple SISO flat fading sub-channels through appropriately cancelling both inter-symbol-interference (ISI) and the inter-user-interference (IUI) from the received signal. The refined channel estimates and the corresponding FO estimates are then obtained for each resolved MIMO multipath tap. The performance of the algorithm is compared with the matched filter bound. In addition to providing superior BER performance, the proposed estimator is also efficient in that it tends to attain the CRLB derived assuming all transmitted symbols in the burst are known pilot symbols.

Chapter 5: Parameter estimation and equalization techniques for a MIMO-OFDM system with time-varying channels are proposed. To combat multipath delay spread in high data rate wireless systems, wireless commu-

nication standards such as IEEE 802.11 adopted an OFDM transmission scheme which transforms a multipath channel into parallel independent flat-fading subchannels. OFDM systems are very sensitive to FOs, and an iterative technique is proposal to estimate and track FOs. Initial estimates of the channel gains and FOs are obtained using the long training signal available in OFDM. These estimates are used to obtain the soft estimates of the data symbols in the subsequent packets in an iterative manner to track carrier FOs. The merit of this iterative method is its ability to track FOs. The proposed iterative technique has the ability to resolve multipaths, bringing the multiple FO problem into the estimation of distinct FOs. Simulation results show a superior BER performance for the proposed algorithm over a scheme that does not consider FO correction.

Chapter 6: Conclusions are drawn and possible future research directions are outlined.

Chapter 2

PARAMETER ESTIMATION
AND EQUALIZATION

The demand for wireless communication systems that can potentially support high quality and high data rate multimedia and interactive services is continuously increasing. The channels in mobile radio systems are usually frequency selective and multipaths may give rise to intersymbol interference (ISI), which limits high data rate transmission [15]. In order to remove the effect of ISI, an equalizer is generally required, which in turn requires a channel estimator.
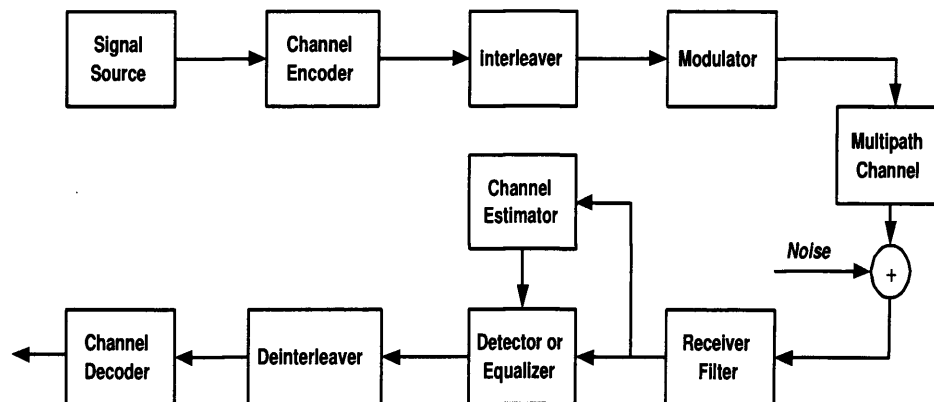
Figure 2.1. Block diagram of a baseband wireless communication system utilizing channel estimator and equalizer.

Fig. 2.1 depicts a block diagram of a baseband wireless communication system, which employs a channel estimator and equalizer at the receiver. The signal is usually first protected by channel coding and interleaving against fading phenomena, after that the binary signal is modulated and transmitted over the multipath fading channel. At the receiver, the task of the equalizer is to remove or mitigate the effect of ISI introduced by the multipath channels. A significant amount of research has been performed in the area of equalization over the last few decades and several well known techniques are available [6,15]. However, equalizers such as the maximum likelihood sequence estimator (MLSE) or maximum a posteriori proba- bility (MAP) detector need to know the channel impulse response (CIR) to ensure successful equalization (removal of ISI). Usually, the channel estimation is based on a known sequence of bits, which is unique for a cer- tain transmitter and known to the receiver. The channel estimator could estimate CIR for each burst separately by exploiting the known transmit- ted bits and the corresponding received samples. Note that equalization without separate channel estimation (e.g., adaptive linear and decision- feedback equalizer) is also possible, however their performance might not be sufficient for a rapidly varying wireless channel. After equalization, the signal is deinterleaved and decoded to extract the original message. In this chapter, a brief background on channel parameter estimation and equalization is presented.

2.1 Channel parameter estimation techniques

An important part of a receiver design is to develop an accurate channel estimation technique. Even with limited knowledge of the wireless channel properties, a receiver can gain insight into the information that was sent by the transmitter using a known pilot signal. The channel need to be

estimated before equalization and this is the focus of this section.

3 Tail bits	58 data bits	26 Training sequence	58 data bits	3 Tail bits
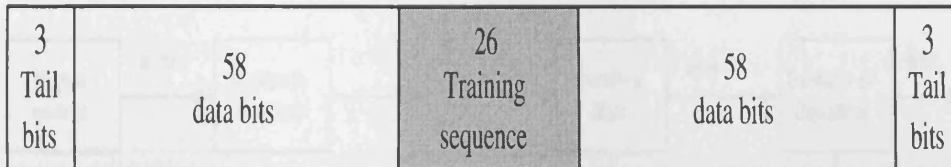
Figure 2.2. GSM burst structure; channel estimator utilizes the known training bits.

In a burst digital communication system, for example GSM [16], the 26 training bits in the middle of the burst are dedicated for channel estimation as shown in Fig. 2.2. The receiver can utilize the known training bits and the corresponding received samples to estimate CIR for each burst separately. The best known channel estimation methods are Maximum likelihood estimation (MLE) and Least-squares (LS) estimation [17].

2.1.1   Maximum likelihood estimation

Consider a baseband communication system, which is assumed to be corrupted by zero mean additive white Gaussian noise (AWGN) as depicted in Fig. 2.3.

The digital signal $s(n)$ from a finite constellation is transmitted over a fading multipath channel of length L, where 'n' denotes the discrete tone index. Thermal noise is generated at the receiver and it is modelled by the zero mean Gaussian distribution. The received signal is passed through a filter which is matched to the frequency band of the transmitter. Therefore, if the sampling rate at the receiver is equal to the symbol transmission rate, then the received signal can be written in the convolution form as

Noise w(n)
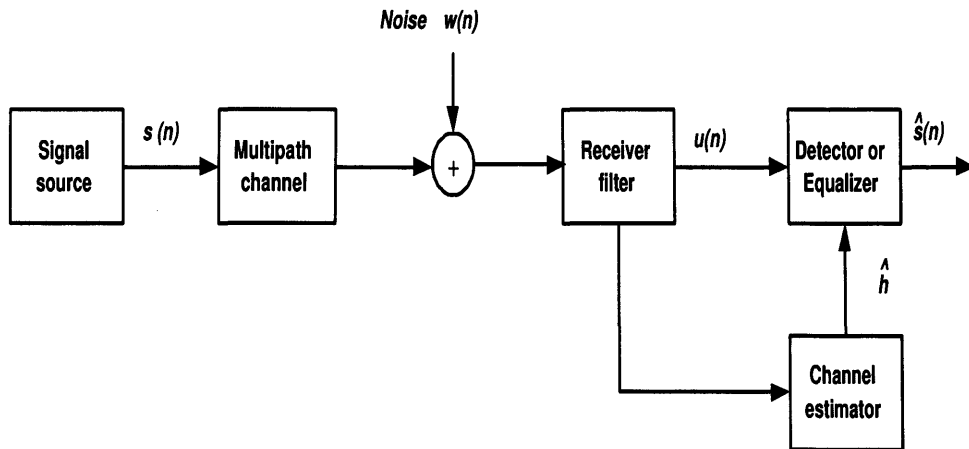
Figure 2.3. Block diagram of a noise-corrupted baseband communication system.

$$u(n) = \sum_{l=0}^{L-1} h(l)s(n-l) + \omega(n) \qquad (2.1.1)$$

where $h(l)$ is the unknown complex channel gain for the lth tap, L is the length of the channel and $\omega(n)$ is additive circularly symmetric zero mean white (complex) Gaussian noise with variance σ_ω^2.

The method of maximum likelihood determines the parameters that maximize the likelihood of the available set of observed data. In principle, the MLE technique may be applied to most of the data models [17], however, the implementation could be computationally expensive. The M received samples in (2.1.1) can be written in a vector form as

$$\mathbf{u} = \mathbf{S}\mathbf{h} + \boldsymbol{\omega} \qquad (2.1.2)$$

where

$$\mathbf{u} = \left[\begin{array}{cccc} u(0) & u(1) & \cdots & u(M-1) \end{array} \right]^T$$

$$\mathbf{S} = \left[\begin{array}{cccc} s(0) & s(-1) & \cdots & s(1-L) \\ s(1) & s(0) & \cdots & s(2-L) \\ \vdots & \ddots & \ddots & \cdots \\ s(M-1) & s(M-2) & \cdots & s(M-L) \end{array} \right],$$

$$\mathbf{h} = \left[\begin{array}{cccc} h(0) & h(1) & \cdots & h(L-1) \end{array} \right]^T$$

and

$$\boldsymbol{\omega} = \left[\begin{array}{cccc} \omega(0) & \omega(1) & \cdots & \omega(M-1) \end{array} \right]^T.$$

The likelihood function of the received samples can be written as

$$p(\mathbf{u}; \mathbf{h}) = \prod_{i=0}^{M-1} p\left[u(i); \mathbf{h}\right]. \tag{2.1.3}$$

In many cases, it is more convenient to work with the natural logarithm of the likelihood function, rather than with the likelihood function itself. Thus

$$
\begin{aligned}
\ln[p(\mathbf{u}; \mathbf{h})] &= \sum_{i=0}^{M-1} \ln p\left[u(i); \mathbf{h}\right] \\
&= \ln \frac{1}{(\pi\sigma_\omega^2)^{M/2}} e^{-\frac{(\mathbf{u}-\mathbf{Sh})^H(\mathbf{u}-\mathbf{Sh})}{\sigma_\omega^2}} \\
&= \frac{-M}{2} \ln(\pi\sigma_\omega^2) - \frac{(\mathbf{u}-\mathbf{Sh})^H(\mathbf{u}-\mathbf{Sh})}{\sigma_\omega^2}
\end{aligned}
$$

The logarithmic function $\ln[p(\mathbf{u}; h)]$ is a monotonically increasing function of $p(\mathbf{u}; h)$ between 0 and 1. Therefore, the parameter vector for

which the likelihood function $p(\mathbf{u}; \boldsymbol{h})$ is a maximum is exactly the same as the parameter vector for which the log-likelihood function $\ln[p(\mathbf{u}; \boldsymbol{h})]$ is a maximum. Taking the derivative of the log-likelihood function produces

$$\frac{\partial \ln p(\mathbf{u}; \mathbf{h})}{\partial \mathbf{h}^*} = \frac{1}{\sigma_\omega^2}(\mathbf{S}^H\mathbf{u} - \mathbf{S}^H\mathbf{Sh})$$

$$= \frac{1}{\sigma_\omega^2}(\mathbf{S}^H\mathbf{S})\left\{(\mathbf{S}^H\mathbf{S})^{-1}\mathbf{S}^H\mathbf{u} - \mathbf{h}\right\}$$

which upon being set to zero yields the MLE

$$\hat{\mathbf{h}} = (\mathbf{S}^H\mathbf{S})^{-1}\mathbf{S}^H\mathbf{u}. \tag{2.1.4}$$

To find how effective the maximum likelihood method is, a lower bound, namely the Cramer Rao Lower Bound (CRLB), on the variance of any unbiased estimate is derived in section 2.3. If the variance of an unbiased estimator is equal to the CRLB [17], then, the estimator is said to be efficient.

An MLE has the following three salient properties [17],

- Maximum-likelihood estimators are consistent, i.e., increasing the sample size of a maximum likelihood estimator decreases the variance of the estimate. It attains the CRLB asymptotically.

- Maximum-likelihood estimators are asymptotically unbiased; that is $\lim_{N \to \infty} E\{\hat{\theta}\} = \theta$.

- The distribution of the maximum-likelihood estimators are asymptotically Gaussian.

The drawback of the MLE can be its complexity and its difficult to apply for the signal models where the noise is not Gaussian.

2.1.2 Least squares estimation

Least squares estimation (LSE) is widely used in practice due to its ease of implementation and optimality in Gaussian noise. A salient feature of the method is that no probabilistic assumptions are made about the data, only a signal model is assumed. The main drawback of the least squares estimator is that it does not generally guarantee the optimality of the estimator. Furthermore, the statistical performance cannot be assessed without some specific assumptions about the probabilistic structure of the data. An LSE of an unknown parameter vector, $\boldsymbol{\theta}$, minimizes the sum of the squared error between the real observed data, $u(n)$ and the estimate $s(n)$ as [17]

$$J(\boldsymbol{\theta}) = \sum_{n=0}^{M-1} [u(n) - s(n)]^2$$

where the observation interval is assumed to be $n = 0, 1, \cdots, M-1$, and the dependence of J on θ is via $s(n)$. The value of θ that minimizes $J(\theta)$ is the LSE. The performance of the LSE will undoubtedly depend upon the properties of the corrupting noise as well as any modelling errors. LSE is usually applied in situations where a precise statistical characterization of the data is unknown or where an optimal estimator cannot be found or may be too complicated to apply in practice [17].

2.1.3 Joint estimation of channel impulse response (CIR) and frequency offset (FO)

In this section, an approximate maximum likelihood (AML) estimator of the complex channel gains (CGs) and a single FO is considered. It is assumed that the signal is propagated through L different paths and each path has the same Doppler shift (DS) f_d. The received complex baseband

signal is given by

$$u(n) = \sum_{l=0}^{L-1} h(l)s(n-l)e^{j2\pi f_d n} + \omega(n) \qquad (2.1.5)$$

and M received samples in a vector form can be expressed as

$$\mathbf{u} = \boldsymbol{\Delta}_d \mathbf{S} \mathbf{h} + \boldsymbol{\omega} \qquad (2.1.6)$$

where

$$\boldsymbol{\Delta}_d = \begin{bmatrix} 1 & 0 & 0 & 0 \\ 0 & e^{j2\pi f_d} & 0 & 0 \\ 0 & 0 & \ddots & 0 \\ 0 & 0 & 0 & e^{j2\pi f_d(M-1)} \end{bmatrix} \qquad (2.1.7)$$

The training signal matrix, $\mathbf{S}$, and the multipath gains (MGs) vector, $\mathbf{h}$, have been defined in the previous section. Thus, the log-likelihood function of the received signal can be expressed as (ignoring the constant terms)

$$\ln p(\mathbf{u}; \mathbf{h}; f_d) = -(\mathbf{u} - \boldsymbol{\Delta}_d \mathbf{S} \mathbf{h})^H (\mathbf{u} - \boldsymbol{\Delta}_d \mathbf{S} \mathbf{h}) \qquad (2.1.8)$$

where $(.)^H$ denotes conjugate transpose. Maximization of the log-likelihood function (2.1.8) is equivalent to minimizing the following cost function [18]

$$J(\mathbf{h}; f_d) = (\mathbf{u} - \boldsymbol{\Delta}_d \mathbf{S} \mathbf{h})^H (\mathbf{u} - \boldsymbol{\Delta}_d \mathbf{S} \mathbf{h}) \qquad (2.1.9)$$

which is a nonlinear least-squares problem. Minimization of (2.1.9) with respect to $\mathbf{h}^*$ yields

$$\frac{\partial J(\mathbf{h}; f_d)}{\partial \mathbf{h}^*} = -\mathbf{S}^H \boldsymbol{\Delta}_d^H \mathbf{u} + \mathbf{S}^H \mathbf{S} \mathbf{h}, \qquad (2.1.10)$$

Equating it to zero, then

$$\hat{\mathbf{h}} = (\mathbf{S}^H \mathbf{S})^{-1} \mathbf{S}^H \mathbf{\Delta}_d^H \mathbf{u}. \qquad (2.1.11)$$

The matrix $\mathbf{\Delta}_d$ is unknown and depends on f_d. Therefore $\mathbf{h}$ in (2.1.11) can not be estimated in the current form. The FO is estimated by minimizing the cost function, $J(f_d)$, obtained by substituting (2.1.11) into (2.1.9)

$$J(f_d) = \mathbf{u}^H \mathbf{u} - \mathbf{u}^H \mathbf{\Delta}_d \mathbf{S} (\mathbf{S}^H \mathbf{S})^{-1} \mathbf{S}^H \mathbf{\Delta}_d^H \mathbf{u} \qquad (2.1.12)$$

Note that the training samples $s(n)$ are assumed uncorrelated. Therefore $\mathbf{S}^H \mathbf{S} \approx k\mathbf{I}$, where k is constant over the frame considered. The minimization of (2.1.12) is therefore equivalent to maximization of the second term in (2.1.12) that can be written as [18]

$$\begin{aligned}
\phi(f_d) &= \mathbf{u}^H \mathbf{\Delta}_d \mathbf{S} \mathbf{S}^H \mathbf{\Delta}_d^H \mathbf{u} \\
&= \frac{1}{M} \sum_{n=0}^{M-1} \sum_{l=0}^{L-1} \left| u(n) e^{j2\pi f_d n} s(n-l) \right|^2,
\end{aligned} \qquad (2.1.13)$$

The maximum likelihood solution of f_d is therefore,

$$\hat{f}_d = \arg \max_f \phi(f) \qquad (2.1.14)$$

The FO f_d can be estimated using a grid search method. The grid search method could determine the frequency bin that maximizes (2.1.13), but it requires a very high computational complexity. However, in practice [15] a less computationally expensive approach called the Fast Fourier Transform (FFT) can be used. Once the FOs are estimated, the CGs, $\mathbf{h}$, can be estimated using (2.1.11).

2.2 Frequency estimation techniques

A frequency offset creates an extra burden for the equalizer in order to track channel variations. In such cases the equalizer can be simplified by estimating the FO and removing it as much as possible before equalization starts. Frequency offset estimation can be divided into two broad categories, data-aided and non-data-aided or blind techniques.

For known training signals and channel information, an FO estimator based upon the maximum-likelihood (ML) criterion was presented in [19]. Likewise, [20] and [21] proposed methods where only the training signals are required to be known. In [20], the least squares (LS) criterion has been employed, while in [21], the ML criterion has been adopted to jointly estimate the channel and the FO. How to choose the best training sequence for the above estimation problem has been addressed in [8, 22]. When the training signals are periodic, Moose [23] provided an ML estimator for the FO based on two identical OFDM symbols. The maximum offset that can be handled is one subcarrier spacing. However a scheme using one training OFDM symbol with two identical components, where the estimation range is two subcarrier spacing has been proposed in [24]. A narrow estimation range means that oscillators with high precision should be used, thus improving the cost of the system. In [25], an enhanced FO estimation scheme was proposed to extend the estimation range to M subcarriers spacing, using one OFDM symbol with M identical components. The methods in [26] and [27] exploit the redundancy associated with a cyclic prefix.

Various techniques are available for the estimation of frequency components. Among them, the following two technique are very powerful.

2.2.1 Classical techniques based on Fourier transform

Spectral analysis based on the frequency domain transformations of the received signal is a basic technique for the estimation of FO. The received signal samples are converted into the frequency domain by using the discrete Fourier transform (DFT). The FOs in the received signal samples can be estimated by determining the frequency at which the periodogram, or "spectrum", attains its maximum [28]. The amplitude of the received samples at different frequencies can be determined by using the discrete Fourier transform [17, 29–31],

$$F(f) = \frac{1}{M} \sum_{n=0}^{M-1} u(n) e^{-j2\pi f n} \qquad (2.2.1)$$

where $F(f)$ is the complex amplitude of the received signal at frequency f and $u(n)$ is the received signal sample. One drawback of this method is that it is difficult to determine the frequency offsets when multiple frequency offsets are present in the multipath channel.

2.2.2 Subspace methods

Subspace methods can provide high resolution frequency estimation but could result in increased computational complexity. These techniques are based on the principle of separating the noisy data into a signal subspace and a noise subspace. The FO is determined using the fact that the signal vectors will be orthogonal to the noise subspace. V. F. Pisarenko, first introduced this concept in 1973 and his technique is known as the Pisarenko harmonic decomposition [32]. This concept was later used to develop more advanced techniques such as MUSIC (multiple signal classification) and ESPRIT (estimation of signal parameters via rotational invariance) [33–35]. These methods require an eigenvalue decomposition

of the received sample covariance matrix $\mathbf{R}$ to determine the signal and the noise subspaces

$$\mathbf{R} = \mathbf{Q}\mathbf{\Lambda}\mathbf{Q}^H \qquad (2.2.2)$$

where $\mathbf{\Lambda}$ is a diagonal matrix of eigenvalues of the covariance matrix, and

$$\mathbf{Q} = [\mathbf{Q}_S \quad \mathbf{Q}_N] \qquad (2.2.3)$$

where $\mathbf{Q}_S$ and $\mathbf{Q}_N$ contain the basis vectors for the signal and the noise subspaces respectively. Thus the MUSIC based spectral estimator is formed as the inverse of the sum of inner products between the signal vector and the vectors in the noise subspace. The frequencies of the signal components are taken to be the peaks of the MUSIC spectral estimate [34]

$$S_{MUSIC}(f) = \frac{1}{\mathbf{s}^H(f)\mathbf{Q}_N\mathbf{Q}_N^H\mathbf{s}(f)} \qquad f \epsilon (-\frac{1}{2}, \frac{1}{2}] \qquad (2.2.4)$$

where $\mathbf{s}(f) = \begin{bmatrix} 1 & e^{-j2\pi f} & ... & e^{-j2\pi fN} \end{bmatrix}^T$ is the frequency scanning vector, and N is the order of the covariance matrix. A drawback in using sub-space based algorithms is that as the number of frequency components in the received signal increases, the order of the associated covariance matrix needs to be increased. Therefore, performing eigenvalue decomposition of a higher order covariance matrix, requires very high computational complexity.

2.2.3 Blind parameter estimation

Most existing FO estimation techniques rely on periodic transmission of pilot symbols, which could inevitably reduce bandwidth efficiency. A blind

FO estimation technique is attractive because it saves bandwidth, i.e., no training signals are required. However, blind algorithms generally require a very large set of data to estimate the parameters, hence they are suitable only when the channel changes slowly. Therefore, they are not good for burst communication, where only a small number of bits is available. Various blind FO estimation techniques can be found in [36–38] and the references therein. Since these techniques are not suitable for a highly dynamic wireless environment, this approach will therefore not be considered in this thesis.

2.3 Cramér Rao lower bound

Being able to place a lower bound on the variance of any unbiased estimator is extremely useful in practice. There are various methods available to determine the lower bound on the variance of the estimators, e.g. [17,39], but the Cramer-Rao Lower Bound (CRLB) [17] is straightforward to determine. An estimator that is unbiased and whose variance is always minimum when compared to other estimators but is not less than CRLB is called the Minimum Variance Unbiased estimator (MVUE).

2.3.1 The estimation problem

Assume real sample u(n) contains the parameter of interest θ corrupted by noise $\omega(n)$,

$$u(n) = \theta + \omega(n) \qquad (2.3.1)$$

where $\omega(n)$ is an additive white Gaussian noise (AWGN) process with PDF $N(0, \sigma^2)$. The observation of θ made at M intervals is given by the data set $[u(0), u(1), \cdots, u(M-1)]$. The joint probability distribution of data is given by $p(u(0), u(1), \cdots, u(M-1); \theta)$ or simply in vector

form as

$$p(\mathbf{u};\theta) = \frac{1}{(2\pi\sigma)^{M/2}} \exp[-\frac{1}{2\sigma^2} \sum_{n=0}^{M-1} (u(n) - \theta)^2] \qquad (2.3.2)$$

The PDF is a function of both the data $\mathbf{u}$ and the unknown parameter θ. When the PDF is viewed as a function of the unknown parameter θ it is called the likelihood function. Intuitively, the PDF describes how accurately the parameter θ can be estimated.

If the probability distribution of the data is known, then the problem of finding an estimator $\hat{\theta}$ is simply finding a function of data which maximizes the likelihood function. The variability of the estimates determines the efficiency of the estimator. The higher the variance of the estimates the less effective (or reliable) the estimates are. Hence various estimators can be found for the data but the one with the lowest variance is the best estimator.

2.3.2   Minimum variance unbiased estimation

Efficient estimation of channel parameters is very important to decode the transmitted data accurately. Therefore, it is very important to determine whether the estimator being designed is unbiased or biased and if it is unbiased what is its variance about the true value. An estimator is said to be unbiased iff

$$E\{\hat{\theta}\} = \theta, \quad a < \theta < b$$

where a and b represent the start and end range of possible values of θ. On the other hand an estimator is said to be biased if

$$b(\hat{\theta}) = E\{\hat{\theta}\} - \theta \neq 0$$

which is the bias of the estimate. The mean squared error (MSE) can be denoted as

$$
\begin{aligned}
\text{MSE}\{\hat{\theta}\} &= E\{(\hat{\theta} - \theta)^2\} \\
&= E\{[(\hat{\theta} - E(\hat{\theta})) + (E(\hat{\theta}) - \theta)]^2\} \\
&= Var(\hat{\theta}) + [E(\hat{\theta}) - \theta]^2 \\
&= Var(\hat{\theta}) + b^2(\hat{\theta})
\end{aligned}
$$

It can be seen that the MSE takes into account the variance of the estimator as well as its bias. If the estimator is constrained to be unbiased, and determined as the one with minimum variance, such an estimator is called minimum variance unbiased estimator (MVUE).

There are several methods for determining the MVUE. The most common ones are based on the Cramér Rao Lower Bound (CRLB).

2.3.3 Cramér Rao lower bound

The theory of the CRLB allows the determination of the MVUE, if it exists. Therefore, if the PDF $p(\mathbf{u}; \theta)$ satisfies the regularity condition [17]

$$
E\left\{\frac{\partial \ln p(\mathbf{u}; \theta)}{\partial \theta}\right\} = 0 \qquad for\ all\ \ \theta \tag{2.3.3}
$$

where the expectation is taken with respect to $p(\mathbf{u}; \theta)$ and if $\hat{\theta}$ is the estimator of θ, then the bound on the variance of an unbiased estimator is given as

$$
\sigma_{\hat{\theta}}^2(\theta) \geq \frac{1}{-E\left\{\frac{\partial^2 \ln p(\mathbf{u};\theta)}{\partial \theta^2}\right\}} \tag{2.3.4}
$$

Equality is the so called CRLB and the condition for equality is

$$\frac{\partial \ln p(\mathbf{u}; \theta)}{\partial \theta} = \frac{1}{c(\theta)}(\hat{\theta} - \theta) \tag{2.3.5}$$

where $c(\theta)$ is a scalar constant whose value may depend on θ. Therefore, this equation implies that if the log-likelihood function can be written in this form then $\hat{\theta}$ will be the MVUE. By differentiating (2.3.5) again, the value of $c(\theta)$ can be found as

$$\frac{\partial}{\partial \theta} \frac{\partial \ln p(\mathbf{u}; \theta)}{\partial \theta} = \frac{\partial}{\partial \theta}\left(\frac{1}{c(\theta)}(\hat{\theta} - \theta)\right)$$

$$\frac{\partial^2 \ln p(\mathbf{u}; \theta)}{\partial \theta^2} = -\frac{1}{c(\theta)} + \frac{\partial(\frac{1}{c(\theta)})}{\partial \theta}(\hat{\theta} - \theta)$$

$$c(\theta) = \frac{1}{-E\left\{\frac{\partial^2 \ln p(\mathbf{u};\theta)}{\partial \theta^2}\right\}}$$

Therefore, if (2.3.5) can be written in general form

$$\frac{\partial \ln p(\mathbf{u}; \theta)}{\partial \theta} = I(\theta)\left(g(\mathbf{u}) - \theta\right), \tag{2.3.6}$$

then the efficient MVUE and its variance bounded by the CRLB are given by (2.3.7) and (2.3.8) respectively.

$$\hat{\theta} = g(\mathbf{u}) \tag{2.3.7}$$

$$VAR(\hat{\theta}) = \frac{1}{I(\theta)} \tag{2.3.8}$$

where $I(\theta)$ is termed the Fisher information. An example is given below [17]. Consider a DC level estimation problem for samples observed in zero mean white Gaussian noise.

$$u(n) = \theta + \omega(n) \qquad n = 0, 1, ..., N - 1 \tag{2.3.9}$$

where $\omega(n)$ is WGN with variance σ^2. The likelihood function can be written as

$$p(\mathbf{u};\theta) = \frac{1}{(2\pi\sigma)^{M/2}} \exp[-\frac{1}{2\sigma^2} \sum_{n=0}^{M-1} (u(n) - \theta)^2] \qquad (2.3.10)$$

Taking the first derivative

$$
\begin{aligned}
\frac{\partial \ln p(\mathbf{u};\theta)}{\partial \theta} &= \frac{\partial}{\partial \theta} \left\{ -ln[(2\pi\sigma^2)^{\frac{M}{2}}] - \frac{1}{2\sigma^2} \sum_{n=0}^{M-1} (u(n) - \theta)^2 \right\} \\
&= \frac{1}{\sigma^2} \sum_{n=0}^{M-1} (u(n) - \theta) \\
&= \frac{M}{\sigma^2}(\bar{u} - \theta) \qquad (2.3.11)
\end{aligned}
$$

This can be compared to (2.3.5), where $\bar{u}$ is the sample mean. Differentiating (2.3.11) again,

$$\frac{\partial^2 \ln p(\mathbf{u};\theta)}{\partial \theta^2} = -\frac{M}{\sigma^2} \qquad (2.3.12)$$

In this case, the second derivative is a constant, and the CRLB is given as

$$Var(\hat{\theta}) \geq \frac{\sigma^2}{M} \qquad (2.3.13)$$

The CRLB derived in this section can easily be extended for vector parameters and it will be used throughout the thesis to assess the performance of the estimators [17].

2.4   Equalization techniques

Equalization techniques have been developed from the 1960s, [40–42]. An equalizer is required at the receiver in order to mitigate the effect of ISI. Equalization techniques fall into two broad categories: linear and non-linear. The linear equalization techniques are generally the simplest to

implement. However, linear equalization techniques typically suffer from more noise enhancement than the nonlinear equalizers, and therefore they are not used in most wireless applications. Among nonlinear equalization techniques, decision-feedback equalization (DFE) is the most common, since it is fairly simple to implement and generally performs well.

Noise w(n)

$s(n)$ → | H(z) | → (+) → $u(n)$ | Equalizer | → $\hat{s}(n)$
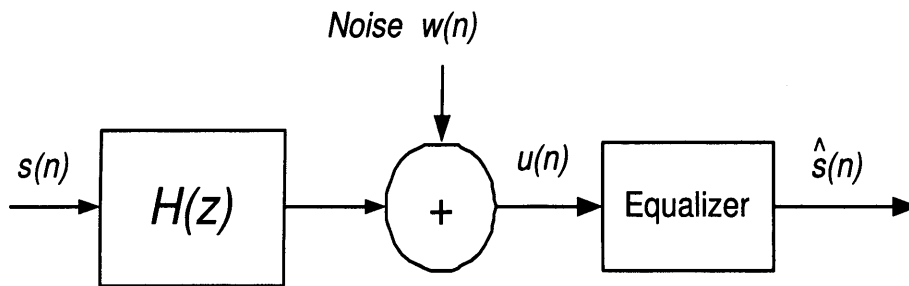
Figure 2.4. Baseband representation of a channel and an equalizer.

For the discussion, the system model in Fig. 2.4 will be used. The transmitted signal $s(n)$ is passed through an ISI channel modelled as a Finite Impulse Response (FIR) filter with z-domain transfer function $H(z)$. As in (2.1.1), the distorted channel output $u(n)$ is then processed by an equalizer that provides an estimate of the transmitted symbol $\hat{s}(n)$.

2.4.1 Linear transversal MMSE equalizer

A linear equalizer can be implemented using an FIR filter. The current and the past values of the received signal are linearly weighted by the filter coefficients and summed to produce the output, as shown in Fig. 2.5. The equalizer input $u(n)$ and the output $\hat{s}(n)$ before decision making can be expressed in the convolution form as [6]

$$\hat{s}(n) = \sum_{p=0}^{P-1} w^*(p)u(n-p) = \mathbf{w}^H\mathbf{u}(n) \qquad (2.4.1)$$
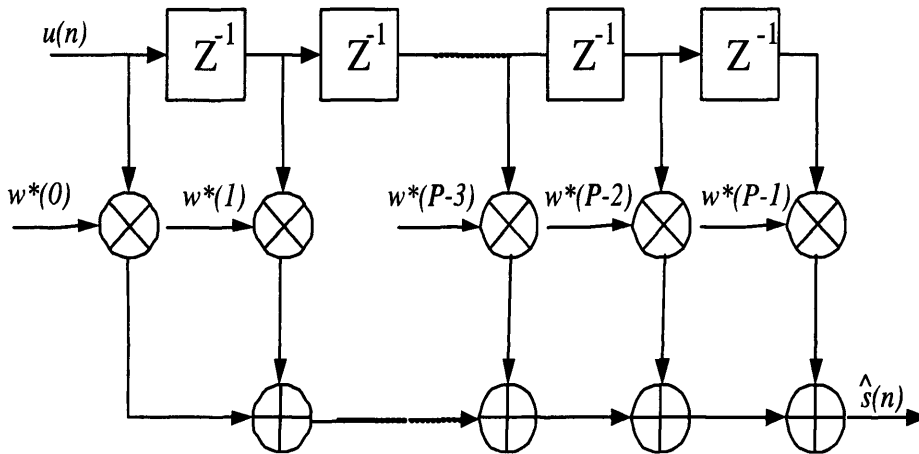
Figure 2.5. A linear equalizer implemented as a transversal filter.

where P is the length of the equalizer, $\mathbf{w} = [w(0), \; w(1), \; \cdots, \; w(P-1)]^T$ represents the equalizer tap weight vector, and the received signal vector is denoted as $\mathbf{u} = [u(0), \; u(n-1), \; \cdots, \; u(n-P-1)]^T$. If the equalizer approximates the inverse of the channel, this is referred to as a zero-forcing equalizer where the coefficients are chosen based on the zero-ISI criterion [43]. Normally, this leads to a very long equalizer and large noise amplification when the signal is weak. Instead of using the zero-ISI criterion, the LE coefficients can be chosen such that $\hat{s}(n)$ becomes as closer to s(n) as possible in the mean square error sense. This is a well-known and widely used approach and known as a Minimum Mean Square Error (MMSE) filter. Since the complex MMSE equalizer design will be of special interest in Chapter 3, 4 and 5, thus only a brief introduction to MMSE equalizer design is provided here. Suppose the equalizer is designed to retrieve the transmitted signal, $s(n)$, with a delay d, the mean square error can be written as

$$J = E\big\{|\ \hat{s}(n) - s(n - d)\ |^2\big\}$$

$$= E\big\{|\ \mathbf{w}^H \mathbf{u}(n) - s(n - d)\ |^2\big\}$$

$$= \mathbf{w}^H E\big\{\mathbf{u}(n)\mathbf{u}^H(n)\big\}\mathbf{w} - \mathbf{w}^H E\big\{\mathbf{u}(n)s^*(n - d)\big\}$$

$$- E\big\{\mathbf{u}^H(n)s(n - d)\big\}\mathbf{w} + E\big\{|\ s(n)\ |^2\big\} \qquad (2.4.2)$$

where the statistical expectation E is taken over the statistics of the noise and the data sequence. Define a channel convolution matrix $\mathbf{H}$ of dimensions $P \times (L + P - 1)$ as

$$\boldsymbol{H} = \begin{bmatrix} h_0 & h_1 & \ldots & h_{L-1} & 0 & \ldots & 0 \\ 0 & h_0 & \ldots & h_{L-2} & h_{L-1} & \ddots & \vdots \\ \vdots & 0 & \ddots & \vdots & \ddots & \ldots & 0 \\ 0 & \ldots & 0 & h_0 & h_1 & \ldots & h_{L-1} \end{bmatrix} \qquad (2.4.3)$$

Differentiating the cost function in (2.4.2) with respect to $\mathbf{w}^*$, the MMSE equalizer is obtained as [17, 18]

$$\mathbf{w} = \left(\mathbf{HH}^H + \frac{\sigma_\omega^2}{\sigma_s^2}\mathbf{I}\right)^{-1}\mathbf{Hc_d} \qquad (2.4.4)$$

where $\mathbf{I}$ is an identity matrix and $\mathbf{c_d}$ is a coordinate vector such that $\mathbf{Hc_d}$ chooses the dth column of $\mathbf{H}$.

2.4.2 Decision feedback equalization

The DFE has been of considerable attention due to its improved performance over a linear equalizer and reduced implementation complexity as compared to a nonlinear maximum-likelihood receiver. The basic idea behind decision feedback equalization is that once an information symbol has been detected and decided upon, the ISI that it induces on the future

symbols can be estimated and subtracted out before detection of subsequent symbols [15]. This is done by a feedforward filter (FFF) $A(z)$ and a supplementary feedback filter (FBF) $B(z)$. The FBF is driven by the decision on the output of the detector, and its coefficients can be adjusted to cancel the ISI on the current symbol from past detected symbols. A block diagram of the DFE structure is shown in Fig. 2.6.
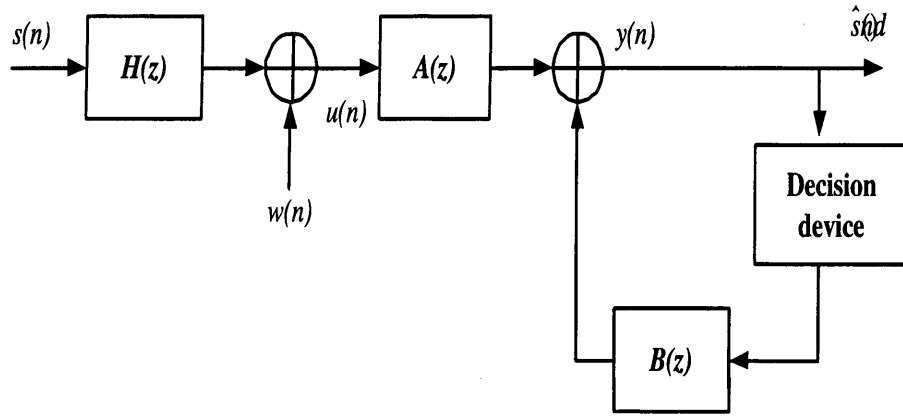
Figure 2.6. The baseband model of a channel and a decision feedback equalizer (DFE).

Assuming that the equalizer has N_f taps in the feed forward filter and N_b taps in the feedback filter, the filters A(z) and B(z) are written as

$$A(z) = \sum_{i=0}^{N_f-1} f_i^* z^{-i} \qquad (2.4.5)$$

$$B(z) = \sum_{k=1}^{N_b} b_k^* z^{-k} \qquad (2.4.6)$$

Combining the output of the feedforward and feedback filters, the equalizer output can be expressed as

$$y(n) = \sum_{i=0}^{N_f-1} f_i^* u(n-i) - \sum_{k=1}^{N_b} b_k^* \hat{s}(n-d-k)$$

$$= \mathbf{f}^H \mathbf{u} - \mathbf{b}^H \hat{\mathbf{s}}$$

$$= \mathbf{f}^H (\mathbf{H}\mathbf{s} + \boldsymbol{\omega}) - \mathbf{b}^H \mathbf{M}\mathbf{s} \qquad (2.4.7)$$

where $\hat{s}(n-d)$ is the hard decision of the previously estimated symbols at the output of a nonlinear decision device, and $\mathbf{f} = [f_0 \; f_1 \; \cdots \; f_{(N_f-1)}]^H$ is the forward filter tap weight vector and $\mathbf{b} = [b_1 \; b_2 \; \cdots \; b_{N_b}]^H$ is the feedback tap weight vector. The vector $\hat{\mathbf{s}}$ is related to $\mathbf{s}$ through the matrix $\mathbf{M}$ as

$$\hat{\mathbf{s}}_{N_b \times 1} = [\mathbf{0}_{N_b \times d} \; \mathbf{I}_{N_b \times N_b} \; \mathbf{0}_{N_b \times (N_f + N_h - 1 - N_b - d)}] \mathbf{s}_{(N_f + N_h - 1) \times 1} = \mathbf{M}\mathbf{s} \quad (2.4.8)$$

where N_h is the channel length. The mean squared error function can be written as

$$J(\mathbf{f}, \mathbf{b}) = E\{| y(n) - s(n-d) |^2\}$$

$$= (\mathbf{f}^H \mathbf{H} - \mathbf{b}^H \mathbf{M})(\mathbf{H}^H \mathbf{f} - \mathbf{M}^H \mathbf{b})\sigma_s^2 + \mathbf{f}^H \mathbf{f}\sigma_\omega^2 - (\mathbf{f}^H \mathbf{H} - \mathbf{b}^H \mathbf{M})\sigma_s^2 \mathbf{c}_d$$

$$- \mathbf{c}_d^H (\mathbf{H}^H \mathbf{f} - \mathbf{M}^H \mathbf{b})\sigma_s^2 + \sigma_s^2 \qquad (2.4.9)$$

where $\mathbf{c}_d$ is a coordinate vector. The expressions for the feedback and feedforward tap weights can be obtained as

$$\mathbf{b} = \mathbf{M}\mathbf{H}^H \mathbf{f} \qquad (2.4.10)$$

$$\mathbf{f} = (\mathbf{H}(\mathbf{I} - \mathbf{M}^H \mathbf{M})\mathbf{H}^H + \frac{\sigma_\omega^2}{\sigma_s^2})^{-1} \mathbf{H}\mathbf{c}_d \qquad (2.4.11)$$

The DFE is known to outperform the traditional linear equalizer, particularly if the channel has deep spectral nulls in its frequency response [15]. However, performance degradation in the DFE occurs when incorrectly

detected symbols are fed through the FBF. The DFE output reflects this error during the next few symbols. This phenomenon is called error propagation. Various techniques for mitigating error propagation have been proposed [44, 45], including DFE structures that contain a soft decision device in the feedback path to compensate for unreliable decisions. Most of these approaches require an increased complexity. In the work in this thesis, a soft decision based iterative equalizer is adopted which will be explained in the next section.

2.4.3   Iterative equalization

Iterative equalizers (turbo equalizers) work similarly to the DFE, the difference is that, in DFEs, previously estimated symbols are fedback and a decision on the current symbol is made only once. However, in iterative equalization the previously estimated symbols are fedback and decisions on the current symbol are made more than once. Hence the iterative methods can obtain more accurate estimates. Turbo equalizers were first proposed in [46] and further developed in [47], [48]. MAP-based techniques, most often a Viterbi algorithm (VA) producing soft output information [49], are used exclusively for both equalization and decoding [46], [47]. Furthermore, in [50] it is shown that a combined turbo coding and equalization, could yield tremendous improvement in terms of bit error rate (BER) performance.

The MAP/ML based methods often suffer from high computational complexity. A major research issue has been the complexity reduction of such iterative algorithms. The work in [51] proposed a joint coding and equalization approach, distinct from turbo equalization, working with convolutional coding and a DFE. Here, within the DFE, soft information from the DFE feedforward filter and tentative (hard) decisions from the decoder

using the VA are fed back. Wang and Poor [52] proposed a turbo equaliza-
tion based multiuser detector for code division multiple access (CDMA)
schemes. This iterative scheme is based on turbo equalization using an
LE to reduce ISI and MAP decoding. The MAP equalizer is thus replaced
with an LE, where the filter parameters are updated using the MMSE
criterion.
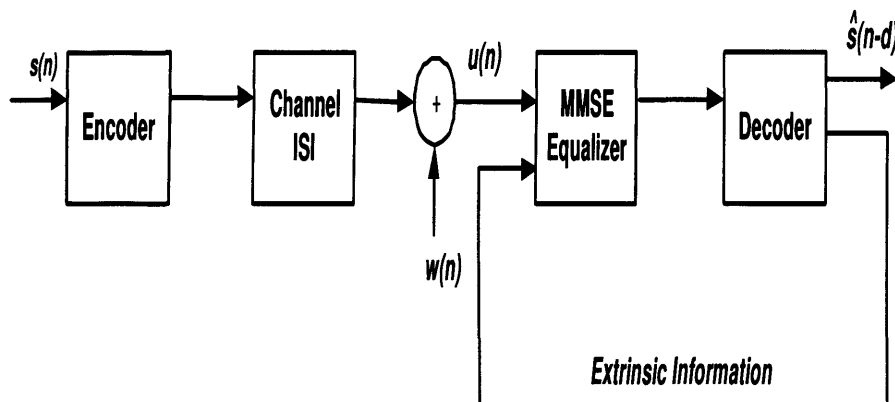
Figure 2.7. An MMSE iterative equalization scheme.

A SISO MMSE iterative equalization scheme is shown in Fig. 2.7. The
noise is assumed to be uncorrelated and zero mean. Therefore, $E\{\omega_n\} = 0$,
$E\{\omega_n\omega_n^H\} = \sigma_\omega^2 \mathbf{I}$, $E\{\mathbf{s}\omega_n^H\} = 0$. Moreover, let $\bar{s}(n) = E\{s(n)\}$, $\bar{\mathbf{s}} = E\{\mathbf{s}\}$,
$v_s(n) = \text{Cov}[s(n), s(n)]$, and $\mathbf{v}_s = \begin{bmatrix} v_s(0) & v_s(1) & \cdots & v_s(P+L-2) \end{bmatrix}$.
The MMSE equalizer $\mathbf{w}_n$ of length L for the soft estimates of $s(n)$ is given
by [53], [54]

$$\mathbf{w}_n = (\mathbf{H}diag(\mathbf{v}_s)\mathbf{H}^H + \sigma_\omega^2 \mathbf{I})^{-1}\mathbf{h}_d\sigma_s^2 \qquad (2.4.12)$$

where $\mathbf{H}$ is the $P \times (P + L - 1)$ channel convolution matrix, and $\mathbf{h}_d$ is
the dth column of $\mathbf{H}$ [55]. The estimate for $s(n)$ is given by

$$\hat{s}(n) = \bar{s}(n) + \mathbf{w}_n^H(\mathbf{u}(n) - \mathbf{H}\bar{\mathbf{s}}) \qquad (2.4.13)$$

To find a posteriori values of $v_s(n)$ and $\bar{s}(n)$ to use in (2.4.12) and (2.4.13), the following steps are required.

Step 1 By assuming no knowledge in the first iteration about the future decisions, initialize all the mean values $\bar{s}(n) = 0$. This corresponds to $\text{diag}(\mathbf{v}_s) = \mathbf{I}$. The estimate $\hat{s}(n)$ is obtained using(2.4.12) and (2.4.13).

Step 2 The a priori and a posteriori LLRs of s(n) are defined as [50, 55]

$$L[s(n)] = \ln \frac{p\{s(n) = 1\}}{p\{s(n) = -1\}}$$

and

$$L[s(n)|_{\hat{s}(n)}] = \ln \frac{p\{s(n) = 1|_{\hat{s}(n)}\}}{p\{s(n) = -1|_{\hat{s}(n)}\}}$$

The MMSE equalizer output $\hat{s}(n)$ is used to obtain the difference between the posteriori and a priori log-likelihood ratio (LLR), also called the extrinsic information as

$$\Delta L[\hat{s}(n)] = L[s(n)|_{\hat{s}(n)}] - L[s(n)]$$

$$= \ln \frac{p\{s(n) = 1|_{\hat{s}(n)}\}}{p\{s(n) = -1|_{\hat{s}(n)}\}} - \ln \frac{p\{s(n) = 1\}}{p\{s(n) = -1\}} \qquad (2.4.14)$$

Using Bayes' theorem, $p(a|b) = \frac{p(b|a)p(a)}{p(b)}$, (2.4.14) can be written as

$$\Delta L[\hat{s}(n)] = \ln \frac{p\{\hat{s}(n)|_{s(n)=1}\}p\{s(n) = 1\}}{p\{\hat{s}(n)|_{s(n)=-1}\}p\{s(n) = -1\}} - \ln \frac{p\{s(n) = 1\}}{p\{s(n) = -1\}}$$

$$= \ln \frac{p\{\hat{s}(n)|_{s(n)=1}\}}{p\{\hat{s}(n)|_{s(n)=-1}\}}$$

$$= L[\hat{s}(n)|_{s(n)}]$$

To find $L[\hat{s}(n)|_{s(n)}]$, it is assumed that the probability density function (PDF) of $\hat{s}(n)$ is Gaussian with variance σ_s^2, i.e.

$$p\{\hat{s}(n)\} = \frac{1}{\sqrt{\pi\sigma_s^2}} \exp\left(-\frac{(\hat{s}(n) - E\{\hat{s}(n)\})(\hat{s}(n) - E\{\hat{s}(n)\})^*}{\sigma_s^2} \right)$$

Therefore, the conditional PDF of $\hat{s}(n)$ becomes

$$p\{\hat{s}(n)|_{s(n)=b}\} = \frac{1}{\sqrt{\pi\sigma_s^2|_{s(n)=b}}} \exp\left(-\frac{(\hat{s}(n) - m_b)(\hat{s}(n) - m_b)^*}{\sigma_s^2|_{s(n)=b}}\right),$$

where m_b and $\sigma_s^2|_{s(n)=b}$ are respectively the conditional mean and variance of $\hat{s}(n)$. Here, a binary phase shift keying (BPSK) system is considered for which $b = \{+1, -1\}$, therefore, for the above PDF, the conditional mean and the variance are obtained from the knowledge of the channel and the equalizer as follows [55], (e.g. d = 0),

$$
\begin{aligned}
m_b &= E[\hat{s}(n)|_{s(n)=b}] \\
&= E[\mathbf{w}_n^H(\mathbf{H}(\mathbf{s} - \bar{\mathbf{s}}) + \boldsymbol{\omega})] \\
&= E[\mathbf{w}_n^H(\mathbf{h}_0 s(n) + \sum_{i \neq 0} h_i(s(n-i) - \bar{s}(n-i)) + \boldsymbol{\omega})] \\
&= \mathbf{w}_n^H \mathbf{h}_0 b
\end{aligned}
$$

$$
\begin{aligned}
\sigma_{s|s(n)=b}^2 &= \text{Cov}\{\hat{s}(n), \hat{s}(n)|_{s(n)=b}\} \\
&= E\{\hat{s}(n)\hat{s}(n)^*\} - m_b m_b^* \\
&= \mathbf{w}_n^H(\mathbf{H}diag(\mathbf{v}_s)\mathbf{H}^H + \sigma_\omega^2 \mathbf{I})\mathbf{w}_n - \mathbf{w}_n^H \mathbf{h}_0 \mathbf{h}_0^H \mathbf{w}_n \\
&= \mathbf{w}_n^H \mathbf{h}_0(1 - \mathbf{h}_0^H \mathbf{w}_n) \quad\quad\quad\quad\quad\quad (2.4.15)
\end{aligned}
$$

In general, when the delayed signal $s(n - d)$ is estimated, the mean and variance can be written as

$$
m_b = \mathbf{w}_n^H \mathbf{h}_d b
$$
$$
\sigma_{s|s(n)=b}^2 = \mathbf{w}_n^H \mathbf{h}_d(1 - \mathbf{h}_d^H \mathbf{w}_n)
$$

Therefore, the required extrinsic information $L[\hat{s}(n)|_{s(n)}]$ can be expressed as

$$L[\hat{s}(n)|_{s(n)}] = -\frac{(\hat{s}(n) - m_{(+1)})(\hat{s}(n) - m_{(+1)})^*}{\sigma_s^2} +$$

$$\frac{(\hat{s}(n) - m_{(-1)})(\hat{s}(n) - m_{(-1)})^*}{\sigma_s^2}$$

$$= \frac{4\text{Re}\{\hat{s}(n)m_{(+1)}\}}{\sigma_s^2}$$

$$= \frac{4\text{Re}\{\hat{s}(n)\}}{1 - \mathbf{h}_d^H \mathbf{w}_n} \qquad (2.4.16)$$

The mean of the symbol (soft estimate) $\bar{s}_n$ to be used in (2.4.13) is obtained as [55]

$$\bar{s}_n = p\{s(n) = +1|_{\hat{s}(n)}\} - p\{s(n) = -1|_{\hat{s}(n)}\} \qquad (2.4.17)$$

$$= \tanh\left(\frac{L[s(n)|_{\hat{s}(n)}]}{2}\right)$$

The variance required for the MMSE equalizer in (2.4.12) is also computed as follows [53]

$$v_s(n) = \sum_{b \, \varepsilon \, \{+1,-1\}} |b - E[s(n)|_{\hat{s}(n)}]|^2 p(s(n) = b|_{\hat{s}(n)}) \qquad (2.4.18)$$

$$= 1 - |\bar{s}(n)|^2$$

In the subsequent iterations, the iterative methods use the extrinsic information obtained in the previous iteration to estimate the current symbols. Therefore, more and more accurate estimates are obtained by repeating this a number of times.

2.5   Summary

In this chapter, a brief background on the available techniques for mitigating the effect of multipath channels was provided. In order to mitigate the effect of a multipath channel, several linear, nonlinear and adaptive equalization techniques can be used. However, in a fast fading channel,

the adaptive equalizer can not track the channel variations. Therefore, equalization techniques with explicit estimation of the channel parameters are preferred. The problem of channel and frequency offset estimation has been formulated and an overview of various estimation techniques has been provided. The performance of the equalizer depends on the variance of the channel parameter estimators. Therefore, the concepts of Minimum Variance Unbiased Estimation (MVUE) and Cramer-Rao Lower Bound have been introduced.

Chapter 3

ITERATIVE PARAMETER ESTIMATION AND EQUALIZATION FOR SISO CHANNELS WITH MULTIPLE FREQUENCY OFFSETS

Wireless communication channels are subject to channel impairments such as multipath propagation and fading in addition to additive noise. Moreover, the performance of a communication system could seriously degrade when FO introduces time-variations into the multipath channel. For a high data rate transmission, FO is introduced due to movement between the transmitter and the receiver (DS) [56] or poor synchronization between the transmitter and the receiver carrier frequencies. The reason for poor synchronization is due to imperfection of local oscillator due to temperature variations. It could also arise due manufacturing imperfection as certain tolerance is allowed in the components design. It is crucial that the FO should be estimated and taken into account in the receiver design to enable accurate decoding of the transmitted signal.

In this chapter, an iterative channel estimation and data detection technique for a TDMA based communication system is studied. For a TDMA communication system, a SISO channel with each multipath possibly having distinct DS is considered. For linear-time-invariant (LTI) channels equalizers may be easy to implement. Since an FO introduces time selectivity into the channel that degrades the BER performance of an equalizer, it is necessary to estimate the FO and cancel its effect prior to equalization. In a TDMA system, it is difficult to estimate the FO due to the limited number of bits available for training, for example in GSM, each burst of 142 bits contains only 26 training data samples [57]. Therefore, the soft estimate of the transmitted signal could be used as a long pilot sequence to determine the FO in an iterative manner. For a TDMA communication system, various FO estimation techniques have been widely studied. Morelli [13] and Huseyin [58] proposed FO estimation algorithms for flat fading channels based on the autocorrelation of the channel. The channel estimates are noisy and require low pass filtering and the bandwidth of the low pass filter depends on the Doppler spread. Thus, such receivers require adaptive low pass filtering that makes these algorithms complicated. Krasny [14] has proposed optimal and sub-optimal algorithms based on the maximum likelihood method to determine FO, where it is assumed that the channel is non-dispersive but it does not require any filtering. For a dispersive channel, the channel and FOs are estimated in [59] based on channel impulse response estimation. In this method, in order to estimate FO, channel estimation is mandatory. Harish [7] proposed a maximum state accumulation technique of FO estimation that does not require an explicit estimation of the channel. All of these algorithms, assume that the FO is identical for each multipath.

In contrast to previous works, in this chapter, equalization of a channel for

a single transmit and receive antenna system, under a general framework that allows distinct FOs for each multipath, is addressed. This scenario could arise when either the receiver or the transmitter moves at very high speed resulting into various Doppler shifts for paths with different angle of arrivals [18] and [60,61]. A similar scenario could also arise when the same signal is transmitted from various basestations e.g., in cooperative diversity scheme, [62]. In this case, even for a fixed wireless system, local oscillator frequency mismatch associated with various basestations could result in different frequency offsets for different paths. Both scenarios result in an identical mathematical model, i.e. multipaths with multiple frequency offsets. In this scenario, by exploiting the correlation property of the transmitted training symbols an approximative maximum likelihood (AML) estimator is proposed. Here, unlike channel estimation, frequency offset estimation requires a long data sequence to get a reasonably good estimate due to the resolution associated with a maximum likelihood method such as power spectral estimation based on the discrete Fourier transformation (DFT) [17]. Therefore, an iterative estimation and detection technique for multipath channels with multiple frequency offsets is proposed.

3.1 Problem statement

Consider a communication system employing a single transmit and receive antenna, and assume that the signal has propagated through L different paths, with each path possibly having different frequency offset. The received baseband signal is given by

$$u(n) = \bar{u}(n) + \omega(n) = \sum_{l=0}^{L-1} h_l s(n - l) e^{j2\pi f_l n} + \omega(n), \qquad (3.1.1)$$

where h_l and f_l are the unknown complex channel gain and frequency offset for the lth channel tap. Herein, it is assumed that h_l and f_l are quasi-stationary, not changing significantly over the observed data frame, and varying only between the data frames. Further, $s(n)$ is the transmitted signal with variance σ_s^2, and $\omega(n)$ is an additive circularly symmetric zero mean white (complex) Gaussian noise with variance σ_ω^2. Let

$$\mathbf{s}_{l,n} = \begin{bmatrix} s(n-l) & s(n-l-1) & \cdots & s(n-l-M+1) \end{bmatrix}^T \qquad (3.1.2)$$

and $\mathbf{S}_{l,n} = \mathrm{diag}(\mathbf{s}_{l,n})$, where M is the frame length, and $(\cdot)^T$ denotes the matrix transpose. Further, let the vector of dimension $M \times 1$

$$\mathbf{e}_{l,n} = \begin{bmatrix} e^{j2\pi f_l n} & \cdots & e^{j2\pi f_l(n-M+1)} \end{bmatrix}^T \qquad (3.1.3)$$

model the effect of frequency offset on the signal vector of length M associated with the lth path. Define an $M \times L$ matrix

$$\mathbf{Q}_n \triangleq \begin{bmatrix} \mathbf{s}_{0,n} \odot \mathbf{e}_{0,n} & \cdots & \mathbf{s}_{L-1,n} \odot \mathbf{e}_{L-1,n} \end{bmatrix} \qquad (3.1.4)$$

where $\odot$ denotes the Schur-Hadamard product. For example,

$$
\begin{aligned}
\mathbf{s}_{0,n} \odot \mathbf{e}_{0,n} &= \begin{bmatrix} s(n) \\ s(n-1) \\ \vdots \\ s(n-M+1) \end{bmatrix} \odot \begin{bmatrix} e^{j2\pi f_0(n)} \\ e^{j2\pi f_0(n-1)} \\ \vdots \\ e^{j2\pi f_0(n-M+1)} \end{bmatrix} \\
&= \begin{bmatrix} s(n)e^{j2\pi f_0(n)} \\ s(n-1)e^{j2\pi f_0(n-1)} \\ \vdots \\ s(n-M+1)e^{j2\pi f_0(n-M+1)} \end{bmatrix} \qquad (3.1.5)
\end{aligned}
$$

Hence, the frame constructed from M consecutive received samples can be expressed as [18, 63]

$$
\begin{aligned}
\mathbf{u}_n &\stackrel{\triangle}{=} \left[\begin{array}{cccc} u(n) & u(n-1) & \ldots & u(n-M+1) \end{array} \right]^T \\
&= \sum_{l=0}^{L-1} h_l \mathbf{S}_{l,n} \mathbf{e}_{l,n} + \boldsymbol{\omega}_n \\
&= \mathbf{Q}_n \mathbf{h}_L + \boldsymbol{\omega}_n
\end{aligned}
\tag{3.1.6}
$$

where

$$
\mathbf{h}_L = \left[\begin{array}{cccc} h_0 & h_1 & \ldots & h_{L-1} \end{array} \right]^T
$$

and

$$
\boldsymbol{\omega}_n = \left[\begin{array}{cccc} \omega(n) & \omega(n-1) & \ldots & \omega(n-M+1) \end{array} \right]^T .
$$

Here, the problem of interest is that given $\mathbf{u}_n$ and the training symbols $\{s(n)\}$, estimate the unknown parameter vector

$$
\begin{aligned}
\boldsymbol{\theta} &= \left[\begin{array}{cccccccc} h_0 & h_1 & \ldots & h_{L-1} & f_0 & f_1 & \ldots & f_{L-1} \end{array} \right]^T \\
&\stackrel{\triangle}{=} \left[\begin{array}{cc} \mathbf{h}_L^T & \mathbf{f}_L^T \end{array} \right]^T
\end{aligned}
\tag{3.1.7}
$$

where $\mathbf{f}_L = [f_0 \ \ldots \ f_{L-1}]^T$. In the next section, to estimate the unknown channel gains and FOs a computationally efficient approach is presented.

3.2   Estimation of multipath gains and frequency offsets

In this section, an approximative maximum likelihood (AML) estimator of the complex channel gains and the FOs is outlined. Consider that the received signal, as expressed in (3.1.6), is only a function of the complex channel gains and FOs. The likelihood function of the received sample vector to be maximized can be written as

$$
p(\mathbf{u}_n; \boldsymbol{\theta}) = \frac{1}{\sqrt{\pi \sigma_\omega^2}} e^{\frac{-(\mathbf{u}_n - \mathbf{Q}_n \mathbf{h}_L)^H (\mathbf{u}_n - \mathbf{Q}_n \mathbf{h}_L)}{\sigma_\omega^2}}
\tag{3.2.1}
$$

The probability of an event occurring can be between 0 and 1, and $\ln(p)$ is a monotonically increasing function for $p \ \epsilon \ (0 \ 1]$. Therefore, using the log-likelihood function will not alter the maximization problem. The log-likelihood function can be expressed as (ignoring the constant terms)

$$\ln p(\mathbf{u}_n; \boldsymbol{\theta}) \approx -\frac{1}{\sigma_\omega^2} (\mathbf{u}_n - \mathbf{Q}_n \mathbf{h}_L)^H (\mathbf{u}_n - \mathbf{Q}_n \mathbf{h}_L). \tag{3.2.2}$$

Maximization of (3.2.2) with respect to $\mathbf{h}_L$ yields [18]

$$\hat{\mathbf{h}}_L = \left(\mathbf{Q}_n^H \mathbf{Q}_n\right)^{-1} \mathbf{Q}_n^H \mathbf{u}_n \triangleq \mathbf{Q}_n^\dagger \mathbf{u}_n \tag{3.2.3}$$

where $\mathbf{Q}_n^\dagger$ denotes the Moore-Penrose pseudo-inverse. Substituting equation (3.2.3) into (3.2.2), the FOs can be estimated by minimizing the cost function, $J(\mathbf{f}_L)$ [18]

$$J(\mathbf{f}_L) = \mathbf{u}_n^H \mathbf{u}_n - \mathbf{u}_n^H \boldsymbol{\Pi}_{\mathbf{Q}_n} \mathbf{u}_n, \tag{3.2.4}$$

where $\boldsymbol{\Pi}_{\mathbf{Q}_n} = \mathbf{Q}_n \mathbf{Q}_n^\dagger$ is the projection onto the range space of $\mathbf{Q}_n$. The training sequence, $s(n)$ is chosen as $E \left\{ s^*(n - k)s(n - p) \right\} = \delta_{p-k}$, where δ_q denotes the Kronecker delta function, the n-dimensional minimization problem in (3.2.4) can be decoupled into n one-dimensional problems, hence the complexity of the minimization can be significantly reduced. Here $\mathbf{Q}_n^H \mathbf{Q}_n$ will be dominated by the large diagonal terms, with almost negligible contribution from the off-diagonal terms, if $s(n)$ is chosen as a pseudo-random sequence (as in the case of a training signal). Therefore, $\mathbf{Q}_n^H \mathbf{Q}_n \approx \sum_{n=0}^{N-1} |s(n)|^2 \mathbf{I} \triangleq q\mathbf{I}$, where q is constant over the frame considered, enabling the minimization of (3.2.4) to be approximated as the maximum of [18]

$$J'(\mathbf{f}_L) \;=\; \mathbf{u}^H \mathbf{Q}_n \mathbf{Q}_n^H \mathbf{u}_n$$

$$= \sum_{p=0}^{L-1} \left| \sum_{n=0}^{M-1} u^*(n) s(n-p) e^{j2\pi f_p n} \right|^2 \tag{3.2.5}$$

maximising the cost function in (3.2.5) with respect to $\mathbf{f}_L$, the approximate maximum likelihood (AML) estimator of each individual FO is written as [18]

$$\hat{f}_x \;=\; \arg\max_{f} \left| \sum_{n=0}^{M-1} u^*(n) s(n-x) e^{j2\pi f n} \right|^2 \tag{3.2.6}$$

The approximation is due to the assumption $\mathbf{Q}_n^H \mathbf{Q}_n$ is an identical matrix, hence multidimensional search is reduced to single dimension search for frequency offsets. The equation in (3.2.6) can be efficiently evaluated using the fast Fourier transform (FFT). Once the FOs are estimated, the channel gains, $\mathbf{h}_l$, can be estimated using (3.2.3).

3.3   MMSE equalizer design

As discussed earlier, identical FOs from each multipath can be compensated easily before equalization by rotating channel outputs by appropriate phase angles. However distinct FOs are difficult to compensate. Distinct FOs produce time selectivity in the channel that could severely degrade the BER performance. Therefore, the estimation of FO and its exploitation in equalization is crucial to enable accurate decoding of the transmitted information.

3.3.1   Equalizer for channels without frequency offsets

In this section, initially the MMSE equalizer for communication channels not affected by FOs is considered. For an equalizer of length M, the received signal vector is given by

$$\mathbf{u}_n = \mathbf{H}\mathbf{s}_n + \boldsymbol{\omega}_n \tag{3.3.1}$$

where

$$\mathbf{u}_n = \left[\begin{array}{ccc} u(n) & \ldots & u(n-M+1) \end{array}\right]^T$$

$$\mathbf{s}_n = \left[\begin{array}{ccc} s(n) & \ldots & s(n-M-L+2) \end{array}\right]^T$$

$$\boldsymbol{\omega}_n = \left[\begin{array}{ccc} \omega(n) & \ldots & \omega(n-M+1) \end{array}\right]^T$$

and $\mathbf{H}$ is the $M \times (L + M - 1)$ channel convolution matrix,

$$\boldsymbol{H} = \begin{bmatrix} h_0 & h_1 & \ldots & h_{L-1} & 0 & \ldots & 0 \\ 0 & h_0 & \ldots & h_{L-2} & h_{L-1} & \ddots & \vdots \\ \vdots & 0 & \ddots & \vdots & \ddots & \ldots & 0 \\ 0 & \ldots & 0 & h_0 & h_1 & \ldots & h_{L-1} \end{bmatrix} \tag{3.3.2}$$

By minimizing the cost function

$$J(\mathbf{w}) = E\{| s(n-v) - \mathbf{w}^H \mathbf{u}_n |^2\}$$

the MMSE equalizer aimed to retrieve the transmitted signal with delay v, i.e., s(n-d) is obtained as [17, 18],

$$\mathbf{w} = \left(\mathbf{H}\mathbf{H}^H + \frac{\sigma_\omega^2}{\sigma_s^2}\mathbf{I}\right)^{-1}\mathbf{H}\mathbf{c}_d \tag{3.3.3}$$

where $\mathbf{I}$ is the identity matrix and $\mathbf{c}_d$ is a coordinate vector, only containing a non-zero component at the dth position, i.e.,

$$\mathbf{c}_d = \left[\begin{array}{ccccccc} 0 & \ldots & 0 & 1 & 0 & \ldots & 0 \end{array}\right]^T$$

3.3.2 Equalizer for channels with frequency offsets

In the presence of frequency offsets, the effective channel convolution matrix $\mathbf{H}$ will vary over time. For an equalizer of length M, the received signal vector of dimension $M \times 1$ is given as [18]

$$\mathbf{u}_n = (\mathbf{H} \odot \boldsymbol{\eta}_L) \, \mathbf{s}_n + \boldsymbol{\omega}_n \triangleq \mathbf{H}_c \mathbf{s}_n + \boldsymbol{\omega}_n \qquad (3.3.4)$$

where $\boldsymbol{\omega}_n$ is the additive white Gaussian noise vector, $\mathbf{H}$ is the $M \times (L + M - 1)$ channel convolution matrix,

$$H = \begin{bmatrix} h_0 & h_1 & \ldots & h_{L-1} & 0 & \ldots & 0 \\ 0 & h_0 & \ldots & h_{L-2} & h_{L-1} & \ddots & \vdots \\ \vdots & 0 & \ddots & \vdots & \ddots & \ldots & 0 \\ 0 & \ldots & 0 & h_0 & h_1 & \ldots & h_{L-1} \end{bmatrix} \qquad (3.3.5)$$

and the matrix $\boldsymbol{\eta}_L$ accounts for the frequency offsets,

$$\boldsymbol{\eta}_L = \begin{bmatrix} \boldsymbol{\iota}_n^T & 0 & \ldots & 0 \\ 0 & \boldsymbol{\iota}_{n-1}^T & 0 & \vdots \\ \vdots & 0 & \ddots & 0 \\ 0 & \ldots & 0 & \boldsymbol{\iota}_{n-M+1}^T \end{bmatrix}, \qquad (3.3.6)$$

$$\boldsymbol{\iota}_n = \begin{bmatrix} e^{j2\pi f_0 n} & \ldots & e^{j2\pi f_{L-1} n} \end{bmatrix}^T. \qquad (3.3.7)$$

Set the equalizer length the same as the channel length, i.e., $M = L$. (Note: The equalizer length is set same as the channel length only for the iterative MMSE equalizer. However, when the signal is equalized at the first time, a conventional MMSE equalizer is used whose length is set much large than the channel length). For this case (i.e. m = L), the matrix $\boldsymbol{H}_c$ in (3.3.4) will appear as

$$H_c = \begin{bmatrix} h_0 e^{j2\pi f_0(n)} & h_1 e^{j2\pi f_1(n)} & \ldots & h_{L-1} e^{j2\pi f_{L-1}(n)} & 0 & \ldots & 0 \\ 0 & h_0 e^{j2\pi f_0(n-1)} & \ldots & h_{L-2} e^{j2\pi f_{L-2}(n-1)} & h_{L-1} e^{j2\pi f_{L-1}(n-1)} & \ddots & \vdots \\ \vdots & 0 & \ddots & \vdots & \ddots & \ldots & 0 \\ 0 & \ldots & 0 & h_0 e^{j2\pi f_0(n-L+1)} & h_1 e^{j2\pi f_1(n-L+1)} & \ldots & h_{L-1} e^{j2\pi f_{L-1}(n-L+1)} \end{bmatrix}$$

$$(3.3.8)$$

Also decompose (3.3.4) to explicitly show the symbol with delay $L - 1$ as

$$\mathbf{u}_n = \mathbf{H}_c \tilde{\mathbf{s}}_n + \mathbf{H}_c \mathbf{c}_L s(n - L + 1) + \boldsymbol{\omega}_n \qquad (3.3.9)$$

where operator $\mathbf{c}_L$ is a coordinate vector such that $\mathbf{H}_c \mathbf{c}_L$ will choose the Lth column of $\mathbf{H}_c$, and the vector $\tilde{\mathbf{s}}_n$ includes all the elements of $\mathbf{s}_n$ except $s(n - L + 1)$, i.e.,

$$\tilde{\mathbf{s}}_n = [s(n) \ \ldots \ s(n - L + 2) \ \ 0 \ \ s(n - L) \ \ldots \ s(n - 2L + 2)]^T \qquad (3.3.10)$$

Note

$$\mathbf{H}_c \mathbf{c}_L = \begin{bmatrix} h_{L-1} \\ h_{L-2} \\ \vdots \\ h_0 \end{bmatrix} \odot \begin{bmatrix} e^{j2\pi f_{L-1}(n)} \\ e^{j2\pi f_{L-2}(n-1)} \\ \vdots \\ e^{j2\pi f_0(n-L+1)} \end{bmatrix} \qquad (3.3.11)$$

Therefore, the FOs can be removed by

$$\begin{aligned} \tilde{\mathbf{u}}_n &= (\mathbf{u}_n - \mathbf{H}_c \tilde{\mathbf{s}}_n) \odot \begin{bmatrix} e^{-j2\pi f_{L-1}(n)} \\ e^{-j2\pi f_{L-2}(n-1)} \\ \vdots \\ e^{-j2\pi f_0(n-L+1)} \end{bmatrix} \\ &= \mathbf{D}(\mathbf{H}_c \mathbf{s}_n + \boldsymbol{\omega}_n - \mathbf{H}_c \tilde{\mathbf{s}}_n) \\ &= \mathbf{D}\left(\mathbf{H}_c(\mathbf{s}_n - \tilde{\mathbf{s}}_n) + \boldsymbol{\omega}_n\right) \qquad (3.3.12) \end{aligned}$$

where $\mathbf{D} = \text{diag}(\boldsymbol{\beta})$, $\boldsymbol{\beta} = [e^{-j2\pi f_{L-1}(n)} \quad e^{-j2\pi f_{L-2}(n-1)} \quad \ldots \quad e^{-j2\pi f_0(n-L+1)}]^T$ and $\bar{\mathbf{s}}_n$ is the mean of $\tilde{\mathbf{s}}_n$ obtained from the extrinsic information passed by the Bahl, Cocke, Jelinek, and Raviv (BCJR) based MAP decoder in Fig. 3.2. The estimate of the transmitted symbol with delay $L - 1$ is obtained using an iterative MMSE equalizer as $\hat{s}(n - L + 1) = \mathbf{w}_n^H \tilde{\mathbf{u}}_n$. Minimization of the mean square error with respect to $\mathbf{w}_n^*$ yields,

$$E\{\tilde{\mathbf{u}}_n \tilde{\mathbf{u}}_n^H\} \mathbf{w}_n - 2E\{s(n - L + 1)\tilde{\mathbf{u}}_n\} = 0 \qquad (3.3.13)$$

Assuming transmitted symbols are temporally uncorrelated, $E\{(\mathbf{s}_n - \bar{\mathbf{s}}_n)(\mathbf{s}_n - \bar{\mathbf{s}}_n)^H\}$ can be written as a diagonal matrix $diag(\mathbf{v}_n)$, where $\mathbf{v}_n$ is constructed from the variance of the symbols as in (3.4.6). Note the Lth element of $\mathbf{v}_n$ is equal to $E\{| s(n) |^2\} = \sigma_s^2$ because the Lth element of $\bar{\mathbf{s}}_n$ is zero. Hence

$$E\{\tilde{\mathbf{u}}_n \tilde{\mathbf{u}}_n^H\} = \mathbf{D}(\mathbf{H}_c \text{diag}(\mathbf{v}_n)\mathbf{H}_c^H + \sigma_\omega^2 \mathbf{I})\mathbf{D}^H \qquad (3.3.14)$$

and

$$E\{s(n - L + 1)\tilde{\mathbf{u}}_n\} = E\{s(n - L + 1)\mathbf{D}\left(\mathbf{H}_c(\mathbf{s}_n - \bar{\mathbf{s}}_n) + \boldsymbol{\omega}_n\right)\} = \mathbf{D}\mathbf{H}_c \mathbf{c}_L$$
$$(3.3.15)$$

where $E\{s(n - L + 1)\bar{\mathbf{s}}_n\}$ is $\mathbf{0}$ because $\bar{\mathbf{s}}_n$ does not contain $s(n - L + 1)$ and all other symbols in $\bar{\mathbf{s}}_n$ are uncorrelated with $s(n - L + 1)$. Hence the MMSE equalizer is written as,

$$\mathbf{w}_n = \left(\mathbf{D}(\mathbf{H}_c \text{diag}(\mathbf{v}_n)\mathbf{H}_c^H + \sigma_\omega^2 \mathbf{I})\mathbf{D}^H\right)^{-1} \mathbf{D}\mathbf{H}_c \mathbf{c}_L \qquad (3.3.16)$$
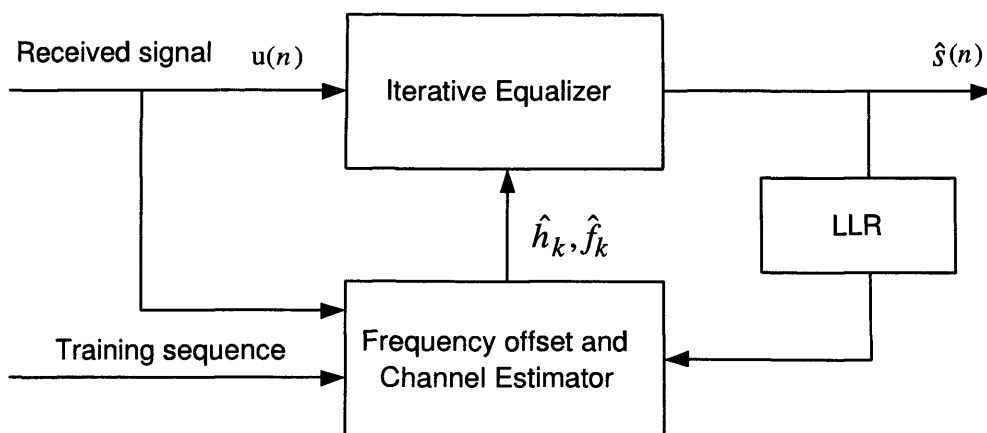
The MMSE equalizer in (3.3.16) requires knowledge of the channel parameter matrix $\mathbf{H}_c$ and the frequency offsets $\mathbf{f}_L$ (in $\mathbf{D}$).

Figure 3.1. The block diagram describing iterative channel estimation and equalization at the receiver.

3.4 Iterative channel estimation

Short pilot symbols are inadequate to estimate the frequency offsets due to the limitation on the resolution associated with DFT. Therefore an iterative channel and frequency offset estimation technique where soft estimates of the transmitted signal can use as a pilot signal to improve the estimation performance is proposed.

3.4.1 Iterative channel estimation

The initial channel estimate is obtained from a training sequence contained in the middle of a burst. This estimate is used to design the MMSE equalizer and to obtain an initial estimate of the transmitted data. The soft decision based estimate of the transmitted data is then treated as a pilot signal to obtain a refined estimate of the channel as shown in Fig 3.1. The a priori and a posteriori LLRs of s(n) are defined as [50,55]

$$L[s(n)] = \ln \frac{p\{s(n) = 1\}}{p\{s(n) = -1\}}$$

and

$$L[s(n)|_{\hat{s}(n)}] = \ln \frac{p\{s(n) = 1|_{\hat{s}(n)}\}}{p\{s(n) = -1|_{\hat{s}(n)}\}}.$$

The MMSE equalizer output $\hat{s}(n)$ is used to obtain the difference between the posteriori and a priori log-likelihood ratio (LLR), also called the extrinsic information as

$$\begin{aligned}
\triangle L[\hat{s}(n)] &= L[s(n)|_{\hat{s}(n)}] - L[s(n)] \\
&= \ln \frac{p\{s(n) = 1|_{\hat{s}(n)}\}}{p\{s(n) = -1|_{\hat{s}(n)\}}} - \ln \frac{p\{s(n) = 1\}}{p\{s(n) = -1\}}.
\end{aligned} \tag{3.4.1}$$

Using Bayes' theorem, $p(a|b) = \frac{p(b|a)p(a)}{p(b)}$, (3.4.1) can be written as

$$\begin{aligned}
\triangle L[\hat{s}(n)] &= \ln \frac{p\{\hat{s}(n)|_{s(n)=1}\}p\{s(n) = 1\}}{p\{\hat{s}(n)|_{s(n)=-1}\}p\{s(n) = -1\}} - \ln \frac{p\{s(n) = 1\}}{p\{s(n) = -1\}} \\
&= \ln \frac{p\{\hat{s}(n)|_{s(n)=1}\}}{p\{\hat{s}(n)|_{s(n)=-1}\}} \\
&= L[\hat{s}(n)|_{s(n)}],
\end{aligned}$$

To find $L[\hat{s}(n)|_{s(n)}]$, it is assumed that the probability density function (PDF) of $\hat{s}(n)$ is Gaussian with variance σ_s^2, i.e.

$$p\{\hat{s}(n)\} = \frac{1}{\sqrt{\pi \sigma_s^2}} \exp \left(-\frac{(\hat{s}(n) - E\{\hat{s}(n)\})(\hat{s}(n) - E\{\hat{s}(n)\})^*}{\sigma_s^2} \right).$$

Therefore, the conditional PDF of $\hat{s}(n)$ becomes

$$p\{\hat{s}(n)|_{s(n)=b}\} = \frac{1}{\sqrt{\pi \sigma_s^2|_{s(n)=b}}} \exp \left(-\frac{(\hat{s}(n) - m_b)(\hat{s}(n) - m_b)^*}{\sigma_s^2|_{s(n)=b}} \right),$$

where m_b and $\sigma_s^2|_{s(n)=b}$ are respectively the conditional mean and variance of $\hat{s}(n)$. Here, a binary phase shift keying (BPSK) system is considered for

which $b = \{+1, -1\}$, therefore, for the above PDF, the conditional mean and the variance are obtained from the knowledge of the channel and the equalizer as follows [61]

$$
\begin{aligned}
m_b &= E[\hat{s}(n)|_{s(n)=b}] \\
&= E[\mathbf{w}_n^H \mathbf{D} \left(\mathbf{H}_c(\mathbf{s}_n - \bar{\mathbf{s}}_n) + \boldsymbol{\omega}_n\right)] \\
&= \mathbf{w}_n^H \mathbf{D} \mathbf{H}_c \mathbf{c}_L b
\end{aligned}
\tag{3.4.2}
$$

$$
\begin{aligned}
\sigma^2_{s|s(n)=b} &= \mathrm{Cov}\{\hat{s}(n), \hat{s}(n)|_{s(n)=b}\} \\
&= E\{(\hat{s}(n) - m_b)(\hat{s}(n) - m_b)^*\} \\
&= E\{\hat{s}(n)\hat{s}(n)^*\} - m_b m_b^* \\
&= \mathbf{w}_n^H \mathbf{D} \mathbf{H}_c \mathbf{c}_L (1 - \mathbf{w}_n^H \mathbf{H}_c \mathbf{c}_L)
\end{aligned}
\tag{3.4.3}
$$

Therefore, the required extrinsic information $L[\hat{s}(n)|_{s(n)}]$ can be expressed as

$$
\begin{aligned}
L[\hat{s}(n)|_{s(n)}] &= -\frac{(\hat{s}(n) - m_{(+1)})(\hat{s}(n) - m_{(+1)})^*}{\sigma_s^2} + \frac{(\hat{s}(n) - m_{(-1)})(\hat{s}(n) - m_{(-1)})^*}{\sigma_s^2} \\
&= \frac{4\mathrm{Re}\{\hat{s}(n)m_{(+1)}\}}{\sigma_s^2} \\
&= 4\frac{Re\{\hat{s}(n)\}}{1 - \mathbf{w}_n^H \mathbf{H}_c \mathbf{c}_L}
\end{aligned}
\tag{3.4.4}
$$

The mean of the symbol (soft estimate) $\bar{s}_n$ to be used in (3.3.12) is obtained as [55]

$$
\begin{aligned}
\bar{s}_n &= p\{s(n) = +1|_{\hat{s}(n)}\} - p\{s(n) = -1|_{\hat{s}(n)}\} \\
&= \tanh\left(\frac{L[s(n)|_{\hat{s}(n)}]}{2}\right)
\end{aligned}
\tag{3.4.5}
$$

Then the soft estimates of the transmitted signal are treated as a pilot signal to determine the multiple frequency offsets and to refine the channel estimates in an iterative fashion. The iterative scheme has the ability to resolve multipaths, i.e. each element of $(\mathbf{u}_n - \mathbf{H}_c\bar{\mathbf{s}}_n)$ forms the contribution

of a particular multipath and the corresponding frequency offset. Hence, the frequency offsets by collecting the gleaned samples from $(\mathbf{u}_n - \mathbf{H}_c \bar{\mathbf{s}}_n)$ for all n can be estimated . For example the sequence obtained by collecting the first element of $(\mathbf{u}_n - \mathbf{H}_c \bar{\mathbf{s}}_n)$ will be used to estimate the frequency offset f_{L-1} while the sequence obtained using the Lth terms of $(\mathbf{u}_n - \mathbf{H}_c \bar{\mathbf{s}}_n)$ will be used to obtain the estimate of f_0. Finally, the variance required for the MMSE equalizer in (3.3.16) is computed as [55],

$$\mathbf{v}_n = 1 - |\bar{s}_n|^2 \tag{3.4.6}$$

where $\bar{s}_n$ denotes the soft estimates of the transmitted symbol from the equalizer output.

3.4.2   Iterative channel estimation with MAP decoder

Soft-output equalizers that exploit a priori information on the channel inputs are fed to a soft-input channel decoder, and the soft decoder outputs are used by the equalizer as a priori information to form more reliable estimates of the FO and channel gain in the subsequent iterations [46] as shown in Fig 3.2. Here a packet radio transmission based on four bursts is considered. The data $\mathbf{s}_d(n)$ in the packet are encoded and interleaved to form four bursts. A pilot sequence of length 26 is inserted to each burst and transmitted through a frequency selective channel. At the receiver, the channel corresponding to each burst is estimated and equalized separately, but the data symbols from all four bursts are collected, deinterleaved and decoded. The initial channel estimate is obtained using the pilot sequence contained in the middle of each burst. This estimate is used to design an MMSE equalizer and to obtain an initial estimate of the transmitted data. In the subsequent iterations, the received signal vector $\mathbf{u}_n$ in (3.3.4) is passed to the iterative MMSE equalizer in (3.3.16) together with prior
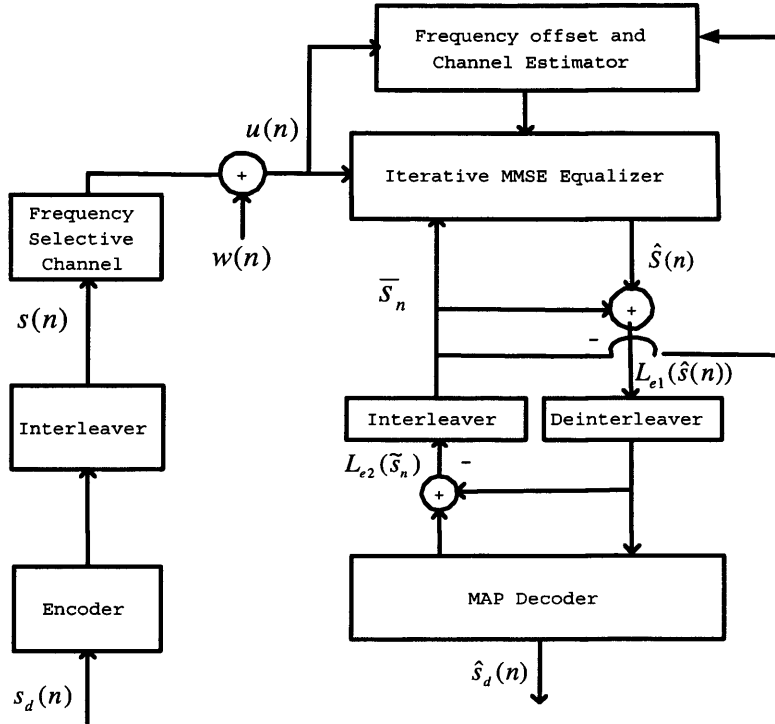
Figure 3.2. The block diagram describing the transmitter as well as the iterative channel estimation, equalization and decoding at the receiver.

information from the decoder so that the contribution of all other symbols except the symbol of interest can be removed from the received signal as in (3.3.12). The LLR of four consecutive bursts from the MMSE equalizer output as shown in (3.4.4) are collected, de-interleaved and decoded using the MAP algorithm [64]. The MAP decoder would then provide the extrinsic information $L_{e2}(\tilde{s}_n)$ of the uncoded symbols. The mean of the symbol (soft estimate) $\bar{s}_n$ to be used in (3.3.12) is then found from this extrinsic information as $\bar{s}_n = \tanh(L_{e2}(\tilde{s}_n))$ [55]. The soft estimates of the transmitted signal are also treated as a pilot signal to determine the multiple frequency offsets and to refine the channel estimates in an

iterative fashion. With reliable estimates of the transmitted symbols from the decoder, the vector $(\mathbf{u}_n - \mathbf{H}_c\bar{\mathbf{s}}_n)$ in (3.3.12) can be approximated to

$$s(n - L + 1) \begin{bmatrix} h_{L-1} \\ h_{L-2} \\ \vdots \\ h_0 \end{bmatrix} \odot \begin{bmatrix} e^{j2\pi f_{L-1}(n)} \\ e^{j2\pi f_{L-2}(n-1)} \\ \vdots \\ e^{j2\pi f_0(n-L+1)} \end{bmatrix}$$

apart from the effect of noise. Hence the iterative scheme has the ability to resolve multipaths, bringing the multiple frequency offset problem into estimation of distinct harmonics. Here the variance required for the MMSE equalizer in (3.3.16) can be computed by using the soft estimates of the transmitted symbol from the decoder output $\bar{s}_n$ in (3.4.6).

3.5 Simulations

To evaluate the performance of the proposed iterative frequency offsets and channel estimator, a normal burst structure as in GSM with 116 data symbols and 26 pilot symbols in the middle [16] is considered. Conventionally the 26 training symbols drawn from binary alphabets are used for time synchronization and channel estimation. In order to assess the performance of the proposed AML estimator, a randomly chosen fixed channel with three paths $[h_0 = -0.3380 - 0.7207i, h_1 = -0.3981 + 0.3426i, h_2 = 0.0492 - 0.2968i]$, and fixed frequency offsets $[f_0 = 0.001, f_1 = 0.002, f_2 = 0.003]$ is considered. The channel is first estimated using the pilot signal of length 26 symbols, and the transmitted signal is retrieved using an MMSE equalizer of length $M = 8$ taps. The soft estimates of the transmitted signal are then used to resolve multipaths, determine the multiple frequency offsets and to refine the channel estimates in an iterative fashion. In each iteration, the soft estimate of the transmitted signal is obtained
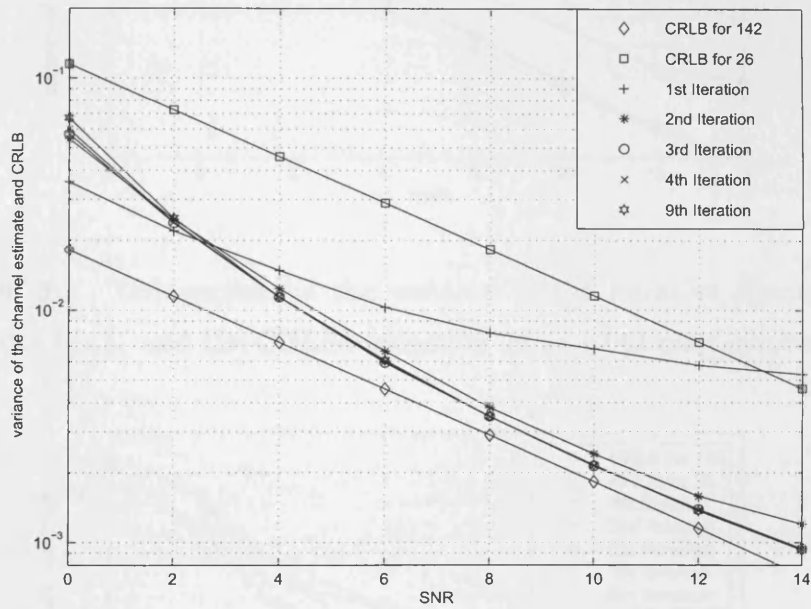
Figure 3.3. Comparison of the variance of the iterative channel gain estimates for h_0 and the CRLBs assuming 26 and 142 pilot symbols.
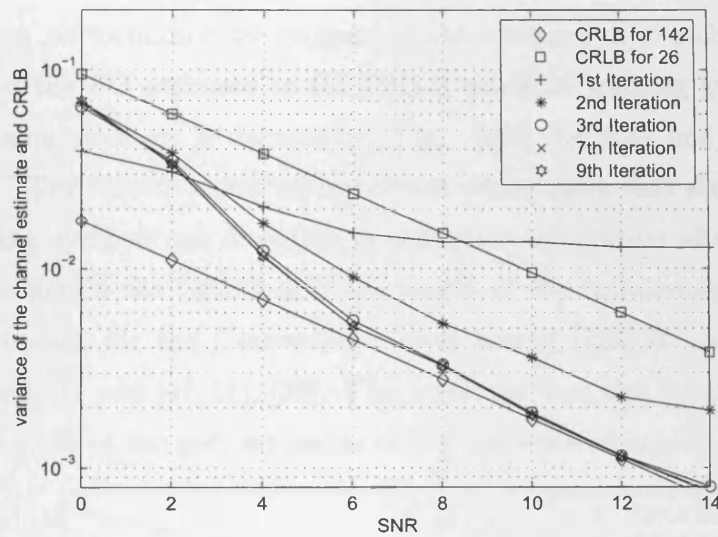
Figure 3.4. Comparison of the variance of the iterative channel gain estimates for h_1 and the CRLBs assuming 26 and 142 pilot symbols.

Figure 3.5. Comparison of the variance of the iterative channel gain estimates for h_2 and the CRLBs assuming 26 and 142 pilot symbols.

using the iterative MMSE equalizer of length three as in (3.3.16). The
estimation performance by comparing the variance of the channel esti-
mate and the FO estimate to the CRLB using 26 training symbols and
142 training symbols is depicted in Fig. {3.3, 3.4 3.5} and Fig. {3.6,
3.7, 3.8}. The results reveal an important observation that although only
26 training symbols are available in the burst, estimators after adequate
iterations attain the CRLB as if the length of the training signal is 142.
The derivation for the Cramér-Rao lower bound (CRLB) can be found
in Appendix 1 and [17, 18], [30]. This confirms that the iterative scheme
makes full use of the soft estimates of the transmitted signal.

Figure 3.6. Comparison of the variance of the iterative frequency offset
estimates for f_0 and the CRLBs assuming 26 and 142 pilot symbols.

In order to evaluate the BER performance, a two path wireless commu-
nication channel and an initial equalizer of length 8 is considered. A ran-
domly chosen fixed channel with two paths $[h_0 = 0.7673 - 0.2365i, h_1 = -0.5208 - 0.2899i]$, and fixed frequency offsets $[f_0 = 0.001, f_1 = 0.005]$ are
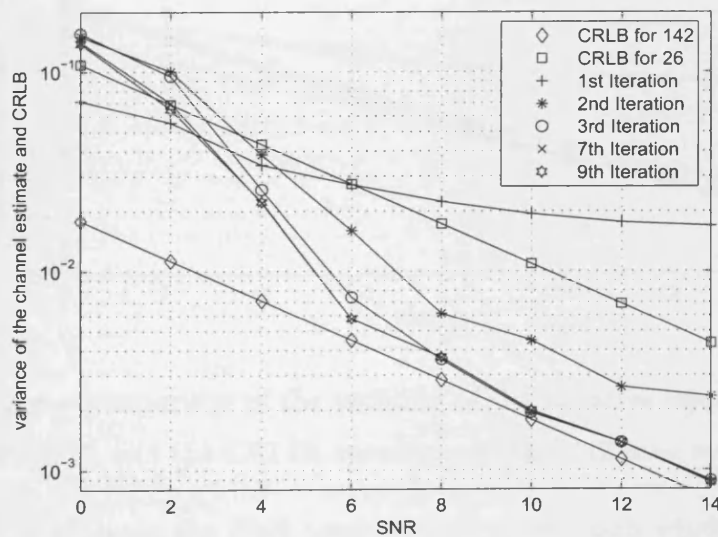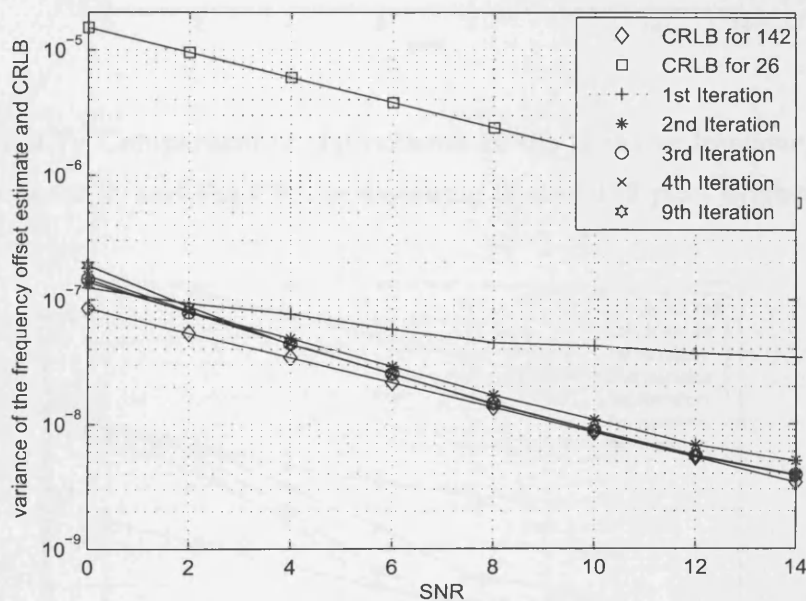
Figure 3.7. Comparison of the variance of the iterative frequency offset estimates for f_1 and the CRLBs assuming 26 and 142 pilot symbols.
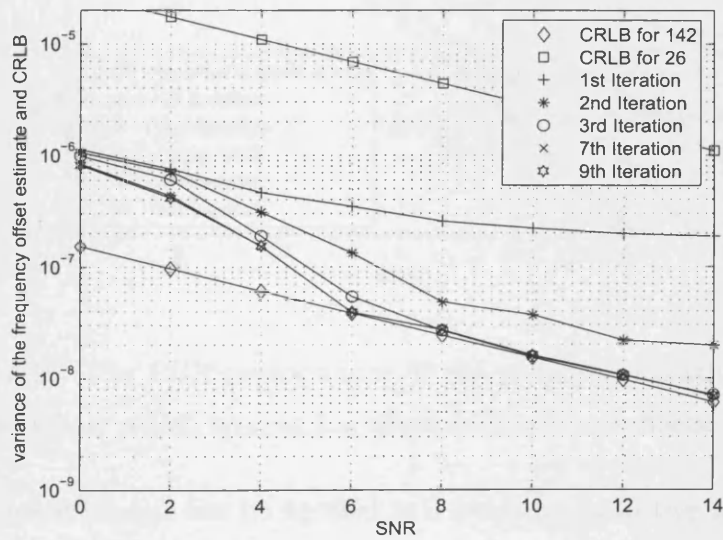
Figure 3.8. Comparison of the variance of the iterative frequency offset estimates for f_2 and the CRLBs assuming 26 and 142 pilot symbols.
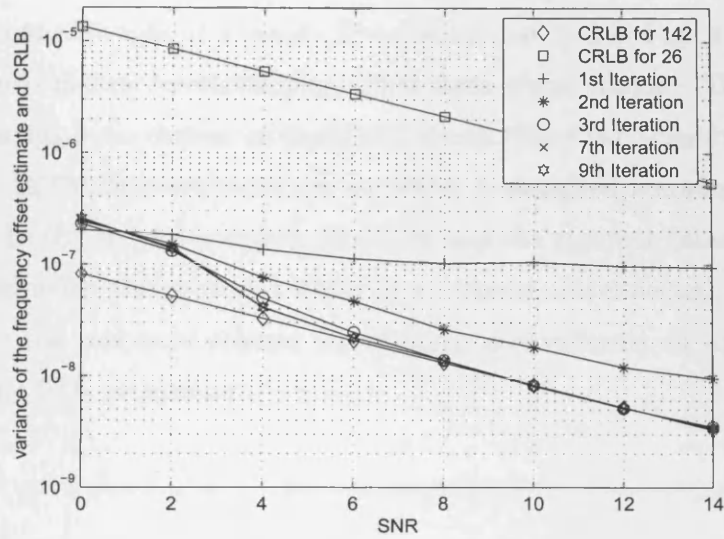
considered. The complex channel gains h_0 and h_1 have been assumed to be constant throughout a burst. The results depicted in Fig. 3.9 show the BER performance by simulating GSM data transmission. The training sequence has been chosen as explained above. Here two scenarios are considered. In the first scenario, an equalizer is designed ignoring the effect of FOs. In the second scenario, the FOs and the channel gains have been estimated using the proposed iterative approach. As expected, the performance of the proposed scheme significantly outperforms an equalizer not employing FOs estimation.
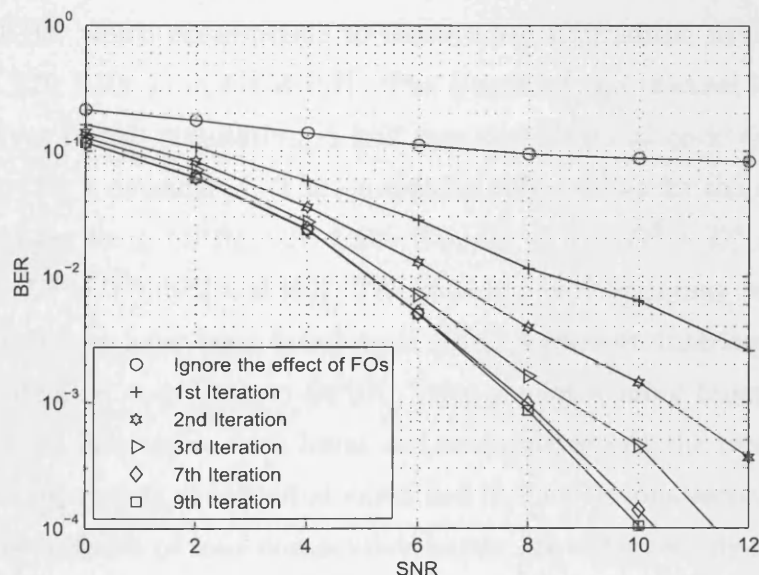
Figure 3.9. The BER performance of the proposed iterative equalizer and an equalizer which ignores the effect of frequency offsets.

The proposed scheme can be applied to a frequency selective fading channel as well. In this case, the channel is assumed to be quasi-stationarity, i.e. the channel is changing for every new burst but remains fixed within a burst. The channel and frequency offset could not be estimated perfectly

during a bad channel condition. However, the performance of the channel and FO estimator can be enhanced, by using the MMSE equalizer output as a priori information and passing them to a MAP decoder as explained in the previous sections. To illustrate this, a quasi-stationary channel with random frequency offsets is considered, so that the channel coefficients and FOs do not change within a burst, but would change between bursts according to a complex Gaussian distribution for the channel coefficients and uniform distribution (between 0 and 0.005) for frequency offsets. This is reasonable as the maximum DS for a vehicular speed of 250 km/h (RA250 channels as defined in GSM standards) at a carrier frequency of 900 MHz is 1.3 KHz, which corresponds to 0.005 when normalised to the symbol rate of 270 KHz as in GSM [57]. The length of the channel is assumed to be five. In this simulation, a half rate convolutional code and a MAP decoder [55] is considered. The generating polynomials for the coder have been chosen as in GPRS CS1-CS3, (i.e, $G0 = 1 + D^3 + D^4$ and $G1 = 1 + D + D^3 + D^4$), [65] and [66]. The data bits corresponding to four consecutive bursts have been interleaved using a random interleaver, coded and modulated according to BPSK. Then a pilot symbol burst of length 26 has been inserted in each burst and transmitted. At the receiver, each bursts is separately equalized as explained in the previous section, and the equalizer outputs of four consecutive bursts are collected, de-interleaved and decoded using MAP algorithm. The soft estimates of the uncoded bits are interleaved again and fedback to the iterative equalizers. The result depicted in Figure 3.10 shows the uncoded BER performance for five iterations. The result is also compared to the matched filter bound. For the matched filter bound, the BER of a five path channel assuming no FOs and perfect resolution of multipaths with ideal channel knowledge at the receiver is assumed. The result also depicts the BER curve of an equalizer that was designed ignoring the effect of FOs. The proposed scheme signif-

icantly outperforms the conventional equalizer and attains a performance
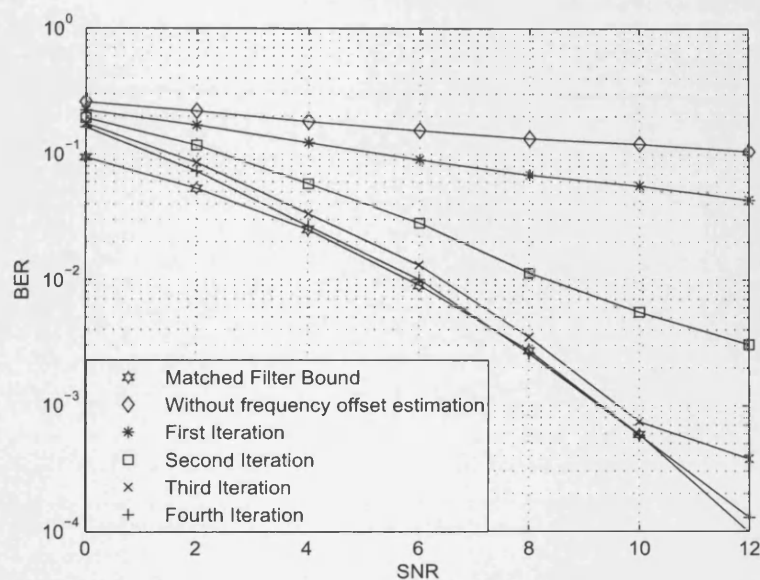closer to the matched filter bound.

Figure 3.10. The uncoded BER performance of the proposed iterative
equalizer and an equalizer which ignores the effect of frequency offsets. A
half rate convolution coding scheme has been used.

3.6 Summary

In this chapter, the estimation and equalization of a frequency selective
channel with distinct FOs have been considered. This problem could arise,
when the receiver or transmitter moves with very high speed with different
paths experiencing distinct DSs, due to different angles of arrival. Accord-
ing to the proposed method, multipath gains are initially estimated using
the available short pilot sequence, and then the soft estimates of the trans-
mitted signal are used to estimate the frequency offsets and to refine the
channel estimates iteratively. In addition to providing superior BER per-

formance, the proposed estimator is also efficient in that it attains the CRLB derived assuming all 142 symbols in the burst are known pilot symbols.

3.7   Appendix 1

The Cramér Rao lower bound (CRLB) for the estimates of MGs and FOs is derived [18]. Let

$$\bar{\mathbf{u}}(\boldsymbol{\theta}) = \left[\begin{array}{ccc} \bar{u}(n) & \ldots & \bar{u}(n - M + 1) \end{array} \right]^T \tag{3.7.1}$$

and

$$\boldsymbol{\theta} = \left[\begin{array}{ccc} \mathrm{Re}(\mathbf{h}_L)^T & \mathrm{Im}(\mathbf{h}_L)^T & \mathbf{f}_L^T \end{array} \right]^T \tag{3.7.2}$$

Under the assumption that $\omega(n)$ is complex white Gaussian with zero mean and variance σ_ω^2, the CRLB can be found using Slepian-Bangs formula [30],

$$\left[\mathbf{P}_{CRLB}^{-1}(\boldsymbol{\theta}) \right]_{l,p} = 2\sigma_\omega^{-2} \mathrm{Re} \left\{ \frac{\partial \bar{\mathbf{u}}^H(\boldsymbol{\theta})}{\partial \theta_l} \frac{\partial \bar{\mathbf{u}}(\boldsymbol{\theta})}{\partial \theta_p} \right\} \tag{3.7.3}$$

where $[\boldsymbol{P}]_{l,p}$ denotes the (l,p)th element of $\boldsymbol{P}$, and

$$\mathbf{P} \triangleq E \left\{ (\hat{\boldsymbol{\theta}} - \boldsymbol{\theta})(\hat{\boldsymbol{\theta}} - \boldsymbol{\theta})^H \right\} \geq \mathbf{P}_{CRLB} \tag{3.7.4}$$

Further note that

$$\frac{\partial \bar{u}(n)}{\partial h_l^r} = e^{j2\pi f_l n} \bar{u}(n - l)$$

$$\frac{\partial \bar{u}(n)}{\partial h_l^i} = j e^{j2\pi f_l n} \bar{u}(n - l)$$

$$\frac{\partial \bar{u}(n)}{\partial f_l} = j2\pi n h_l e^{j2\pi f_l n} \bar{u}(n - l) \tag{3.7.5}$$

where h_l^r and h_l^i are the lth element of $\mathrm{Re}(\mathbf{h}_L)$ and $\mathrm{Im}(\mathbf{h}_L)$.

Chapter 4

ITERATIVE PARAMETER

ESTIMATION AND

EQUALIZATION FOR MIMO

CHANNELS WITH MULTIPLE

FREQUENCY OFFSETS

The use of multiple input multiple output (MIMO) communication channels for enhancing system capacity and link reliability has become a major research topic within the last decade [67–69]. With multi-element antenna arrays at both the transmitter and the receiver, independent data streams could share the same frequency band and time slot to increase spectral efficiency enormously [68]. It has been shown that the theoretical capacity increases linearly with the number of antennas in rich scattering environments [69]. However, to realise its full potential, it is also very important to have efficient channel and frequency offset estimation techniques. Often, MIMO transmission schemes proposed in the literature are based on somewhat idealized assumptions. Most MIMO transmission schemes are designed for frequency-flat channels [70,71]. However, if there are multipath signals with large propagation delays, the assumption of a

62

frequency-flat channel may not be valid, depending on the symbol duration.

Besson [70] discussed the estimation of FOs for MIMO flat fading channels with distinct FOs between each transmitter and receiver. Sajid [63] and Qiang [72, 73] extended this work for MIMO frequency selective channels that allows distinct FOs for each multipath between each transmit and receive antenna. As discussed in chapter 3, the performance of such multiple antenna based systems may seriously degrade in the presence of FOs. Therefore, it is of importance to determine these FOs and to take them into account in the equalizer design. In this scenario, to estimate the FOs and MGs, an AML estimator is proposed that exploits the correlation property of the transmitted training sequence. However, in a TDMA system, for example GSM, the pilot symbols are generally inadequate to obtain an accurate estimate of the FOs due to limitation on the frequency resolution of the estimator. Therefore, in this chapter, an iterative estimation and detection technique for MIMO frequency selective channels with multiple frequency offsets is proposed. Accordingly, an initial channel estimate is obtained using a very short pilot (training) signal and the soft estimate of the transmitted signal is then treated as a pilot signal to determine multiple frequency offsets and to refine the channel estimates iteratively. Even though the proposed iterative scheme does not need to adhere to a specific standard, in order to evaluate the performance, a burst structure with pilot sequences of 26 symbols, and 116 data symbols for each user as in the global system for mobile communication (GSM) standards [16] is considered. In addition to the superior BER performance, the estimation performance through comparison of the variance of the estimates with the corresponding CRLBs is given.

4.1 Problem statement

Consider a MIMO communication system with N_t transmit and N_r receive antennas, where the signal is propagated through L different paths for each transmit-receive antenna pair, with each path possibly having different frequency offsets. The received baseband signal at antenna q is therefore written as

$$
\begin{aligned}
r_q(n) &= u_q(n) + \omega_q(n) \\
&= \sum_{t=1}^{N_t} \sum_{l=0}^{L-1} h_{qt}(l) e^{j2\pi f_{qtl} n} s_t(n-l) + \omega_q(n),
\end{aligned} \tag{4.1.1}
$$

where $q = 1, \dots, N_r$, and $h_{qt}(l)$ and f_{qtl} are the unknown complex channel gain and the frequency offset between the receive antenna q and the transmit antenna t, for the multipath tap l; each channel is assumed to be quasi-stationary and frequency selective, i.e., the channel impulse response and frequency offsets remain fixed during a burst interval but change between bursts. Here $\{s_t(n)\}$ is the signal transmitted from the tth antenna and $\omega_q(n)$ is additive, circularly symmetric zero mean (complex) Gaussian noise with variance σ_ω^2 and is assumed to be temporarily and spatially uncorrelated. Let

$$
\mathbf{s}_{tl} = \begin{bmatrix} s_t(n-l) & \dots & s_t(n-l-M+1) \end{bmatrix}^T \tag{4.1.2}
$$

and $\mathbf{S}_{tl} = \text{diag}(\mathbf{s}_{tl})$, where M is the frame length, and $(\cdot)^T$ denotes the matrix transpose.

$$
\mathbf{e}_{qt}(l) = \begin{bmatrix} e^{j2\pi f_{qtl} n} & \dots & e^{j2\pi f_{qtl}(n-M+1)} \end{bmatrix}^T \tag{4.1.3}
$$

is a vector containing the FO between the receive antenna q and the transmit antenna t for the lth path. Further, suppose that

$$\mathbf{Q}_{qt} = \begin{bmatrix} \mathbf{S}_{t0}\mathbf{e}_{qt}(0) & \cdots & \mathbf{S}_{t(L-1)}\mathbf{e}_{qt}(L-1) \end{bmatrix} \quad (M \times L)$$

$$\mathbf{Q}_q = \begin{bmatrix} \mathbf{Q}_{q1} & \mathbf{Q}_{q2} & \cdots & \mathbf{Q}_{qN_t} \end{bmatrix} \quad (M \times N_t L)$$

Hence, the frame constructed from M consecutive received samples can be expressed as [63]

$$\mathbf{u}_q \triangleq \begin{bmatrix} u_q(n) & \ldots & u_q(n - M + 1) \end{bmatrix}^T$$
$$= \mathbf{Q}_q\mathbf{h}_q + \boldsymbol{\omega}_q \tag{4.1.4}$$

where

$$\mathbf{h}_{qt} = \begin{bmatrix} \mathbf{h}_{qt}(0) & \cdots & \mathbf{h}_{qt}(L-1) \end{bmatrix}^T$$
$$\mathbf{h}_q = \begin{bmatrix} \mathbf{h}_{q1}^T & \mathbf{h}_{q2}^T & \cdots & \mathbf{h}_{qN_T}^T \end{bmatrix}^T$$

$$\boldsymbol{\omega}_{qt} = \begin{bmatrix} \boldsymbol{\omega}_{qt}(0) & \cdots & \boldsymbol{\omega}_{qt}(L-1) \end{bmatrix}^T$$
$$\boldsymbol{\omega}_q = \begin{bmatrix} \boldsymbol{\omega}_{q1}^T & \cdots & \boldsymbol{\omega}_{qN_T}^T \end{bmatrix}^T$$

Estimating various channel gains, $\mathbf{h}_{qt}(l)$ and frequency offsets $\mathbf{f}_{qtl}$, is the target. Let

$$\mathbf{f}_{qt} = \begin{bmatrix} f_{qt0} & f_{qt1} & \cdots & f_{qt(L-1)} \end{bmatrix}^T \tag{4.1.5}$$

$$\mathbf{f}_q = \begin{bmatrix} \mathbf{f}_{q1}^T & \mathbf{f}_{q2}^T & \cdots & \mathbf{f}_{qN_t}^T \end{bmatrix}^T \tag{4.1.6}$$

Then the unknown parameter vector, $\boldsymbol{\theta}_q$, corresponding to receive antenna q, can be written as $\boldsymbol{\theta}_q = \begin{bmatrix} \mathbf{h}_q^T & \mathbf{f}_q^T \end{bmatrix}^T$. In the next section, the problem of estimating $\boldsymbol{\theta}_q$ is considered.

4.2   Estimation of multipath gains and frequency offsets

In this section, an approximate maximum likelihood (AML) estimator is outlined, which fully exploits the structure of the transmitted training sequence. Since the noise, $\omega_q(n)$, at each receive antenna is spatially uncorrelated, the parameters associated with each receiver can be estimated independently from the received signal. Considering (4.1.4), the likelihood function of $\mathbf{u}_q$ can be written as [17]

$$p(\mathbf{u}_q;\ \boldsymbol{\theta}_q) = \frac{1}{(\pi\sigma_\omega^2)^{M/2}}\, e^{-\frac{(\mathbf{u}_q - \mathbf{Q}_q\mathbf{h}_q)^H(\mathbf{u}_q - \mathbf{Q}_q\mathbf{h}_q)}{\sigma_\omega^2}}, \qquad (4.2.1)$$

Taking the natural logarithm and ignoring the constant terms, as they will not affect the maximization of the likelihood function, (4.2.1) can be formulated as minimization of

$$\ln p(\mathbf{u}_q;\ \boldsymbol{\theta}_q) \approx \frac{1}{\sigma_{\omega_q}^2}\,(\mathbf{u}_q - \mathbf{Q}_q\mathbf{h}_q)^H\,(\mathbf{u}_q - \mathbf{Q}_q\mathbf{h}_q) \qquad (4.2.2)$$

This yields

$$\hat{\mathbf{h}}_q = (\mathbf{Q}_q^H\mathbf{Q}_q)^{-1}\mathbf{Q}_q^H\mathbf{u}_q, \qquad (4.2.3)$$

Substituting the optimal solution of (4.2.3) into (4.2.2) function, and minimizing with respect to $\mathbf{f}_q$, and considering a given path k, from the transmit antenna j to the receive antenna q, the approximative maximum likelihood (AML) estimator of the frequency offsets is obtained as follows [18],

$$\hat{f}_{qjk} = \arg\max_f \left| \sum_{n=0}^{M-1} u_q^*(n)s_j(n-k)e^{j2\pi fn} \right|^2 \qquad (4.2.4)$$

The optimization involved in (4.2.4) can be efficiently evaluated using the FFT. Once the FOs are estimated, the MGs, $\mathbf{h}_q$, can be estimated by inserting the estimated values of the FOs in (4.2.3).

4.3   MIMO MMSE equalizer design

For an equalizer of length M, the received signal vector of dimension $N_r M \times 1$ is given as [63]

$$\mathbf{u}(n) = \mathbf{H}_c(n)\mathbf{s}(n) + \boldsymbol{\omega}(n) \tag{4.3.1}$$

where $\boldsymbol{\omega}(n)$ is additive white Gaussian noise vector and $\mathbf{H}_c(n)$ is the $N_r M \times N_t(L + M - 1)$ channel convolution matrix and $\mathbf{s}(n)$ is the $N_t(M + L - 1) \times 1$ transmitted signal vector and are defined as

$$\mathbf{u}(n) = \left[\begin{array}{ccc} \mathbf{u}_1^T(n) & \ldots & \mathbf{u}_{N_r}^T(n) \end{array}\right]^T,$$

$$\mathbf{u}_q(n) = \left[\begin{array}{ccc} u_q(n) & \ldots & u_q(n - M + 1) \end{array}\right]^T,$$

$$\mathbf{s}(n) = \left[\begin{array}{ccc} \mathbf{s}_1^T(n) & \ldots & \mathbf{s}_{N_t}^T(n) \end{array}\right]^T,$$

$$\mathbf{s}_t(n) = \left[\begin{array}{ccc} s_t(n) & \ldots & s_t(n - M - L + 2) \end{array}\right]^T,$$

$$\mathbf{H}_c(n) = \left[\begin{array}{cccc} \mathbf{H}_{11}(n) & \mathbf{H}_{12}(n) & \ldots & \mathbf{H}_{1N_t}(n) \\ \mathbf{H}_{21}(n) & \mathbf{H}_{22}(n) & \ldots & \mathbf{H}_{2N_t}(n) \\ \vdots & \vdots & \vdots & \vdots \\ \mathbf{H}_{N_r 1}(n) & \mathbf{H}_{N_r 2}(n) & \ldots & \mathbf{H}_{N_r N_t}(n) \end{array}\right],$$

and

$$\mathbf{H}_{ij}(n) = \left[\begin{array}{ccccccc} \mathbf{h}(0)^n & \mathbf{h}(1)^n & \ldots & \mathbf{h}(L-1)^n & 0 & \ldots & 0 \\ 0 & \mathbf{h}(0)^{(n-1)} & \ldots & \mathbf{h}(L-2)^{(n-1)} & \mathbf{h}(L-1)^{(n-1)} & \ddots & \vdots \\ \vdots & 0 & \ddots & \vdots & & \ddots & \ldots & 0 \\ 0 & \ldots & 0 & \mathbf{h}(0)^{(n-M+1)} & \mathbf{h}(1)^{(n-M+1)} & \ldots & \mathbf{h}(L-1)^{(n-M+1)} \end{array}\right]$$

where $\mathbf{h}(l)^n = [h_{ij}(l)e^{j2\pi f_{ij}l n}]$. Using these definitions, the equalizer output for the symbol transmitted from antenna t can be written as

$$y_t(n) = \mathbf{w}_t^H \mathbf{H}_c(n)\mathbf{s}(n) + \mathbf{w}_t^H \boldsymbol{\omega}(n) \tag{4.3.2}$$

The equalizer is obtained by minimising the mean square error cost function

$$J = E\{(y_t(n) - s_t(n - d))^*(y_t(n) - s_t(n - d))\} \tag{4.3.3}$$

where $t \in (1, 2, \ldots, N_t)$ and $d \in (0, 1, \ldots, M + L - 2)$, therefore

$$\mathbf{w}_t = \left(\mathbf{H}_c(n)\mathbf{H}_c^H(n) + \frac{\sigma_\omega^2}{\sigma_s^2}\mathbf{I} \right)^{-1} \mathbf{H}_c(n)\mathbf{c}_d \tag{4.3.4}$$

where $\mathbf{c}_d$ is the $N_t(M + L - 1) \times 1$ co-ordinate vector, only containing a nonzero element at position d, i.e.

$$\mathbf{c}_d = \begin{bmatrix} 0 & \ldots & 0 & 1 & 0 & \ldots & 0 \end{bmatrix}^T \tag{4.3.5}$$

The position of the nonzero element in $\mathbf{c}_v$ determines the equalizer corresponding to various transmitters $t \in (1, 2, \ldots, N_t)$ and retrieval delays $d \in (0, 1, \ldots, M + L - 2)$.

Remark 1. Here, to estimate the transmitted symbols perfect (apart from the effect of noise) the condition $n_R M \geq n_T(M + L - 1)$ must be satisfied or [74]

$$n_R \geq n_T \left(1 + \frac{L - 1}{M} \right),$$

which implies that for a multipath channel $n_R > n_T$. Moreover, $M \geq \left(\frac{n_T}{n_R - n_T}(L - 1) \right)$.

4.4 Iterative MIMO MMSE equalizer design

In the presence of FOs, the effective channel convolution matrix $\mathbf{H}_c(n)$ is time varying. Set the temporal equalizer length the same as the channel length, i.e., $M = L$ (M = L is adequate for the iterative method as this has the ability to resolve multipaths and the equalizer converges to a matched filter), and decompose (4.3.1) to explicitly show user t symbol with delay $(L\text{-}1)$ as

$$\mathbf{u}(n) = \mathbf{H}_c(n)\tilde{\mathbf{s}}(n) + \mathbf{H}_c(n)\mathbf{c}_{tL}s_t(n - L + 1) + \boldsymbol{\omega}(n) \qquad (4.4.1)$$

where operator $\mathbf{c}_{tL}$ is a coordinate vector such that $\mathbf{H}_c(n)\mathbf{c}_{tL}$ will choose the Lth column of $\mathbf{H}_c(n)$ corresponding to the tth transmitter antenna. The vector $\tilde{\mathbf{s}}(n)$ includes all the elements of $\mathbf{s}(n)$ except $s_t(n - L + 1)$, i.e.,

$$\tilde{\mathbf{s}}(n) = \begin{bmatrix} \tilde{\mathbf{s}}_1^T(n) & \ldots & \tilde{\mathbf{s}}_{N_t}^T(n) \end{bmatrix}^T \qquad (4.4.2)$$

where $\mathbf{s}_i(n) = [s_i(n) \ \ldots \ s_i(n - L + 2) \ \ 0 \ \ s_i(n - L) \ \ldots \ s_i(n - 2L + 2)]^T$ if $i = t$, and $\mathbf{s}_i(n) = [s_i(n) \ \ldots \ s_i(n - 2L + 2)]^T$ when $i \neq t$. According to (4.4.1) the frequency offsets can be removed by

$$\tilde{\mathbf{u}}(n) = (\mathbf{u}(n) - \mathbf{H}_c(n)\bar{\mathbf{s}}(n)) \odot \begin{bmatrix} e^{-j2\pi\mathbf{f}_{t,1}} \\ \vdots \\ e^{-j2\pi\mathbf{f}_{t,N_r}} \end{bmatrix}$$

$$= \mathbf{D}_t \left(\mathbf{H}_c(n)(\mathbf{s}(n) - \bar{\mathbf{s}}(n)) + \boldsymbol{\omega}(n) \right) \qquad (4.4.3)$$

where $\odot$ denotes the Schur-Hadamard product, $\mathbf{f}_{t,q} = [f_{t,qL-1}(n) \ \ldots$ $f_{t,q0}(n - L + 1)]^T$, $\bar{\mathbf{s}}(n)$ is the mean of $\tilde{\mathbf{s}}(n)$ obtained from the extrinsic information passed from the BCJR based MAP decoder and $\mathbf{D}_t =$

$\text{diag}(\beta)$, $\beta = [e^{-j2\pi f_{t,q}} \ldots e^{-j2\pi f_{t,N_r}}]^T$. Assuming that the transmitted symbols are temporally uncorrelated, denoting $E\{(\mathbf{s}(n) - \bar{\mathbf{s}}(n))(\mathbf{s}(n) - \bar{\mathbf{s}}(n))^H\}$ as a diagonal matrix $\text{diag}(\mathbf{v}_t(n))$, where $\mathbf{v}_t(n)$ provides the variance of the symbols transmitted from antenna t as in (4.5.4). Hence

$$E\{\tilde{\mathbf{u}}(n)\tilde{\mathbf{u}}(n)^H\} = \mathbf{D}_t(\mathbf{H}_c(n)\text{diag}(\mathbf{v}_t(n))\mathbf{H}_c(n)^H + \sigma_\omega^2\mathbf{I})\mathbf{D}_t^H \qquad (4.4.4)$$

and

$$
\begin{aligned}
E\{s_t(n - L + 1)\tilde{\mathbf{u}}(n)\} &= E\{s_t(n - L + 1)\mathbf{D}_t(\mathbf{H}_c(n)(\mathbf{s}(n) - \bar{\mathbf{s}}(n)) + \boldsymbol{\omega}(n))\} \\
&= \mathbf{D}_t\mathbf{H}_c(n)\mathbf{c}_{tL} \qquad (4.4.5)
\end{aligned}
$$

where $E\{s_t(n - L + 1)\bar{\mathbf{s}}(n)\}$ is $\mathbf{0}$ because $\bar{\mathbf{s}}(n)$ does not contain $s_t(n - L + 1)$ and all other symbols in $\bar{\mathbf{s}}(n)$ are uncorrelated with $s_t(n - L + 1)$. Hence the iterative MIMO MMSE equalizer is written as,

$$\mathbf{w}_t(n) = \left(\mathbf{D}_t(\mathbf{H}_c(n)\text{diag}(\mathbf{v}_t(n))\mathbf{H}_c(n)^H + \sigma_\omega^2\mathbf{I})\mathbf{D}_t^H\right)^{-1}\mathbf{D}_t\mathbf{H}_c(n)\mathbf{c}_{tL}$$

$$(4.4.6)$$

The symbol with delay $L - 1$ is estimated as

$$\hat{s}_t(n - L + 1) = \mathbf{w}_t(n)^H\tilde{\mathbf{u}}(n) \qquad (4.4.7)$$

The MIMO MMSE equalizer in (4.4.6) requires knowledge of the channel parameter matrix $\mathbf{H}_c(n)$ and the frequency offsets $\mathbf{f}_{t,q}$ (in $\mathbf{D}$). However short pilot symbols are inadequate to estimate the frequency offsets due to limitation on the resolution associated with the DFT. Therefore an iterative channel and FO estimation technique is proposed where soft estimates of the transmitted signal are used as a pilot signal to improve the estimation performance.
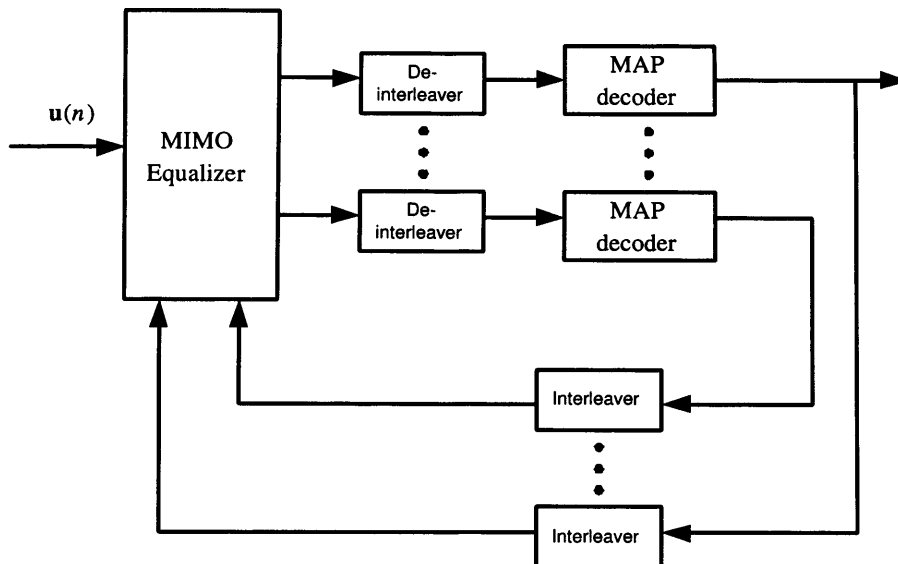
Figure 4.1. Iterative MIMO receiver.

4.5   Iterative Channel Estimation

The initial channel estimate is obtained using the training sequence contained in the middle of a burst. This estimate is used to design a MIMO MMSE equalizer as in (4.3.4) and to obtain an initial estimate of the transmitted data. The initial estimates of the transmitted signal at the linear MIMO equalizer output are deinterleaved and passed to a MAP decoder as shown in Fig. 4.1. The MAP decoder would provide the likelihood ratios (soft estimates) of the uncoded transmitted symbols which are interleaved and passed to the iterative MMSE equalizer. At each iteration, the received signal vector $\mathbf{u}(n)$ in (4.3.1) will be passed to the iterative MIMO MMSE equalizer in (4.4.6) together with the prior information from the decoder so that the contribution of all other users except the user of interest can be removed from the received signal as in (4.4.3) for each user t. The MIMO MMSE equalizer output $\hat{\mathbf{s}}_t(n)$ is used to obtain a posterior log-likelihood ratios as follows [50,55]

$$\Delta L[\hat{s}_t(n)] = ln\frac{p\{\hat{s}_t(n)|_{s_t(n)} = 1\}}{p\{\hat{s}_t(n)|_{s_t(n)} = -1\}}$$

$$= \frac{4Re\{\hat{s}_t(n)\}}{1 - \mathbf{w}_t(n)^H\mathbf{H}_c(n)\mathbf{c}_{tL}} \qquad (4.5.1)$$

where $p\{\hat{s}_t(n)|_{s_t(n)} = b\}$ is determined using a Gaussian distribution assumption as follows

$$p[\hat{s}_t(n)] = \frac{1}{\sqrt{\pi}\sigma_{s_t}}e^{-\frac{(\hat{s}_t(n) - m_b)^2}{\sigma_{s_t}^2}} \qquad (4.5.2)$$

For the above PDF the conditional mean and the variance are obtained from the knowledge of the channel and equalizer as follows [55]

$$m_b = E[\hat{s}_t(n)|_{s_t(n)} = b] = \mathbf{w}_t(n)^H\mathbf{D}_t\mathbf{H}_c(n)\mathbf{c}_{tL}b \qquad (4.5.3)$$

$$\sigma_{s_t|s_t(n)=b}^2 = \text{Cov}\{\hat{s}_t(n), \hat{s}_t(n)|_{s_t(n)} = b\}$$

$$= E\{\hat{s}_t(n)\hat{s}_t(n)^*\} - m_b m_b^*$$

$$= \mathbf{w}_t(n)^H\mathbf{D}_t\mathbf{H}_c(n)\mathbf{c}_{tL}(1 - \mathbf{w}_t(n)^H\mathbf{H}_c(n)\mathbf{c}_{tL})$$

The log-likelihood ratios of all user symbols will be determined in a similar way. As in the SISO case, a four-bursts based packet radio transmission is considered. Therefore each burst is separately equalized and the equalizer outputs of four consecutive bursts for each user are collected, de-interleaved and decoded using MAP algorithm [64]. The MAP decoder provides a log-likelihood ratio (LLR) estimate of the coded and uncoded symbols after each iterations. The mean of the symbol $\bar{s}(n)$ in (4.4.3) is found from the LLRs; updated de-interleaved and pilot symbols are reinserted. The soft estimate of the transmitted signal is then used to separate users and to determine the multiple frequency offsets and to refine the channel estimates in an iterative fashion. The variance required for the MIMO MMSE equalizer in [72] is also computed as follows

$$\mathbf{v}_t(n) = 1 - \tilde{\tilde{s}}_t(n)^2 \tag{4.5.4}$$

where $\tilde{\tilde{s}}_t(n)$ denotes the soft estimates (real) of the transmitted symbol from the decoder output.

4.6 Simulations

In order to examine the performance of the proposed iterative FOs and channel estimator, a system using two transmit and three receive antennas is simulated. As in the SISO case, a normal burst structure as in GSM with 116 data symbols and 26 pilot symbols in the middle is considered. For each user, a pilot sequence was generated randomly from binary alphabets. The length of each channel is five. Also a half rate convolutional code and a MAP decoder is considered. The generator polynomials have been chosen as in GPRS CS1-CS3, (i.e, G0 $= 1 + D^3 + D^4$ and G1 $= 1 + D + D^3 + D^4$), [65] and [66]. The data bits corresponding to four consecutive bursts have been added, interleaved using a random interleaver, and modulated according to BPSK. Then a pilot symbol burst of length 26 has been inserted in each burst and transmitted. At the receiver, each burst is separately equalized as explained in the previous section, and the equalizer outputs of four consecutive bursts for each user are collected, de-interleaved and decoded using the MAP algorithm. The soft estimates of the uncoded bits are interleaved again and fedback to the iterative equalizers.

In the simulation, parameters are estimated and the variances of the estimators are compared with the corresponding CRLB, which is derived in Appendix 2 and [17], [30], [63]. Fig. 4.2 and Fig. 4.3 depict the variance of the estimators for the MGs and the FOs, respectively. In this simulation, the results are presented only for the first transmit-receive

antenna pair, but similar results were observed for the remaining antennas. Here, a randomly chosen fixed channel with five paths is considered. Frequency offsets were also chosen randomly in the interval 0 and 0.005 using a uniform distribution. The channel is first estimated using the pilot signal burst of length 26, and the transmitted signal are retrieved using an MMSE equalizer of length eight and a half rate convolutional decoder. (The equalizer length is set same as the channel length only for iterative MMSE equalizer. However, when the signal is equalized at the first time, a conventional MMSE equalizer is used whose length is set much greater than the channel length). The soft estimates of the transmitted signal are then used to separate users, resolve multipaths, determine the multiple frequency offsets and to refine the channel estimates in an iterative fashion. In each iteration, the soft estimates of the transmitted signal are obtained using the iterative MMSE equalizer of temporal length five as in (4.4.6). The results depicted in Fig. 4.2 and Fig. 4.3 for the channel and the frequency offset estimation reveal an important observation that although only 26 training symbols are available in the burst, estimators after adequate iterations approach the CRLB as if the length of the training signal is 142. However, MIMO channel need a very powerful decoder in order to cancel both ISI and IUI. A possible way to reduce the gap between the variance of the estimate and CRLB in Fig. 4.2 and Fig. 4.3 is to increase the code rate or to use more powerful coding scheme such as turbo codes.

In order to evaluate the BER performance, a frequency selective MIMO channel with random frequency offsets is used, so that the channel coefficients and frequency offsets do not change within a burst, but would change between bursts according to a complex Gaussian distribution for the channel coefficients and uniform distribution (between 0 and 0.005) for FOs. The uncoded BER performance for five iterations has been pro-
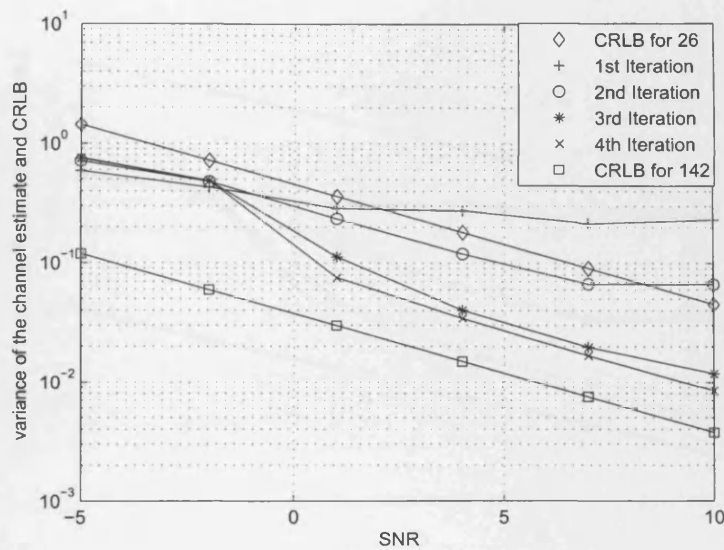
Figure 4.2. Comparison of the variance of the iterative channel gain estimate for h_{11} and the CRLBs assuming 26 and 142 pilot symbols. h_{qt} is the channel gain between the first receive antenna and the transmit antenna t for path k. The estimation performance for h_{qt} is also similar to that of h_{11}, hence not depicted.

duced, and compared with the single-user matched filter bound in Fig. 4.4. For the matched filter bound, the BER of a three receive antenna and five path channel assuming no frequency offsets and perfect resolution of the multipath with ideal channel knowledge at the receiver is obtained. The BER curve of a MIMO equalizer that was designed ignoring the effect of FOs has also been produced. The proposed scheme significantly outperforms the conventional equalizer and attains a performance closer to the matched filter bound.
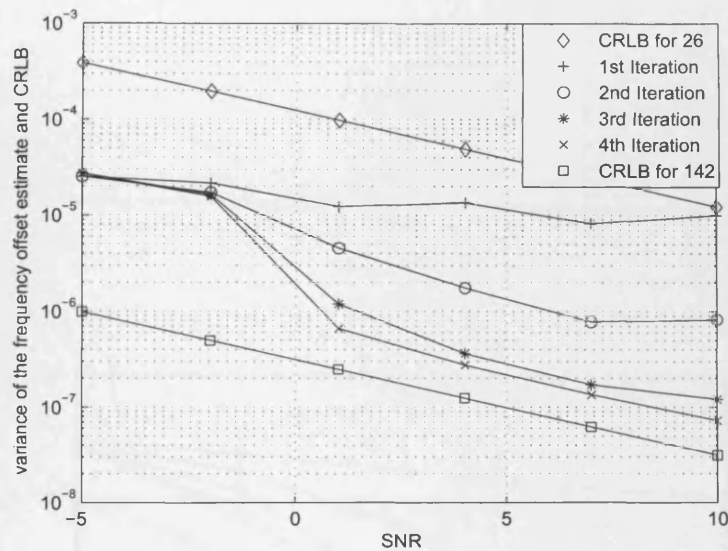
Figure 4.3. Comparison of the variance of the iterative frequency offset estimate for f_{11} and the CRLBs assuming 26 and 142 pilot symbols. f_{qt} is the frequency offset between the first receive antenna and the transmit antenna t for path k. The estimation performance for f_{qt} is also similar to that of f_{11}, hence not depicted.

4.7   Summary

In this chapter, an iterative algorithm for the estimation of MGs and FOs for the frequency selective MIMO channel with distinct FOs is provided. According to the proposed method, multipath gains are initially estimated using the available short pilot sequence, and then the soft estimates of the transmitted signal are used to estimate the frequency offsets and to refine the channel estimates iteratively. In addition to providing a superior BER performance, the proposed estimator is also efficient in that it tends to attain the CRLB assuming all 142 symbols in the burst are known pilot symbols.
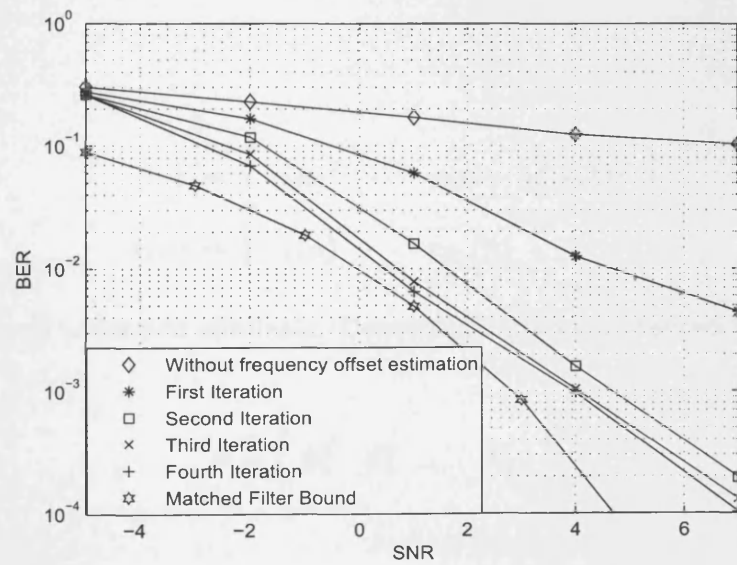
Figure 4.4. The BER performance of the proposed MIMO iterative equalizer and a MIMO equalizer which ignores the effect of frequency offsets.

4.8 Appendices 2

The Cramér Rao lower bound (CRLB) for the estimates of MGs and FOs
for a MIMO environment is derived [63]. Recalling (4.1.1), and stacking
all the received samples from time n to $(n - M + 1)$, from all antennas,
(4.1.1) can be written in vector form as

$$\mathbf{r} = \mathbf{u} + \boldsymbol{\omega}, \qquad (4.8.1)$$

where

$$\mathbf{r} = \begin{bmatrix} \mathbf{r}(n)^T & \cdots & \mathbf{r}(n - M + 1)^T \end{bmatrix}$$

$$\mathbf{r}(n) = \begin{bmatrix} r_1(n) & \cdots & r_{N_r}(n) \end{bmatrix}^T$$

with $\mathbf{u}$ and $\boldsymbol{\omega}$ formed similarly. Denote the unknown desired vector para-
meters

$$\boldsymbol{\theta} \triangleq \begin{bmatrix} \boldsymbol{\theta}_1^T & \boldsymbol{\theta}_2^T & \ldots & \boldsymbol{\theta}_{N_r}^T \end{bmatrix}^T, \qquad (4.8.2)$$

where

$$\boldsymbol{\theta}_q \triangleq \begin{bmatrix} Re(\mathbf{h}_q)^T & Im(\mathbf{h}_q)^T & \mathbf{f}_q^T \end{bmatrix}^T. \qquad (4.8.3)$$

Since the noise sequence $\omega_q(n)$ is spatially uncorrelated, the Fisher infor-
mation matrix (FIM) for the estimation of θ can be found using Slepian-
Bangs formula [17, 30].

$$\mathbf{F}(q, t) = \frac{2}{\sigma_\omega^2} Re \left(\frac{\partial \mathbf{u}^H}{\partial \boldsymbol{\theta}_q} \frac{\partial \mathbf{u}}{\partial \boldsymbol{\theta}_t^T} \right)$$

$$= \frac{2}{\sigma_\omega^2} Re \sum_{n=0}^{N-1} \left(\frac{\partial \mathbf{u}^H(n)}{\partial \boldsymbol{\theta}_q} \frac{\partial \mathbf{u}(n)}{\partial \boldsymbol{\theta}_t^T} \right), \qquad (4.8.4)$$

where

$$\frac{\partial \mathbf{u}^H}{\partial \boldsymbol{\theta}_q} = \begin{bmatrix} \frac{\partial \mathbf{u}^H}{\partial Re(\mathbf{h}_q)} \\ \frac{\partial \mathbf{u}^H}{\partial Im(\mathbf{h}_q)} \\ \frac{\partial \mathbf{u}^H}{\partial \mathbf{f}_q} \end{bmatrix} \quad (3N_t L \times N_r M)$$

$$\frac{\partial \mathbf{u}}{\partial \boldsymbol{\theta}_t^T} = \begin{bmatrix} \frac{\partial \mathbf{u}}{\partial Re(\mathbf{h}_t{}^T)} & \frac{\partial \mathbf{u}}{\partial Im(\mathbf{h}_t{}^T)} & \frac{\partial \mathbf{u}}{\partial \mathbf{f}_t{}^T} \end{bmatrix} \quad (N_r M \times 3N_t L)$$

Here, $q, t = 1, 2, ..., N_r$. The FIM can be written as

$$\mathbf{F} = \begin{bmatrix} \mathbf{F}(1,1) & \mathbf{F}(1,2) & \cdots & \mathbf{F}(1, N_r) \\ \mathbf{F}(2,1) & \mathbf{F}(2,2) & \cdots & \mathbf{F}(2, N_r) \\ \vdots & \vdots & \ddots & \vdots \\ \mathbf{F}(N_r, 1) & \mathbf{F}(N_r, 2) & \cdots & \mathbf{F}(N_r, N_r) \end{bmatrix} \tag{4.8.5}$$

where $\mathbf{F}(q, t)$ denotes the (q, t)th sub-matrix of the FIM corresponding to the parameters $\boldsymbol{\theta}_q$ and $\boldsymbol{\theta}_t$. From (4.8.4), it can be noted that $\mathbf{F}(q, t) = \mathbf{0}$ whenever $q \neq t$. Hence, there is a decoupling between the estimation error in parameters corresponding to two different receive antennas and the FIM is block diagonal, which justifies that the parameters corresponding to each receive antenna can be estimated independently. Let $\mathbf{F}_q = \mathbf{F}(q, q)$, the FIM of size $3N_t L \times 3N_t L$ corresponding to the estimation of $\boldsymbol{\theta}_q = [Re(\mathbf{h}_q)^T \ Im(\mathbf{h}_q)^T \ \mathbf{f}_q^T]^T$, then $\mathbf{F}_q$ can be represented as

$$\mathbf{F}_q = \frac{2}{\sigma_\omega^2} \begin{bmatrix} \mathbf{F}_q[Re(\mathbf{h}_q), Re(\mathbf{h}_q)] & \mathbf{F}_q[Re(\mathbf{h}_q), Im(\mathbf{h}_q)] & \mathbf{F}_q[Re(\mathbf{h}_q), \mathbf{f}_q] \\ \mathbf{F}_q[Im(\mathbf{h}_q), Re(\mathbf{h}_q)] & \mathbf{F}_q[Im(\mathbf{h}_q), Im(\mathbf{h}_q)] & \mathbf{F}_q[Im(\mathbf{h}_q), \mathbf{f}_q] \\ \mathbf{F}_q[\mathbf{f}_q, Re(\mathbf{h}_q)] & \mathbf{F}_q[\mathbf{f}_q, Im(\mathbf{h}_q)] & \mathbf{F}_q[\mathbf{f}_q, \mathbf{f}_q] \end{bmatrix}$$
$$\tag{4.8.6}$$

and the elements of $\mathbf{F}_q$ can be found using the differentials

$$\frac{\partial u_q(n)}{\partial Reh_{qt}(l)} = e^{j2\pi f_{qtl}n} s_t(n-l) \tag{4.8.7a}$$

$$\frac{\partial u_q(n)}{\partial Imh_{qt}(l)} = je^{j2\pi f_{qtl}n} s_t(n-l) \tag{4.8.7b}$$

$$\frac{\partial u_q(n)}{\partial f_{qtl}} = jnh_{qt}(l)e^{j2\pi f_{qtl}n} s_t(n-l) \tag{4.8.7c}$$

Introduce

$$\mathbf{U}_q = \mathbf{P}_q^H \mathbf{P}_q$$

$$\mathbf{P}_q = [\, \mathbf{p}_{q1}(0) \quad \cdots \quad \mathbf{p}_{q1}(L-1) \quad \cdots \quad \mathbf{p}_{qN_t}(L-1)]$$

$$\mathbf{p}_{qt}(l) = \mathbf{S}_{qk}\mathbf{e}_{qt}(l)$$

$$\mathbf{D}_n = diag\,(0, 1, \cdots, N-1)$$

$$\mathbf{D}_h = diag\,(h_{q1}(0), \cdots h_{q1}(L-1), \cdots, h_{qN_t}(L-1))$$

$$\mathbf{T}_q = \mathbf{P}_q^H \mathbf{D}_n \mathbf{P}_q \mathbf{D}_h$$

$$\mathbf{G}_q = \mathbf{D}_h^H \mathbf{P}_q^H \mathbf{D}_n^2 \mathbf{P}_q \mathbf{D}_h$$

$$\mathbf{B} = [Re(\mathbf{G}_q - \mathbf{T}_q^H \mathbf{U}_q^{-1} \mathbf{T}_q)]^{-1}$$

The individual elements corresponding to the estimation of $\boldsymbol{\theta}_q$ can be found from (4.8.4). Therefore, the initial row of the submatrices in (4.8.6) can be written as

$$\mathbf{F}_q\,[Re(\mathbf{h}_q), Re(\mathbf{h}_q)] = Re\left[\mathbf{P}_q^H \mathbf{P}_q\right] \tag{4.8.8}$$

$$\mathbf{F}_q\,[Re(\mathbf{h}_q), Im(\mathbf{h}_q)] = -Im\left[\mathbf{P}_q^H \mathbf{P}_q\right] \tag{4.8.9}$$

$$\mathbf{F}_q\,[Re(\mathbf{h}_q), f_q] = -Im\left[\mathbf{P}_q^H \mathbf{D}_n \mathbf{P}_q \mathbf{D}_h\right] \tag{4.8.10}$$

The second row of matrices can be written as

$$\mathbf{F}_q\,[Im(\mathbf{h}_q), Re(\mathbf{h}_q)] = Im\left[\mathbf{P}_q^H \mathbf{P}_q\right] \tag{4.8.11}$$

$$\mathbf{F}_q\,[Im(\mathbf{h}_q), Im(\mathbf{h}_q)] = Re\left[\mathbf{P}_q^H \mathbf{P}_q\right] \tag{4.8.12}$$

$$\mathbf{F}_q\left[Im(\mathbf{h}_q), \boldsymbol{f}_q\right] = Re\left[\mathbf{P}_q^H \mathbf{D}_n \mathbf{P}_q \mathbf{D}_h\right] \tag{4.8.13}$$

Similarly, the third row of matrices can be written as

$$\mathbf{F}_q\left[\boldsymbol{f}_q, Re(\mathbf{h}_q)\right] = -Im\left[\mathbf{P}_q^H \mathbf{D}_n \mathbf{P}_q \mathbf{D}_h\right]^H \tag{4.8.14}$$

$$\mathbf{F}_q\left[\boldsymbol{f}_q, Im(\mathbf{h}_q)\right] = Re\left[\mathbf{P}_q^H \mathbf{D}_n \mathbf{P}_q \mathbf{D}_h\right]^H \tag{4.8.15}$$

$$\mathbf{F}_q\left[\boldsymbol{f}_q, \boldsymbol{f}_q\right] = Re[\mathbf{D}_h^H \mathbf{P}_q^H \mathbf{D}_n^2 \mathbf{P}_q \mathbf{D}_h] \tag{4.8.16}$$

In compact form (4.8.6) can be written as

$$\mathbf{F}_q = \frac{2}{\sigma_\omega^2} \begin{bmatrix} Re(\mathbf{U}_q) & -Im(\mathbf{U}_q) & -Im(\mathbf{T}_q) \\ Im(\mathbf{U}_q) & Re(\mathbf{U}_q) & Re(\mathbf{T}_q) \\ -Im(\mathbf{T}_q)^T & Re(\mathbf{T}_q)^T & Re(\mathbf{G}_q) \end{bmatrix} \tag{4.8.17}$$

Note that there is a coupling in the estimation error between the channel parameters and the FOs. The CRLB is obtained as the inverse of the FIM, i.e.,

$$\mathbf{CRLB}(\boldsymbol{\theta}_q) = \mathbf{F}_q^{-1}. \tag{4.8.18}$$

The inverse of $\mathbf{F}_q$ can be calculated by using the matrix inversion lemma, i.e,

$$\mathbf{CRLB}(\boldsymbol{\theta}_q) = \frac{\sigma_\omega^2}{2} \begin{bmatrix} Re(\mathbf{U}_q^{-1}) & -Im(\mathbf{U}_q^{-1}) & 0 \\ Im(\mathbf{U}_q^{-1}) & Re(\mathbf{U}_q^{-1}) & 0 \\ 0 & 0 & 0 \end{bmatrix}$$
$$+ \begin{bmatrix} Im(\mathbf{U}_q^{-1}\mathbf{T}_q) \\ -Re(\mathbf{U}_q^{-1}\mathbf{T}_q) \\ \mathbf{I} \end{bmatrix} \left[Re(\mathbf{G}_q - \mathbf{T}_q^H \mathbf{U}_q^{-1} \mathbf{T}_q)\right]^{-1}$$
$$\times \begin{bmatrix} Im(\mathbf{U}_q^{-1}\mathbf{T}_q)^T & -Re(\mathbf{U}_q^{-1}\mathbf{T}_q)^T & \mathbf{I} \end{bmatrix} \tag{4.8.19}$$

From (4.8.19), the CRLB associated with the FOs becomes

$$\mathbf{CRLB}(\boldsymbol{f}_q) = \left[Re(\mathbf{G}_q - \mathbf{T}_q^H \mathbf{U}_q^{-1} \mathbf{T}_q)\right]^{-1}, \qquad (4.8.20)$$

and the CRLB for the real and the imaginary parts of the MGs are given as

$$\mathbf{CRLB}[Re(\mathbf{h}_q)] = \left[Re(\mathbf{U}_q^{-1}) + Im(\mathbf{U}_q^{-1}\mathbf{T}_q)\mathbf{B}Im(\mathbf{U}_q^{-1}\mathbf{T}_q)^T\right]$$

$$\mathbf{CRLB}[Im(\mathbf{h}_q)] = \left[Re(\mathbf{U}_q^{-1}) + Re(\mathbf{U}_q^{-1}\mathbf{T}_q)\mathbf{B}Re(\mathbf{U}_q^{-1}\mathbf{T}_q)^T\right]$$

Chapter 5

FREQUENCY SYNCHRONIZATION AND CHANNEL ESTIMATION TECHNIQUES FOR MIMO OFDM SYSTEMS

Most future wireless communication networks will be based on broadband transmission and reception. The broadband services require reliable and high data rate communications over time-dispersive (frequency-selective) channels with limited spectrum and intersymbol interference (ISI) caused by multipath fading. Orthogonal frequency division multiplexing (OFDM) is a leading modulation and access technique for broadband wireless communications. This combined with multiple input multiple output (MIMO) transmission systems [68] promises a substantial increase in the through-put to support data intensive services such as multimedia and interactive applications.

OFDM is very similar to the well known and widely used technique of frequency division multiplexing (FDM). It uses the same principle as in

FDM to allow multiple messages to be sent over a single radio channel. The main difference between FDM and OFDM is that in OFDM, the spectrum of the individual carriers could mutually overlap. These sub-carries overlap in the frequency domain but do not cause ICI due to the orthogonal nature of the subcarriers. Another advantage of OFDM is its ability to transform a wideband frequency-selective channel into a set of parallel flat fading narrowband channels. This substantially simplifies the channel equalization problem. The principal weakness of OFDM is its sensitivity to frequency offsets caused by Doppler shifts and/or local oscillator mismatches. In particular, the presence of frequency offset introduces inter-carrier interference (ICI) that could significantly degrade the radio link performance [75]. In this chapter, the basics of OFDM are reviewed and the frequency synchronization problem is studied in detail. Issues such as timing synchronization and sampling clock synchronization are important, but will not be treated here. Assuming that the system has perfect frame and time synchronization, only carrier frequency offset estimation is considered here. Several FO schemes for OFDM have been proposed in the literature. Tracking of the frequency offsets using pilots has been analyzed for single-antenna systems in [76]. Lately, MIMO OFDM has been considered, and several papers investigated both pilot design [77] and FO estimation techniques [78].

Again all previous works assumed single FOs. However, in this chapter, estimation and detection techniques for OFDM channels with multiple FOs is investigated.

5.1 A brief overview of an OFDM system

Assume that the information symbols are transmitted at the rate of R symbols per second over a multipath channel. The duration of each sym-

bol is therefore $T_s = 1/R$. If the delay spread, $\tau_{max} > T_s/10$, then the receive signal may suffer from significant intersymbol interference (ISI). Such a channel is said to be dispersive or frequency selective. There are two main approaches to cope with such channels. The first approach is to use a single carrier system with an equalizer at the receiver to compensate for the ISI. The implementation of the equalizer may become very challenging for channels with large delay spreads, specially at very high data rates. The second approach is based on multicarrier modulation, such as orthogonal frequency division multiplexing (OFDM). In this chapter, OFDM is focus on investigating. A SISO based OFDM system is first investigated and then generalised to a MIMO system. The basic principle of an OFDM system is that the available bandwidth is divided into a large number of subbands, and over each subband the wireless channel can be considered nondispersive or flat fading. The original data stream at rate R is split into K parallel data streams, each at the rate R/K. The symbol duration, T, for these parallel data streams is therefore increased by a factor of K, i.e., $T = KT_s$. Conceptually, each of the data streams modulates a carrier with a different frequency and the resulting signals are transmitted simultaneously. Correspondingly, the receiver consists of K parallel receiver paths. Due to the increased symbol duration, the ISI over each channel is reduced to $\tau_{max}/(KT_s)$ symbols.

OFDM systems transmit low-rate signals simultaneously over a single transmission path. Low symbol rate makes OFDM resistant to the effects of ISI caused by multipath propagation. The effects of ISI on an OFDM signal can be further improved by the addition of a guard period at the start of each symbol in the time domain. The guard period is generally a cyclic copy of the last bits of the actual data being transmitted. The length of the cyclic prefix is kept at least equal to $L - 1$ samples. Under
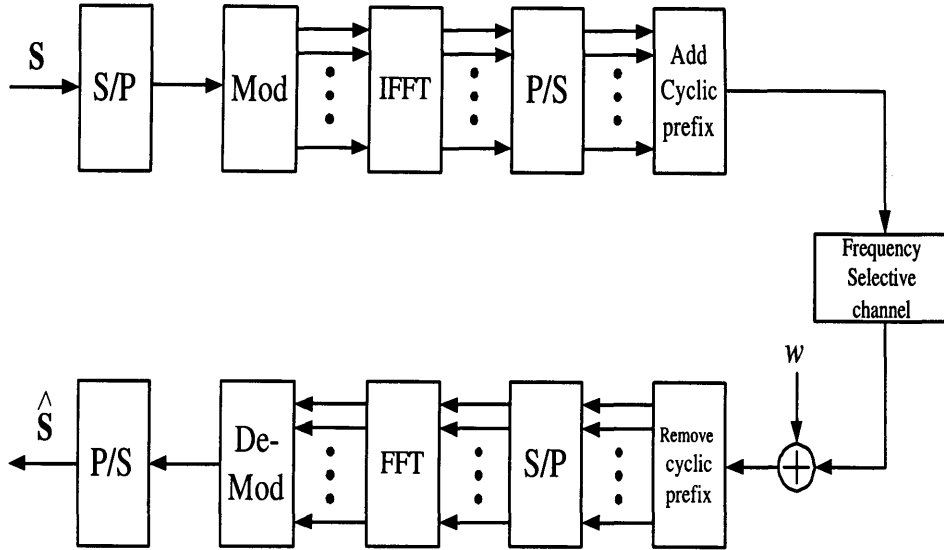
Figure 5.1. Baseband OFDM system model.

this condition, a linear convolution of the transmitted sequence and the channel is converted to a circular convolution. Therefore, the effects of ISI are easily and completely removed. Moreover, this approach enables the receiver to use the FFT technique for OFDM implementation [79].

5.2 Problem statement (SISO case)

The baseband equivalent representation of an OFDM system is depicted in Fig 5.1. The input data are first fed into a serial to parallel (S/P) converter. For simplicity, BPSK in all N subcarriers is considered. The modulated data symbols, represented by $S(0)$, ..., $S(N-1)$, are then transformed using the inverse fast Fourier transform (IFFT) and parallel to serially converted to obtain the transmitted data in the time domain as $s(n)$.

$$s(n) = \frac{1}{\sqrt{N}} \sum_{k=0}^{N-1} S(k) e^{j \frac{2\pi}{N} kn} \qquad (5.2.1)$$

where the term $\frac{1}{\sqrt{N}}$ is used to ensure the total symbol energy is not changed by the transformation. In order to avoid intersymbol interference (ISI), cyclic prefix (CP) symbols of length v, are added to each OFDM symbol and transmitted though the channel. Let the signal transmitted through the channel be $s(0)$, $s(1)$, ..., $s(N + v - 1)$. The received data sequence $y(0)$, $y(1)$, ..., $y(N + v - 1)$ corrupted by multipath fading and zero mean AWGN is converted back to frequency domain signals $Y(0)$, ..., $Y(N - 1)$ after removing the CP, and performing FFT. A multipath length of L with distinct FOs is considered. The received signal at the channel output is written as [80]

$$y(n) = \sum_{l=0}^{L-1} h_l s(n - l) e^{j2\pi f_l n} + \omega(n), \quad n = 0, 1, ..., N + v - 1 \qquad (5.2.2)$$

where h_l and f_l are the unknown complex channel gain and frequency offset for the lth channel tap, and $\omega(n)$ is an additive circularly symmetric zero mean white (complex) Gaussian noise with variance σ_ω^2.

5.2.1   Time domain estimation

A frame of 60 OFDM symbols with each OFDM symbol consisting of 64 subcarriers is considered. In each frame, the first transmitted OFDM symbol is a long training sequence based on two consecutive identical sets of OFDM samples [81]. Assuming the channel impulse response (CIR) and FOs change from frame to frame according to a complex Gaussian distribution and uniform distribution (0 - 0.005), respectively. Within each frame, the FO for the lth path varies between OFDM symbols according to a random walk model

$$f_l = \alpha f_l + (1 - \alpha)\eta(n) \qquad (5.2.3)$$

where α has been chosen as 0.99 in our simulation. $\eta(n)$ is a zero mean real Gaussian variable with variance equal to 0.001. Furthermore it is assumed that the system has perfect time synchronization. Let $\mathbf{s}_{l,n} = \left[\begin{array}{ccc} \tilde{s}(n-l) & \ldots & \tilde{s}(n-l-N+1) \end{array} \right]^T$ and $\tilde{s}(n)$ be the soft estimate of the transmitted signal $s(n)$. This soft estimate is treated as a pilot signal to determine the multiple frequency offsets and to refine the channel estimates. Further, the vector of dimension $N \times 1$ $\mathbf{e}_{l,n} = \left[\begin{array}{ccc} e^{j2\pi f_l n} & \ldots & e^{j2\pi f_l(n-N+1)} \end{array} \right]^T$ models the effect of frequency offset on the signal vector of length N associated with the lth path. Define an $N \times L$ matrix $\mathbf{Q}_n \stackrel{\triangle}{=}$ $\left[\begin{array}{ccc} \mathbf{s}_{0,n} \odot \mathbf{e}_{0,n} & \ldots & \mathbf{s}_{L-1,n} \odot \mathbf{e}_{L-1,n} \end{array} \right]$, where $\odot$ denotes the Schur-Hadamard product. For example,

$$
\mathbf{s}_{0,n} \odot \mathbf{e}_{0,n} = \left[\begin{array}{c} s(n) \\ s(n-1) \\ \vdots \\ s(n-N+1) \end{array} \right] \odot \left[\begin{array}{c} e^{j2\pi f_0(n)} \\ e^{j2\pi f_0(n-1)} \\ \vdots \\ e^{j2\pi f_0(n-N+1)} \end{array} \right]
$$

$$
= \left[\begin{array}{c} s(n)e^{j2\pi f_0(n)} \\ s(n-1)e^{j2\pi f_0(n-1)} \\ \vdots \\ s(n-N+1)e^{j2\pi f_0(n-N+1)} \end{array} \right] \tag{5.2.4}
$$

Therefore equation (5.2.2) using the soft estimate of the transmitted signal can be written in a vector form as

$$
\mathbf{y}_n = \sum_{l=0}^{L-1} h_l \mathbf{S}_{l,n} \mathbf{e}_{l,n} + \boldsymbol{\omega}_n = \mathbf{Q}_n \mathbf{h}_L + \boldsymbol{\omega}_n \tag{5.2.5}
$$

where $\mathbf{h}_L = [h_0 \ \ldots \ h_{L-1}]^T$, $\boldsymbol{\omega}_n = [\omega(n) \ \ldots \ \omega(n-N+1)]^T$ and $\mathbf{S}_{l,n} = \mathrm{diag}(\mathbf{s}_{l,n})$. The various channel gains, $\mathbf{h}_L$ and frequency offsets $\mathbf{f}_L = [f_0 \ \ldots \ f_{L-1}]^T$ are estimated in the time domain using the received signal $y(n)$ and the soft estimate of $s(n)$. The unknown parameter vector

θ can be written as $\theta = [h_0 \ \ldots \ h_{L-1} \ f_0 \ \ldots \ f_{L-1}]^T \triangleq [\mathbf{h}_L^T \ \mathbf{f}_L^T]^T$. The log-likelihood function is given by [18],

$$\ln p(\mathbf{y}_n; \theta) \approx -\frac{1}{\sigma_\omega^2} \left(\mathbf{y}_n - \mathbf{Q}_n\mathbf{h}_L\right)^H \left(\mathbf{y}_n - \mathbf{Q}_n\mathbf{h}_L\right) \qquad (5.2.6)$$

By maximising (5.2.6) with respect to $\mathbf{h}_L$, the maximum likelihood estimate of $\mathbf{h}_L$ is obtained as follows [18]

$$\hat{\mathbf{h}}_L = \left(\mathbf{Q}_n^H\mathbf{Q}_n\right)^{-1}\mathbf{Q}_n^H\mathbf{y}_n \qquad (5.2.7)$$

Substituting the optimal solution (5.2.7) into (5.2.6), and minimising with respect to f_L, the approximative maximum likelihood (AML) estimator of frequency offsets is obtained as follows [18],

$$\hat{f}_x = \arg\max_f \left|\sum_{n=0}^{P-1} y^*(n)\tilde{s}(n-x)e^{j2\pi fn}\right|^2 \qquad (5.2.8)$$

where P is the number of sample used for the estimation. The optimization involved in (5.2.8) can be efficiently evaluated using the fast Fourier transform (FFT). Once the frequency offsets have been found, the channel gains are obtained using (5.2.7).

5.2.2   Iterative channel and FO estimation in SISO OFDM

The proposed iterative technique for the estimation of multiple FOs uses the long training signal available in OFDM to obtain an initial estimate of channel gains and multiple FOs. It then combines this with the soft estimate of the data to continuously track multiple FOs as shown in Fig. 5.2.

The initial channel estimation is used to obtain the channel gain at each
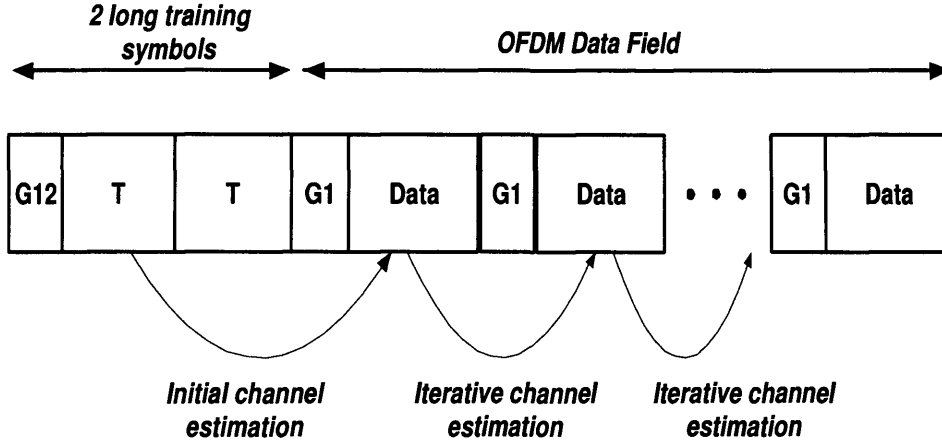
Figure 5.2. OFDM training structure.

subcarrier. Denote the gain in the nth subcarrier as H_n. In a conventional OFDM receiver, a per tone MMSE equalizer is employed as

$$W_n = (H_n H_n^* + \frac{\sigma_\omega^2}{\sigma_s^2})^{-1} H_n \qquad (5.2.9)$$

Using this per tone equalizer, the soft estimate of the transmitted signal is obtained as

$$\hat{S}(n) = W_n^* Y(n) \qquad (5.2.10)$$

where $Y(n)$ is the received signal at the nth subcarrier (after FFT). The a priori and a posteriori LLRs of $S(n)$ are defined as [55]

$$L[S(n)] = \ln \frac{p\{S(n) = 1\}}{p\{S(n) = -1\}}$$

and

$$L[S(n)|_{\hat{S}(n)}] = \ln \frac{p\{S(n) = 1|_{\hat{S}(n)}\}}{p\{S(n) = -1|_{\hat{S}(n)}\}}.$$

The output $\hat{S}(n)$ is used to obtain the difference between the posteriori and a priori log-likelihood ratio (LLR), also called the extrinsic information,

of $S(n)$ is as follows [50, 55]

$$\Delta L[\hat{S}(n)] = L[S(n)|_{\hat{S}(n)}] - L[S(n)]$$

$$= \ln\frac{p\{S(n) = 1|_{\hat{S}(n)}\}}{p\{S(n) = -1|_{\hat{S}(n)}\}} - \ln\frac{p\{S(n) = 1\}}{p\{S(n) = -1\}}. \quad (5.2.11)$$

Using Bayes' theorem, $p(a;b) = \frac{p(b;a)p(a)}{p(b)}$, (5.2.11) can be written as

$$\Delta L[\hat{S}(n)] = \ln\frac{p\{\hat{S}(n)|_{S(n)=1}\}p\{S(n) = 1\}}{p\{\hat{S}(n)|_{S(n)=-1}\}p\{S(n) = -1\}} - \ln\frac{p\{S(n) = 1\}}{p\{S(n) = -1\}}$$

$$= \ln\frac{p\{\hat{S}(n)|_{S(n)=1}\}}{p\{\hat{S}(n)|_{S(n)=-1}\}}$$

$$= \frac{4\text{Re}\{\hat{S}(n)\}}{1 - W_n^* H_n} \qquad (5.2.12)$$

The mean of the symbol (soft estimate) is obtained as

$$\bar{S}(n) = \tanh(\Delta L[\hat{S}(n)]) \qquad (5.2.13)$$

After the IFFT, the soft estimates of the transmitted symbols are then treated as a training signal to determine multiple FOs and to refine the channel estimate and FOs in an iterative fashion. The estimate of the transmitted signal are updated using the new channel estimate and the FOs. Once the FOs are determined, $\hat{f}_l$, at each iteration stage, the FOs can be corrected in the received signal. The correction procedure can be mathematically described as

$$y(n) = \sum_{l=0}^{L-1} y_l(n)e^{-j2\pi f_l n} \qquad (5.2.14)$$

where $y_l(n)$ is the resolved multipath corresponding to path l and obtained using the iterative method as

$$y_l(n) = y(n) - \sum_{m=0,m\neq l}^{L-1} \hat{h}_m \hat{s}(n-m) e^{j2\pi \hat{f}_m n} \qquad (5.2.15)$$

This procedure will be continued until the residual error has no significant effect on the system performance. Having obtained the estimated FOs, the CSI can be updated afterwards.

5.2.3 Simulations results for SISO channels

In this section, it is assumed that 60 OFDM symbols are in each frame, with each OFDM symbol having $N = 64$ subcarriers. For all simulations, the length of the CP is kept equal to the order of the channel and the number of carriers is equal to the number of symbols in an OFDM block. The transmitted frequency domain symbols $\{S(k)\}$ are BPSK. In order to assess the performance of the proposed AML estimator, a randomly chosen fixed channel with two paths $[h_0 = -0.2502 + 0.0363i, h_1 = -0.8932 + 0.3719i]$, and fixed frequency offsets $[f_0 = 0.001, f_1 = 0.005]$ are considered. The channel is first estimated using the long training signal available in OFDM symbol. The soft estimates of the transmitted signal are then used to resolve multipaths, determine multiple FOs and to refine the channel estimates in an iterative fashion. At each iteration, the soft estimate of the transmitted signal are obtained using the new FO and channel estimation. The results are depicted in Fig. 5.3 and Fig. 5.4 for the channel and the FO estimation, respectively. The derivation for the CRLB can be found in [17, 18], [30] and [63]. This confirms that the iterative scheme makes full use of the soft estimates of the transmitted signal at moderate to high SNR.

In order to evaluate the BER performance, a quasi-stationary channel with distinct multipath FOs is considered, so that the FO and channel coefficients change between frames of 60 OFDM symbols according to uniform

(0 - 0.005) and complex Gaussian distributions, respectively. However, the multiple FOs have been assumed to vary between OFDM symbols in each frame according to (5.2.3). The proposed iterative scheme has the ability to track the FOs as depicted in Fig. 5.5. The length of the channel is assumed to be two. The results depicted in Fig. 5.6 show the BER performance of the proposed iterative method for three iterations. The result is compared to a scheme that does not track frequency offsets. A substantial gain in terms of dB is obtained using the proposed method. Note unlike our previous results for TDMA system, the CRLB is achieved only with the first iteration. This is because an initial frequency offset estimation is obtained by using the long training symbol in OFDM.
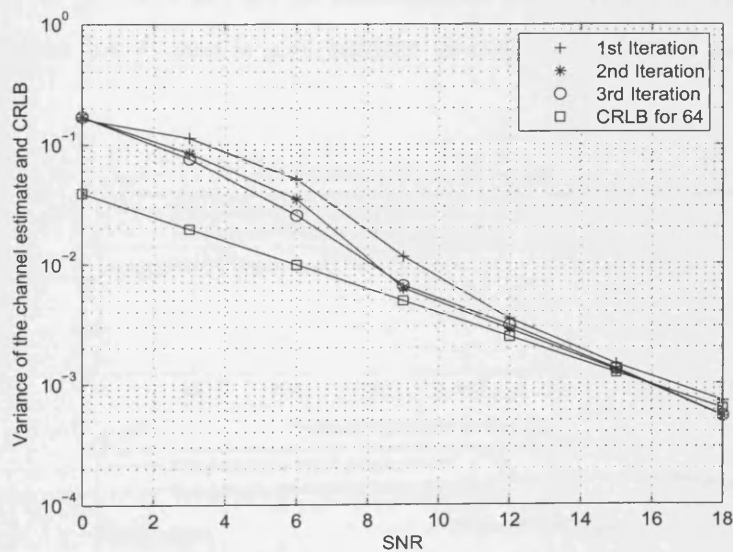
Figure 5.3. Comparison of the variance of the iterative channel gain estimate for h_0 and the CRLBs assuming 64 pilot symbols. The estimation performance for h_1 is also similar to that of h_0, hence not depicted.
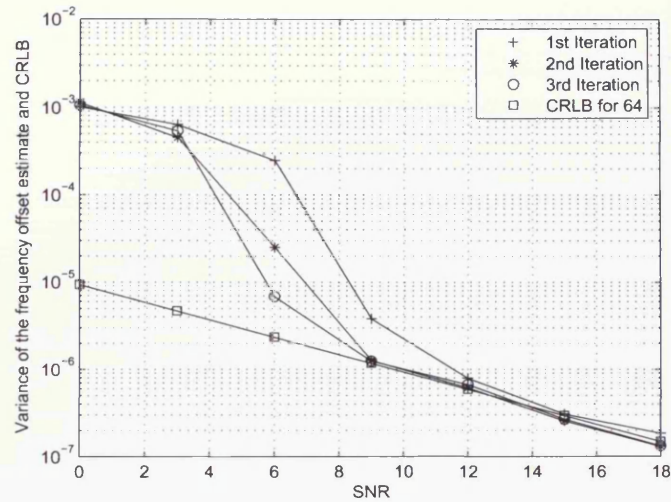
Figure 5.4. Comparison of the variance of the iterative frequency offset estimate for f_0 and the CRLBs assuming 64 pilot symbols. The estimation performance for f_1 and is also similar to that of f_0, hence not depicted.
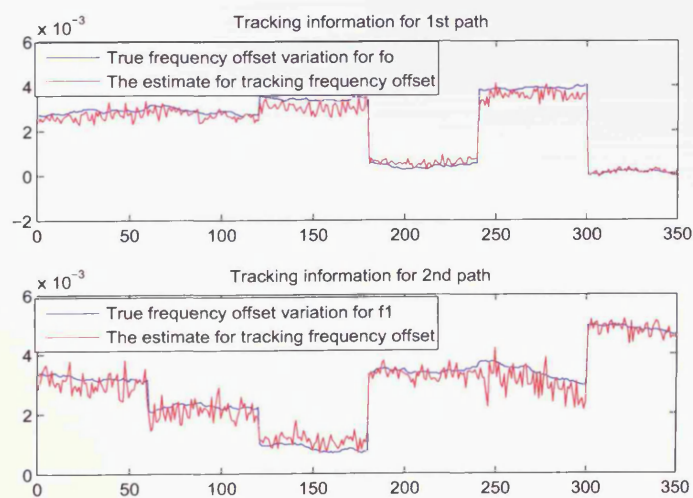
Figure 5.5. Tracking frequency offsets for multipath channel.
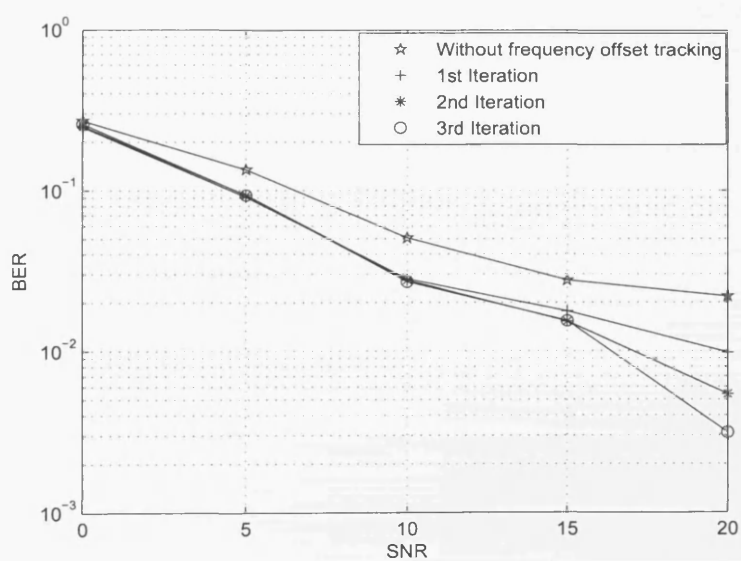
Figure 5.6. The BER performance of the proposed iterative method and the one which does not track the frequency offsets.
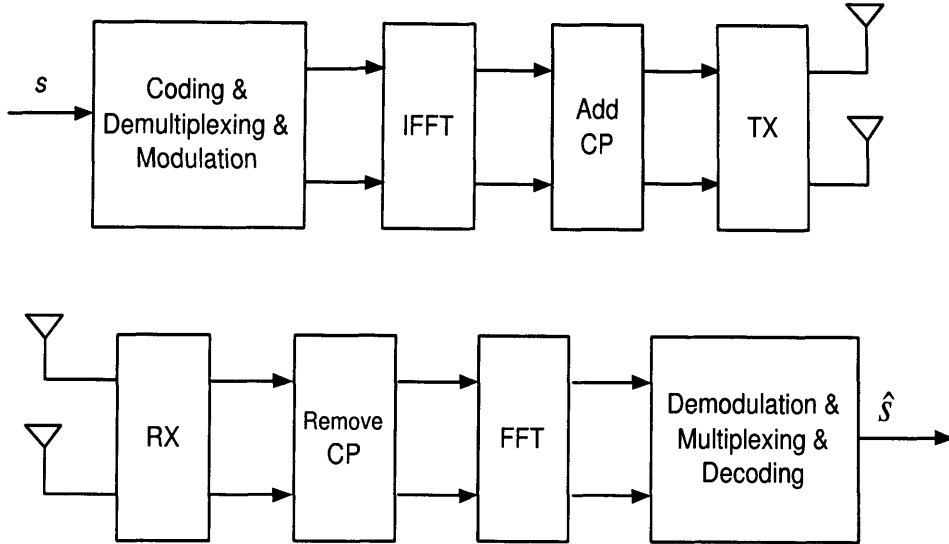
Figure 5.7. 2 × 2 MIMO OFDM baseband system.

5.3   Problem statement (MIMO case)

Fig. 5.7 illustrates a baseband MIMO-OFDM system. The original data stream is first encoded by a convolutional encoder (assumed to be 1/2-rate), interleaved and serial-to-parallel converted into N_T parallel data substream, where N_T is the number of transmit antennas. Each data substream is mapped onto a stream of symbols. After modulation, the IFFT is performed on each stream of symbols, a cyclic prefix of length v is inserted and transmitted. The signal is propagated through L different paths for each transmit-receive antenna pair, with each path possibly having different FOs. The receive signal at the qth receiver antenna is

$$y_q(n) = \sum_{t=0}^{N_T} \sum_{l=0}^{L-1} h_{qt}(l) s_t(n-l) e^{j2\pi f_{qtl} n} + \omega_q(n), \qquad (5.3.1)$$

where $n = 0, 1, ..., N + v - 1$, $h_{qt}(l)$ and f_{qtl} are the unknown complex channel gain and the frequency offset between the receive antenna q and

the transmit antenna t, for the lth path. Here $\{s_t(n)\}$ is the signal transmitted from the tth antenna and $\omega_q(n)$ is an additive, circularly symmetric zero mean white (complex) Gaussian noise with variance σ_ω^2 and assumed to be spatially uncorrelated.

5.3.1   Iterative channel and FO estimation

In this section, the channel impulse response (CIR) and frequency offsets are assumed to change between frames according to a complex Gaussian distribution and uniform distribution (0 - 0.005), respectively. Within each frame, however, the frequency offsets and the channel gains are assumed to be changing between OFDM symbols according to a random walk model

$$f_{qtl}^{m+1} = \alpha f_{qtl}^m + (1 - \alpha)\eta_1(m) \tag{5.3.2}$$

$$h_{qt}^{m+1}(l) = \beta h_{qt}^m(l) + (1 - \beta)\eta_2(m) \tag{5.3.3}$$

where f_{qtl}^m and $h_{qt}^m(l)$ are the FOs and the channel gain for the path l between the tth transmit antenna and q^{th} receive antenna at OFDM symbol number m. $\eta_1(m)$ is the real Gaussian variables with variances equal to 0.001 and $\eta_2(m)$ is zero mean complex Gaussian variables with variances equal to 0.1. The value of α and β are chosen as 0.99.

For the MIMO frequency selective channel, denote the gain in the nth subcarrier as $\mathbf{H}(n)$. Therefore, as in a conventional MIMO OFDM receiver, to decode the transmitted signal, a per-tone MIMO MMSE equalizer is employed as

$$\mathbf{W}(n) = (\mathbf{H}(n)\mathbf{H}(n)^H + \frac{\sigma_\omega^2}{\sigma_s^2}\mathbf{I})^{-1}\mathbf{H}(n) \tag{5.3.4}$$

Using this per tone equalizer, the soft estimate of the transmitted signal is obtained as

$$\hat{S}_t(n) = \mathbf{w}_t^H(n)\mathbf{Y}(n) \tag{5.3.5}$$

where $\mathbf{Y}(n)$ is the received signal at the nth subcarrier (after FFT) and $\mathbf{w}_t(n)$ is the tth column of the MIMO equalizer $\mathbf{W}(n)$. The output $\hat{\mathbf{S}}_t(n)$ is used to obtain the difference between the posteriori and a priori log-likelihood ratio (LLR) as follows [50, 55]

$$
\begin{aligned}
L_{e1}[\hat{S}_t(n)] &= \ln\frac{p\{S_t(n) = +1|_{\hat{S}_t(n)}\}}{p\{S_t(n) = -1|_{\hat{S}_t(n)}\}} - \ln\frac{p\{S_t(n) = +1\}}{p\{S_t(n) = -1\}} \\
&= \ln\frac{p\{\hat{S}_t(n)|_{S_t(n)=+1}\}}{p\{\hat{S}_t(n)|_{S_t(n)=-1}\}} \\
&= \frac{4\mathrm{Re}\{\hat{S}_t(n)\}}{1 - \mathbf{w}_t(n)^H\mathbf{H}_t(n)}
\end{aligned}
\tag{5.3.6}
$$

where $\mathbf{H}_t(n)$ is the tth column of the $\mathbf{H}(n)$. The mean of the symbol (soft estimate) is obtained as

$$\bar{S}_t(n) = \tanh(L_{e1}[\hat{S}_t(n)]) \tag{5.3.7}$$

After the IFFT, the soft estimates of the transmitted symbols are then treated as a training signal to separate users and to determine the multiple FOs and to refine the channel estimate and FOs in an iterative fashion. The estimate of the transmitted signal are updated using the new channel estimate and the frequency offsets. Once the FOs estimate $\hat{\mathbf{f}}_q$ in (4.2.4) is obtained, at each iteration stage, the FO can be corrected in the received signal. The correction procedure can be mathematically described as

$$y_q(n) = \sum_{t=1}^{N_t}\sum_{l=0}^{L-1} y_{qt}^l(n)e^{-j2\pi f_{qtl}n} \tag{5.3.8}$$

where $y_{qt}^l(n)$ is the resolved multipath between the receive antenna q and the transmit antenna t which is obtained using iterative method as

$$y_{qt}^l(n) = y_q(n) - \sum_{t=1}^{N_t} \sum_{m=0, m \neq l}^{L-1} \hat{h}_{qt}(m)\hat{s}_t(n-m)e^{j2\pi f_{qtm}n} \qquad (5.3.9)$$

For each OFDM symbol in the frame, the frequency offsets and the channel gains are estimated, and the estimate of the channel is used to obtain an initial estimate of the transmitted signal in the subsequent OFDM symbol. This procedure continues until the last OFDM symbol is reached in the frame. Once the soft estimates of all OFDM symbols are obtained in the frame (of 60 OFDM symbols), they are deinterleaved and passed to a MAP decoder to obtain soft estimates of the transmitted signal which will be used to perform iterations a number of times to obtain a refined estimate of the channel, frequency offsets and the transmitted symbols.

5.3.2 Simulations results for MIMO channels

Two transmit and two receive antennas have been used for the iterative receiver. The length of the channel is assumed to be two. A half rate convolutional code and a MAP decoder are considered. The generator polynomials have been chosen as $G0 = 1 + D^3 + D^4$ and $G1 = 1 + D + D^3 + D^4$. The data bits with length $60 \times N$ have been interleaved using a random interleaver, and modulated according to OFDM. At the receiver, the equalizer outputs for each user are collected, de-interleaved and decoded using the MAP algorithm. The soft estimation of the uncoded bits are interleaved again and fedback to the iterative equalizers. The soft estimates of the transmitted signal are then used to separate users, resolve multipaths, determine multiple frequency offsets and to refine the channel estimates in an iterative fashion. At each iteration, the soft estimate of the transmitted signal is obtained using the updated frequency offset and channel estimates. The proposed iterative scheme has the ability to track the FOs as depicted in Fig. 5.8. There are two scenarios are considered. In the

first scenario, the FOs are changed according to (5.3.2) between OFDM symbols (64 samples), but the channel is assumed to be fixed throughout the frame. The results are depicted using solid lines in Fig. 5.9. In the second scenario, in addition to frequency offset variation, the channel coefficients also changed according to (5.3.3). The result are depicted using dashed lines in Fig. 5.9. The result shows the BER performance for three iterations, and compares the BER result when the FOs are not tracked. The simulation results show that the proposed iterative scheme outperforms a scheme that assumes fixed channel coefficients within the frame.

5.4 Summary

In this chapter, iterative channel and frequency offset estimation algorithms for multipath channels with multiple frequency offsets for an OFDM environment have been proposed. According to the proposed method, multipath gains are initially estimated using the available long pilot sequence in an OFDM symbol, and then the soft estimates of the transmitted signal are used to estimate the frequency offsets and to refine the channel estimates iteratively. The simulation results demonstrated the proposed technique has the ability to track multiple frequency offsets. In addition to providing superior BER performance, the proposed estimator is also efficient in that it attains the CRLB derived assuming all 64 symbols in the OFDM symbol are known pilot symbols.
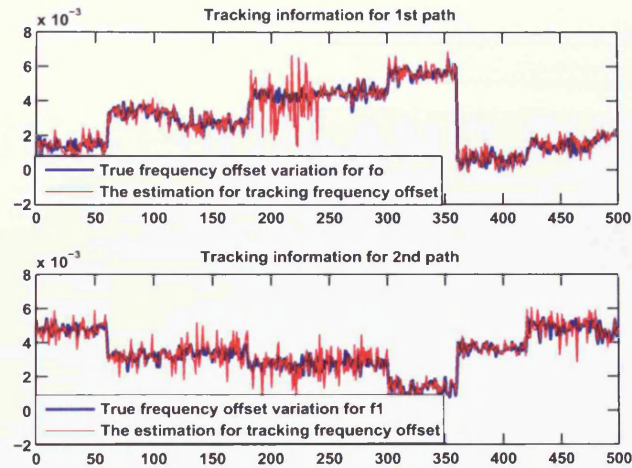
Figure 5.8. Tracking frequency offsets for multipath channel for a MIMO OFDM system.
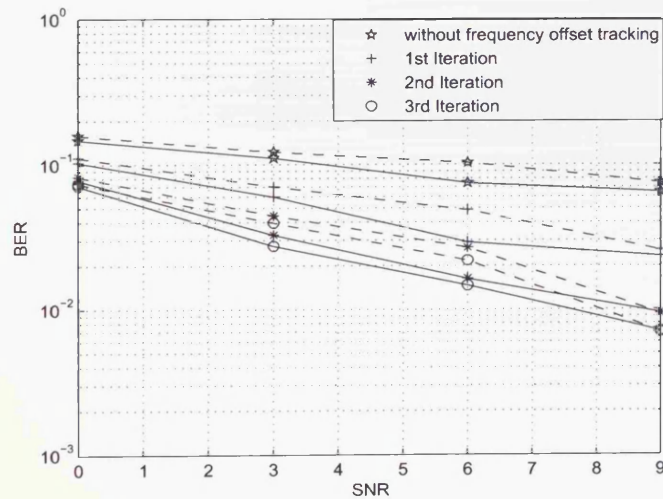
Figure 5.9. The BER performance of the proposed iterative method and the one which does not track frequency offsets for a MIMO OFDM system.

Chapter 6

CONCLUSION AND FUTURE WORK

6.1 Conclusion

For the equalization of wireless channels with long delay profiles, optimal ML techniques are not feasible due to high computational complexity. A review of low complexity LE and DFE equalizers shows that the gain in terms of complexity is traded against reduced performance. In order to keep down complexity while maintaining satisfactory performance, iterative equalization techniques have been adopted. By iteratively processing data, good performance can be achieved. For high data rate transmission, the mobile channel introduces significant Doppler shifts in the carrier frequencies which result from time variations in the frequency selective channels. Estimation of channel parameters becomes a challenging problem in fast time varying channels. Therefore, the main focus of this thesis has been on the parameter estimation and equalization techniques for frequency selective channels, with particular focus on iterative methods.

In the first part of the thesis, a simple time-varying channel has been considered for very high data rate transmission. Due to the relative motion between the transmitter and receiver, various multipaths experience

different DSs due to different angles of arrival. At first, the equalization of a SISO channel that allowed multipaths with distinct DSs was considered. To mitigate the effects of the channel and FOs, the equalizer required knowledge of both CSI and FOs. However, in a GSM system, the pilot symbols are generally inadequate to obtain an accurate estimate of the FOs due to limitation on the frequency resolution of the estimator. Therefore, an iterative algorithm has been considered, so that the soft estimate of the transmitted signal were treated as a long pilot sequence to determine multiple FOs and to refine channel estimates iteratively. To validate the performance of FOs and CSI estimators, the variance of the estimates has been compared with appropriate CRLBs. The BER performance showed superiority of this scheme over conventional equalizers.

In the second part of the thesis, the techniques proposed for SISO channel have been extended to a MIMO frequency selective channel. Using the iterative technique, the MIMO frequency selective channel was decoupled into multiple single-input single-output (SISO) flat fading sub-channels through appropriately cancelling both inter-symbol-interference (ISI) and the inter-user-interference (IUI) from the received signal. As in the case of a SISO channel, the distinct FOs could not be compensated prior to equalization. Therefore, they were accounted for in the iterative equalizer design. The soft estimate of the transmitted signal was used to separate users and to determine the multiple FOs and to refine the channel estimates in an iterative fashion. The simulation results revealed that the iterative scheme made full use of the soft estimates of the transmitted signal.

Finally, the iterative estimation and equalization techniques proposed for SISO and MIMO TDMA systems have been extended to SISO and MIMO

OFDM systems. The OFDM scheme is very sensitive to frequency offsets caused by Doppler shifts and/or local oscillator mismatches. The presence of frequency offset (FO) introduces inter-carrier interference (ICI) that could significantly degrade link layer performance [75]. Using both the time and frequency samples, a low complexity iterative algorithm was proposed. Multipath gains were initially estimated using the available long pilot sequence in OFDM symbol. These time domain estimates were used to design a per tone MMSE equalizer to decode the transmitted signal in the frequency domain. An IFFT was performed on the estimated frequency domain samples to obtain the time domain symbols. These time domain samples were used to estimate the multipath gains and frequency offsets iteratively. The merit of this iterative method is its capability of tracking frequency offsets. The proposed iterative technique has the ability to resolve multipaths, bringing the multiple frequency offset problem into the estimation of distinct frequency offsets. The simulation results demonstrate the superiority of the proposed scheme over a scheme that does not consider frequency offset correction. For most scenarios, the algorithm required only three iterations and provided substantial gain in terms of dB as compared to the conventional scheme.

6.2 Future work

A few possible extensions to the work presented in this thesis are listed below.

In the last three chapters, iterative algorithms have been proposed for SISO and MIMO systems. The EXIT chart analysis could be performed for both SISO and MIMO systems. EXIT charts show the input/output reliability using the mutual information. It is possible to understand the

convergence behavior of the iterative receiver through the EXIT chart mapping (one for the equalizer and the other for the channel decoder).

Another possible extension is to use superimposed training to improve channel and frequency offset estimation. Since training is superimposed with data, this technique could possibly provide better spectrum efficiency. Moreover, using iterative techniques, the data sequence could also be reused together with the training to improve the estimation performance.

Only quasi static fading channels, i.e. channel changed between blocks according to a Rayleigh fading profile, but unchanged within each block were considered in the thesis. The work can be extended to consider variations within each block. This will require estimation of the fading waveforms together with frequency offsets. Use of superimposed training may prove to be beneficial as this provides continuous training for tracking channel variations.

In this work, a mulipath channel with each path experiencing single frequency offset has been considered. However, each path could also experience multiple frequency offsets due to scattering as in a fading channel model. However, this problem has not been considered in this work. It may be possible to extend this work along this direction. In this case, one needs to look for multiple peaks in the power spectral density function.

BIBLIOGRAPHY

[1] W. Mohr and W. Konhauser, "Access network evaluation beyond third generation mobile communications," *IEEE Commun. Magazines*, vol. 38, pp. 122–133, Dec. 2000.

[2] 3GPP Homepage, [online]: http://www.3gpp.org, correct as September 2007.

[3] IEEE 802.11, [online]: http://grouper.ieee.org/groups/802/11/, correct as September 2007.

[4] ETSI DAB Standard, [online]: http://portal.etsi.org/broadcast/dab.asp, correct as September 2007.

[5] ETSI DVB Standard, [online]: http://www.dvb.org, correct as September 2007.

[6] T. S. Rappaport, *Wireless communications, Principles and Practice.* Prentice Hill, 1996.

[7] H. Viswanathan and R. Krishnamoorthy, "A frequency offset estimation technique for frequency selective fading channels," *IEEE Commun. Letters*, vol. 5, pp. 166–168, April 2001.

[8] P. Stoica and O. Besson, "Training sequence design for frequency offset and frequency selective channel estimation," *IEEE Trans. Commun.*, vol. 51, pp. 1910– 1917, Nov. 2003.

[9] K. E. Scott and E. B. Olasz, "Simultaneously clock phase and frequency offset estimation," *IEEE Trans. Commun.*, vol. 43, pp. 2263–2270, July 1995.

[10] H. Murata and S. Yoshida, "Maximum-likelihood sequence estimation receiver with joint frequency offset and delay profile estimation technique," *Global Telecommunications Conference (GLOBECOM 98)*, vol. 6, pp. 3455 – 3459, Nov. 1998.

[11] C. Toker, "Signal Processing Algorithms and Architectures for Communication Transceivers," *PhD thesis, University of London*, Sep. 2004.

[12] S. Ahmed, "Equalization of doubly selective channels using recursive and iterative methods," *PhD thesis, Cardiff university*, Sep. 2005.

[13] M. Morelli, U. Mengali, and G. M. Vitetta, "Further results in carrier frequency estimation for transmissions over flat fading channels," *IEEE Commun. Letters*, vol. 2, pp. 327–330, Dec. 1998.

[14] L. Krasny, H. Arslan, D. Koilpillai, and S. Chennakeshu, "Doppler spread estimation for wireless mobile radio systems," *IEEE Commun. Letters*, vol. 5, pp. 197 – 199, May 2001.

[15] J. G. Proakis, *Digital Communications.* McGraw Hill, 1989.

[16] "Multiplexing and multiple access on radio path," *3GPP TS 45.002,*.

[17] S. M. Kay, *Fundamentals of statistical signal processing, estimation theory.* Englewood Cliffs, N.J.: Prentice-Hall, 1993.

[18] S. Ahmed, S. Lambotharan, A. Jakobsson, and J. Chambers, "Parameter estimation and equalization techniques for communication channels with multipath and multiple frequency offsets," *IEEE Trans. Commun.*, vol. 53, pp. 219–223, Feb. 2005.

[19] M. G. Hebley and D. P. Taylor, "The effect of diversity on a burst-mode carrier-frequency estimator in the frequency-selective multipath channel," *IEEE Trans. Commun.*, vol. 46, no. 4, pp. 553 – 560, Apr. 1998.

[20] E. Jeong, S. Jo, and Y. H. Lee, "Least square frequency estimation in frequency estimation in frequency-selective channels and its application to transmissions with antenna diversity," *IEEE J. Sel. Areas Commun.*, vol. 19, no. 12, pp. 2369 – 2380, Dec. 2001.

[21] M. Morelli and U. Mengali, "Carrier-frequency estimation for transmission over selective channels," *IEEE Trans. Commun.*, vol. 48, no. 9, pp. 1580 – 1589, Sep. 2000.

[22] W. Y. Kuo and M. P. Fitz, "Frequency offset compensation of pilot symbol assisted modulation in frequency flat fading," *IEEE Trans. Commun.*, vol. 45, pp. 1412 – 1416, Nov. 1997.

[23] P. H. Moose, "A technique for Orthogonal Frequency Division Multiplexing Frequency Offset Correction," *IEEE Trans. Commun.*, vol. 42, pp. 2908–2914, Oct. 1994.

[24] T. M. Schmidl and D. C. Cox, "Robust frequency and timing synchronization for OFDM," *IEEE Trans. Commun.*, vol. 45, pp. 1613–1621, Dec. 1997.

[25] M. Morelli and U. Mengali, "An improved frequency offset estimator for OFDM applications," *IEEE Commun. Lett.*, vol. 3, pp. 75–77, Mar. 1999.

[26] F. Daffara and O. Adami, "A New Frequency Detector for Orthogonal Multicarrier Transmission Techniques," *in Proc. IEEE 45th Vehic. Technol. Conf.*, no. 1800-1805, 1995.

[27] J. J. van de Beek, M. Sandell, and P. O. Borjesson, "ML Estimation of Time and Frequency Offset in OFDM Systems," *IEEE Trans. Signal Process.*, vol. 45, pp. 1800–1805, Jul. 1997.

[28] B. B, "Estimating and Interpreting the Instantaneous Frequency of a Signal - Part 2: Algorithms and Applications," *Proceedings of the IEEE*, vol. 80, pp. 540 – 568, April 1992.

[29] A. V. Oppenheim and R. W. Schafer, *Discrete-Time Signal Processing.* Prentice-Hall, 1989.

[30] P. Stoica and R. Moses, *Introduction to Spectral Analysis.* Upper Saddle River, N.J.: Prentice Hall, 1997.

[31] B. Porat, *A Course in Digital Signal Processing.* New York, N.Y.: John Wiley and Sons, Inc., 1997.

[32] V. F. Pisarenko, "The retrieval of harmonics from a covariance function geophysics," *J. Roy. Astron. Soc.*, vol. 33, pp. 347 – 366, 1973.

[33] A. Eriksson, P. Stoica, and T. Soderstrom, "Asymptotical analysis of MUSIC and ESPRIT frequency estimates," *IEEE International Conference on Acoustics, Speech and Signal Processing (ICASSP)*, vol. 4, pp. 556 – 559, Apr. 1993.

[34] S. Haykin, *Adaptive Filter Theory (2nd edition).* Englewood Cliffs, N.J.: Prentice Hall, Inc., 1991.

[35] G. Strang, *Linear algebra and its applications, 3rd Ed.* Thomson Learning, Inc, 1988.

[36] E. Serpedin, A. Chevreuil, G. B. Giannakis, and P. Loubaton, "Blind channel and carrier frequency offset estimation using periodic modulation

precoders," *IEEE Trans. Signal Process.*, vol. 48, pp. 2389–2405, Aug. 2000.

[37] Y. Ma and Y. Huang, "Blind estimation of carrier frequency offset for OFDM in unknown multi-path channels," *IEE Electronics Letter*, vol. 39, pp. 128–130, Jan. 2003.

[38] M. Ghogho and A. Swami, "Blind frequency-offset estimator for OFDM systems transmitting constant-modulus symbols," *IEEE Commun. Letters*, vol. 6, pp. 343 – 345, Aug. 2003.

[39] R. J. McaAulay and E. M. Hofstetter, "Barankin bounds on parameter estimation," *IEEE Trans. Inf. Theory*, vol. 17, pp. 669–676, Nov. 1971.

[40] R. W. Lucky, "Automatic equalization for digital Communication," *Bell System Technical Journal*, vol. 46, pp. 547–588, Nov. 1965.

[41] J. G. Proakis and J. Miller, "An adaptive receiver for digital signaling through channels with inter-symbol-interference," *IEEE Trans. on Inform. Theory*, vol. 15, pp. 484–497, Jul. 1969.

[42] S. Qureshi, "Adaptive equalization," *IEEE Trans. Signal Process.*, vol. 20, pp. 9–16, Mar. 1982.

[43] S. Qureshi, "Adaptive equalization," *IEEE Proceedings*, vol. 73, pp. 1349–1387, Sep. 1985.

[44] Y. H. Kim and S. Shamsunder, "Adaptive algorithms for channel equalization with soft decision feedback," *IEEE Journals on Selected Areas of Commun.*, vol. 16, pp. 1660–1669, Dec. 1998.

[45] M. Chiani, "Introducing erasures in decision-feedback equalization to reduce error propagation," *IEEE Trans. Commun.*, vol. 45, pp. 757–760, July. 1997.

[46] C. Douillard, M. Jezequel, C. Berrou, P. Didier, and A. Glavieux, "Iterative correction of intersymbol iterference: Turbo-equalization," *European Trans. on Telecomm.*, vol. 6, no 5, pp. 507–511, Oct. 1995.

[47] G. Bauch and V. Franz, "A comparision of soft-in/soft-out algorithms for turbo detection," *in Proc. Int. Conf. Telecomm.*, pp. 259 – 263, Jun. 1998.

[48] A. Anastasopoulos and K. Chugg, "Iterative equalization/decoding for tcm for frequency-selective fading channels," *in Conf. Rec. 31th Asilomar Conf. Signals. Systems and Computers*, vol. 1, pp. 177 – 181, Nov. 1997.

[49] J. Hagenauer and P. Hoeher, "A Viterbi algorithm with soft-decision outputs and its applications," *in Proc. IEEE Global Telecomm. Conf.*, pp. 1680 – 1686, 1989.

[50] R. Koetter, A. C. Singer, and M. Tüchler, "Turbo equalization," *IEEE Signal Process. Mag.*, vol. 21, pp. 67–80, Jan. 2004.

[51] S. Ariyavisitakul and Y. Li, "Joint coding and decision feedback equalization for broadband wireless channels," *IEEE J. Select. Areas Commun.*, vol. 16, pp. 1670 – 1678, Dec. 1998.

[52] X. Wang and H. Poor, "Iterative (turbo) soft interference cancellation and decoding for coded cdma," *IEEE Trans. Commun.*, vol. 47, pp. 1046 – 1061, Jul. 1999.

[53] P. Schniter, "Low-Complexity Equalization of OFDM in Doubly Selective Channels," *IEEE Trans. on Signal Process.*, vol. 52, pp. 1002–1010, April 2004.

[54] S. Ahmed, M. Sellathurai, S. Lambotharan, and J. A. Chambers, "Low complexity iterative method of equalization for Single Carrier With Cyclic Prefix in doubly selective channels," *IEEE Signal Process. Lett.*, Jan. 2006.

[55] M. Tüchler, R. Koetter, and A. C. Singer, "Turbo equalization: principles and new results," *IEEE Trans. Commun.*, vol. 50, pp. 754–766, May 2002.

[56] S. Haykin and M. Moher, *Modern Wireless Communications.* Upper Saddle River, N. J.: Prentice Hall, Inc., 2005.

[57] "Multiplexing and multiple access on radio path," *3GPP TS 45.002 (V5.9.0)*, April 2003.

[58] L. Krasny, H. Arslan, D. Koilpillai, and S. Chennakeshu, "Optimal and suboptimal algorithms for Doppler spread estimation in mobile radio systems," *IEEE International Symposium on Personal, Indoor and Mobile Radio Communications (PIMRC 2000)*, vol. 2, pp. 1295 – 1299, Sep. 2000.

[59] A. R. S. Bahai and M. Sarraf, "Frequency offset estimation in frequency selective fading channels," *in Proc. IEEE Vehic. Technol. Conf.*, vol. 3, pp. 1719 – 1723, May 1997.

[60] Q. Yu and S. Lambotharan, "Iterative channel estimation and equalization techniques for multipath channels with multiple frequency offsets," *in Proc. IEEE ICCS, Singapore*, November 2006.

[61] Q. Yu and S. Lambotharan, "Iterative (Turbo) estimation and detection techniques for frequency selective channels with multiple frequency offsets," *IEEE Signal Process. Lett.*, vol. 14, pp. 236–239, April 2007.

[62] K. Azarian, H. E. Gamal, and P. Schniter, "On the achievable diversity-multiplexing tradeoff in half-duplex cooperative channels," *IEEE Trans. Inf. Theory*, vol. 51, pp. 4152–4172, Dec. 2005.

[63] S. Ahmed, S. Lambotharan, A. Jakobsson, and J. A. Chambers, "MIMO frequency selective channels with multiple frequency offsets: es-

timation and detection techniques," *IEE Proc. Commun.*, vol. 152, Aug 2005.

[64] B. Vucetic and J. Yuan, *Turbo codes: principles and applications.* Kluwer Academic Publishers, 2000.

[65] D. Molkdar, W. Featherstone, and S. Lambotharan, "An overview of EGPRS: the packet data component of EDGE," *IEE Electron. Commun. Eng. J.*, pp. 21–38, Feb. 2002.

[66] "Channel coding," *3GPP TS 45.003.*

[67] J. Mietzner and P. A. Hoeher, "Boosting the performance of wireless communication systems: theory and practice of multiple-antenna techniques," *IEEE Commun. Mag.*, pp. 40 – 47, Oct. 2004.

[68] G. J. Foschini and M. G. Gans, "On limits of wireless communications in a fading environment when using multiple antennas," *Wireless Personal Communications*, pp. 311–335, Mar. 1998.

[69] I. E. Telatar, "Capacity of multi-antenna Gaussian channels," *European Trans. on Telecomm.*, pp. 585–595, Nov. 1999.

[70] O. Besson and P. Stoica, "On parameter estimation of MIMO flat-fading channels with frequency offsets," *IEEE Trans. Signal Process.*, vol. 51, pp. 602–613, Mar. 2003.

[71] S. M. Alamouti, "A simple transmit diversity technique for wireless communications," *IEEE Trans. on Select. Areas Commun.*, vol. 16, pp. 1451–1458, Oct. 1998.

[72] Q. Yu and S. Lambotharan, "Iterative (turbo) estimation and detection techniques for frequency selective channels with multiple frequency

offsets in MIMO system," *in Proc. IEEE 65th Vehic. Technol. Conf.*, April 2007.

[73] K. Cumanan, R. Krishna, Q. Yu, and S. Lambotharan, "Maximum likelihood frequency offset estimation for frequency selective mimo channels: An average periodogram interpretation and iterative techniques," *European Signal Processing Conference, Poznan, Poland*, Sept. 2007.

[74] H. Liu and M. D. Zoltowski, "Blind equalization in antenna array CDMA systems," *IEEE Trans. Signal Process.*, vol. 45, pp. 161–172, Jan. 1997.

[75] T. Pollet, M. van Bladel, and M. Moeneclaey, "BER sensitivity of OFDM systems to carrier frequency offset and Wiener phase noise," *IEEE Trans. Commun.*, vol. 43, pp. 191–193, Feb. 1993.

[76] S. S. Das, R. Rajakumar, M. I. Rahman, A. Pal, F. Fitzek, O. Olsen, and R. Prasad, "Low cost residual phase tracking algorithm for ofdm based wlan systems," *in Proc. Commun. Syst., Netw., Digital Signal Process., Newcastle, UK*, pp. 128 – 131, Jul. 2004.

[77] X. Dai and S. Zhang, "Pilot-assisted carrier frequency offset estimation for mimo-ofdm systems," *in Proc. Int. Conf. Comput. Inf. Technol., Wuhan, China*, pp. 681 – 686, Sep. 2004.

[78] C. Oberli and B. Daneshrad, "Maximum likelihood tracking algorithms for mimo-ofdm," *in Proc. Int. Conf. Commun,. Paris, France*, vol. 4, pp. 2468 – 2472, Jun. 2004.

[79] G. L. Stuber, J. R. Barry, S. W. Mclaughlin, and M. A. Ingram, "Broadband MIMO-OFDM wireless Commun.," *Proc. IEEE*, vol. 92, pp. 271 – 294, Feb. 2004.

[80] Q. Yu and S. Lambotharan, "An iterative estimation and detection technique for ofdm systems with multiple frequency offsets (doppler shifts)," *in Proc. IEEE PIMRC, Athens, Greece*, Sept. 2007.

[81] "IEEE Standard for Wireless WLAN Medium Access Control (MAC) and Physical Layer (PHY) Specifications," *IEEE 802.11a*, 1999.